EXPERIMENTAL STUDY OF THE ALKALINE-SURFACTANT-GAS (ASG) FLOODING IN A CARBONATE RESERVOIR

BY

ALI SALEH OMAR BA GERI

A Thesis Presented to the
DEANSHIP OF GRADUATE STUDIES

KING FAHD UNIVERSITY OF PETROLEUM & MINERALS

DHAHRAN, SAUDI ARABIA

In Partial Fulfillment of the
Requirements for the Degree of

MASTER OF SCIENCE

In

PETROLEUM ENGINEERING

May, 2013

KING FAHD UNIVERSITY OF PETROLEUM & MINERALS

DHAHRAN- 31261, SAUDI ARABIA

DEANSHIP OF GRADUATE STUDIES

This thesis, written by **ALI SALEH OMAR BA GERI** under the direction of his thesis advisor and approved by his thesis committee, has been presented and accepted by the Dean of Graduate Studies, in partial fulfillment of the requirements for the degree of **MASTER OF SCIENCE IN PETROLEUM ENGINEERING.**

Dr. Abdullah S. Sultan
(Advisor)

For Dr. Abdullah S. Sultan
Department Chairman

Dr. Darren Malekzadeh
(Member)

Dr. Salam A. Zummo
Dean of Graduate Studies

Dr. Mohamed Mahmoud
(Member)

30/6/13

Date

DEDICATION

This thesis is dedicated to

MY BELOVED MOTHE & FATHER,

MY WIFE, MY DAUGHTER, MY BROTHER& SISTERS

ACKNOWLEDGMENTS

In the name of Allah, most gracious, All praise is to Almighty Allah who gave me courage, knowledge and ability to complete this work and blessing of Allah be upon his prophet Mohammed (Peace be your him).

I wish to express my deep appreciation and thanks to Dr. Abdullah S. Sultan, thesis advisor, Dr. Darren Malekzadeh and Dr. Mohammed Mahmoud, committee members, for providing their invaluable help and guidance through this work.

Acknowledgment is due to King Fahd University of Petroleum & Minerals. My sincere appreciation is extended to all faculty and staff of the Centre for Petroleum and Minerals at Research Institute, and the Petroleum Engineering Department for the contribution to this work.

I am also indebted to the help provided by: Dr. Mohamed Kandil, Mr. Aziz Arshed, Mr. Abdurahim Mohammedeen, and Mr. Noor during my experimental work in the RI laboratories.

Special thanks are due to all my colleagues and friends who help me in my work and made my stay at the University memorable and source of valuable experience.

Finally, I am indebted to Eng. A. A. Bugshan & HEFHD for providing me with scholarship and for their mortal support and encouragement throughout my master program.

TABLE OF CONTENTS

LIST OF TABLES

LIST OF FIGURES

LIST OF ABBREVIATIONS

ASG	:	Alkaline Surfactant Gas
EOR	:	Enhanced Oil Recovery
BP	:	Back Pressure
D	:	Core Diameter, cm
k	:	Permeability, md
Kabs	:	Absolute Permeability (Darcy)
k_o	:	Effective Oil Permeability (md)
k_w	:	Effective Water Permeability (md)
k_{rw}	:	End – Point Water Relative Permeability (md)
L	:	Core Length, cm
M_{dry}	:	Weight of the Dry Core, gm
$M_{sat.}$	:	Weight of the Saturated Core by Brine, gm
OBP	:	Over Burden Pressure
q	:	Flow Rate, cm^3/min
Q_o	:	Oil Rate, cm^3/sec
Qw	:	Brine Rate, cm^3/min
PV	:	Pore Volume, cm^3

S_{oi}	:	Initial Oil Saturation (%)
S_{ro}	:	Residual Oil Saturation (%)
S_{wi}	:	Initial Water Saturation (%)
TDS	:	Total Dissolve Solids, ppm
V_{bulk}	:	Bulk Volume of the Core, cm^3
$V_{injected}$	:	Volume of Oil Injected into the Core, cm^3
V_o	:	Initial Volume of Oil in The Core, cm^3
$V_{produced}$	:	Volume of Collected Oil at Effluent, cm^3
ρ_{brine}	:	Core Density, gm/ cm^3
ΔP	:	Steady Pressure along the Core (atm)
ϕ	:	Porosity, fraction
μ_{brine}	:	Brine Viscosity, cp
μ_{oil}	:	Oil Viscosity, cp

ABSTRACT

Full Name : Ali Saleh Omar Ba geri

Thesis Title : EXPERIMENTAL STUDY OF THE ALKALINE-SURFACTANT-GAS (ASG) FLOODING IN A CARBONATE RESERVOIR

Major Field : Petroleum Engineering

Date of Degree : May, 2013

The use of gas in alkaline-surfactant flooding (Alkaline-Surfactant-Gas (ASG) process) can be an alternative to the use of polymer, especially in carbonate reservoirs that generally have low permeability and contain vugs and fractures, for improving the displacement efficiency. In this process foam performs the role of a mobility control agent; thereby ASG can be capable of recovering some of the oil left behind the primary and secondary recovery.

Two approaches were applied to determine the favorable concentration of each surfactant. First; aqueous stability test; where the solubility and stability of surfactant mixture in electrolyte solution are investigated by changing the salinity. The second approach was to evaluated the foam stability and determine the concentration of each surfactant. From phase behavior tests, oil- and water-solubility, it was observed that the phase behavior is oil-in-water micro-emulsion (Winsor Type I Behavior). It is believed that low IFT can be obtained at high solubility ratio for the optimum salinity concentration.

The performance of foam flooding with nitrogen (N_2) for oil recovery in limestone carbonate rocks was studied. The success of the ASG process was determined by evaluation of oil recovery, coreflood pressure response and effluent from coreflood

experiments. The effects of core permeability, alkaline, and type of surfactants on the performance of the ASG process were evaluated. Maximum recovery of 47.7% of residual oil in place in low permeability was observed compared to 43% of residual oil in place on high permeability. In addition, the more recovery was obtained when using surfactant without alkaline.

ملخص الرسالة

الاسم الكامل: علي صالح عمر باجري

عنوان الرسالة: دراسة مختبرية لعملية الغمر بالقلويات والسيرفاكتنت و الغاز في المكامن الكربونية

التخصص: هندسة البترول

تاريخ الدرجة العلمية: مايو 2013 م

قد يكون استخدام الغاز مع عمليات الغمر بالقلويات والسيرفاكتنت (التي يتم اختصارها ب ASG) بديلا من استخدام البوليمرات, خصوصا في المكامن الكربونية التي عادة لها نفاذية منخفضة وتحتوي على تجاويف صغيرة وشقوق، لتطوير كفاءة الازاحة في عملية الاستخلاص المحسن الكيميائي للنفط. في هذه العملية (ASG)، تقوم الرغوة بوظيفة عامل تحكم للحركية، وبالتالي فإن ASG قادرة على استخلاص بعض النفط المتبقي في الصخور الكربونية.

تم تطبيق طريقتين لتحديد افضل تركيز لكل نوع من السيرفاكتنت. الطريقة الأولى هي اختبار استقراريه المحلول المائي حيث نقوم بالتحقيق في الذوبان والاستقرار من خليط السيرفاكتنت في المحلول الأيوني عن طريق تغيير الملوحة. الطريقة الثانية عن طريق تقييم استقرار الرغوة لتحديد التركيز الأمثل لكل سيرفاكتنت. من اختبارات سلوك الموائع، لوحظ ان سلوك المائع من نوع وينزر النوع الأول. في نسبة الذوبان العالية في الملوحة المثلى يحدث التوتر السطحي المنخفض (IFT).

كما تمت دراسة أدائية الرغوة بالنيتروجين (N2) في الصخور الجيرية الكربونية. و قد تم في هذه الدراسة تحديد نجاح عملية ASG من خلال تقييم استخراج النفط، و استجابة الضغط من تجارب الغمر. كما تمت دراسة تأثير نفاذية العينة واضافة القلويات ونوع السيرفاكتنت على ادائية طريقة الغمر(ASG). في حالة النفاذية المنخفضة كانت أعلى نسبة استخلاص للنفط 47.7 % من النفط المتبقي في المكمن، بينما 43% في حالة النفاذية العالية. اضافة لذلك فإن نسبة الاستخلاص كانت اعلى بدون اضافة المادة القلوية.

ملخص الرسالة

الاسم الكامل: علي صالح عمر باجري

عنوان الرسالة: دراسة مختبرية لعملية الغمر بالقلويات والسيرفاكتنت و الغاز في المكامن الكربونية

التخصص: هندسة البترول

تاريخ الدرجة العلمية: مايو 2013 م

قد يكون استخدام الغاز مع عمليات الغمر بالقلويات والسيرفاكتنت (التي يتم اختصارها ب ASG) بديلا من استخدام البوليمرات, خصوصا في المكامن الكربونية التي عادة لها نفاذية منخفضة وتحتوي على تجاويف صغيرة وشقوق، لتطوير كفاءة الازاحة في عملية الاستخلاص المحسن الكيميائي للنفط. في هذه العملية (ASG)، تقوم الرغوة بوظيفة عامل تحكم للحركية، وبالتالي فإن ASG قادرة على استخلاص بعض النفط المتبقي في الصخور الكربونية.

تم تطبيق طريقتين لتحديد افضل تركيز لكل نوع من السيرفاكتنت. الطريقة الأولى هي اختبار استقراريه المحلول المائي حيث نقوم بالتحقيق في الذوبان والاستقرار من خليط السيرفاكتنت في المحلول الأيوني عن طريق تغيير الملوحة. الطريقة الثانية عن طريق تقييم استقرار الرغوة لتحديد التركيز الأمثل لكل سيرفاكتنت. من اختبارات سلوك الموائع، لوحظ ان سلوك المائع من نوع وينزر النوع الأول. في نسبة الذوبان العالية في الملوحة المثلى يحدث التوتر السطحي المنخفض (IFT).

كما تمت دراسة أدائية الرغوة بالنيتروجين (N2) في الصخور الجيرية الكربونية. و قد تم في هذه الدراسة تحديد نجاح عملية ASG من خلال تقييم استخراج النفط، و استجابة الضغط من تجارب الغمر. كما تمت دراسة تأثير نفاذية العينة واضافة القلويات ونوع السيرفاكتنت على ادائية طريقة الغمر(ASG). في حالة النفاذية المنخفضة كانت أعلى نسبة استخلاص للنفط 47.7 % من النفط المتبقي في المكمن، بينما 43% في حالة النفاذية العالية. اضافة لذلك فإن نسبة الاستخلاص كانت اعلى بدون اضافة المادة القلوية.

CHAPTER 1

INTRODUCTION

1.1 Chemical EOR in carbonate reservoir

Oil recovery operations traditionally have been subdivided into three phases: primary, secondary, and tertiary which is known as enhanced oil recovery (EOR). After primary recovery (utilizing natural drive mechanisms, artificial lift techniques) and secondary recovery (pressure maintenance such as water and gas injection), over 50 % of the original oil in place is left behind in the reservoir (Shah, 1981). This residual oil is a result of high capillary force of water, viscous forces and reservoir heterogeneities which are keeping the oil immobile. Thereby, EOR methods are the only way of producing that residual oil.

EOR methods are basically the injection of gases, liquid chemicals and/or the use of thermal energy. Hydrocarbon gases, carbon dioxide (CO_2), nitrogen (N_2), and flue gases are example of the gases used in gas EOR processes where the recovery efficiency significantly depends on the immiscibility. In addition, liquid chemicals are commonly used, including polymers, surfactants, and hydrocarbon solvents. In thermal processes, steam or hot water are typically used, or rely on the in-situ combustion which is used to generate thermal energy in the reservoir rock. The injection of these fluids achieves

favorable conditions such as lower IFT's, oil swelling, oil viscosity reduction, wettability alteration, or favorable phase behavior, which may permit the residual oil to be mobile.

It is well known that a considerable portion of the world's hydrocarbon is in carbonate reservoirs (Eduardo Manrique and et al, 2010). In chemical EOR method, polymer provides mobility control during Alkaline-Surfactant-Polymer (ASP) slug and polymer drive injection. However, some reservoir conditions are not favorable for the use of polymers. These conditions such as (Srivastava et al, 2009):

- Very low permeability rocks, accordingly high molecular weight polymers can plug the pore through; however using polymers with a lower molecular weight may increase the cost of process.
- In carbonate rocks, which generally have low permeability and contains vugs and fractures, the use of polymer may result in the loss of permeability.
- High temperature reservoirs where many of the commercially available EOR polymers can be unstable
- At high flow rate through chokes or perforations, some polymers can mechanically degrade due to high shear stress
- Unfavorable interactions of polymers with under some conditions

For improving the displacement efficiency in chemical-EOR process, foam can be an alternative to polymer as a mobility control agent by reducing gas mobility. Moreover, foam can block and restrict the flow of undesired fluids; coning of gas or water in production wells; and injected fluids in high permeability streaks or fractures (Green and

Willhite, 1998). Foam is a two-phase system in which gas bubbles are enclosed by liquid since it may contain more or less liquid, according to circumstances (Yan, 2006). However, Hirasaki (1989) defined foam in porous media as "a dispersion of a gas in a liquid such that the liquid phase is continuous (i.e. connected) and at least some part of the gas phase is made discontinuous by thin liquid films called lamellae, Figure 1.1." The concept of using foam for mobility control was first introduced by Lawson and Reisberg in 1980. Foam can be generated by co-injection or alternate injection of gas and foaming agent (surfactant).

In this project, the use of foam as a mobility control agent through a process known as Alkali – Surfactant – Gas (ASG). In ASG process, reducing gas mobility can be achieved by creating more resistance to gas flow since gas bubbles are surrounded in foam by lamella. The addition of surfactant in aqueous phase reduces the interfacial tension between the displacing fluids and the trapped oil, thereby decreasing capillary forces. Foams can also collapse into low permeability regions if capillary forces are sufficiently high enough to drain the liquid in thin films surrounding gas bubbles (Schramm et al., 1994).

Oil displacement relies on the phase behaviour of the injected fluid and crude oil mixtures that are strongly dependent on reservoir temperature, pressure and crude oil composition. As a result, it is important to understand foam performance, strong or stable foam, in ASG process. Rossen (1988) reported a minimum pressure gradient needed to initiate and sustain a foam flow in porous media. Stable foam lowers mobilities of two phases to a favorable value and improves displacement efficiency of the process.

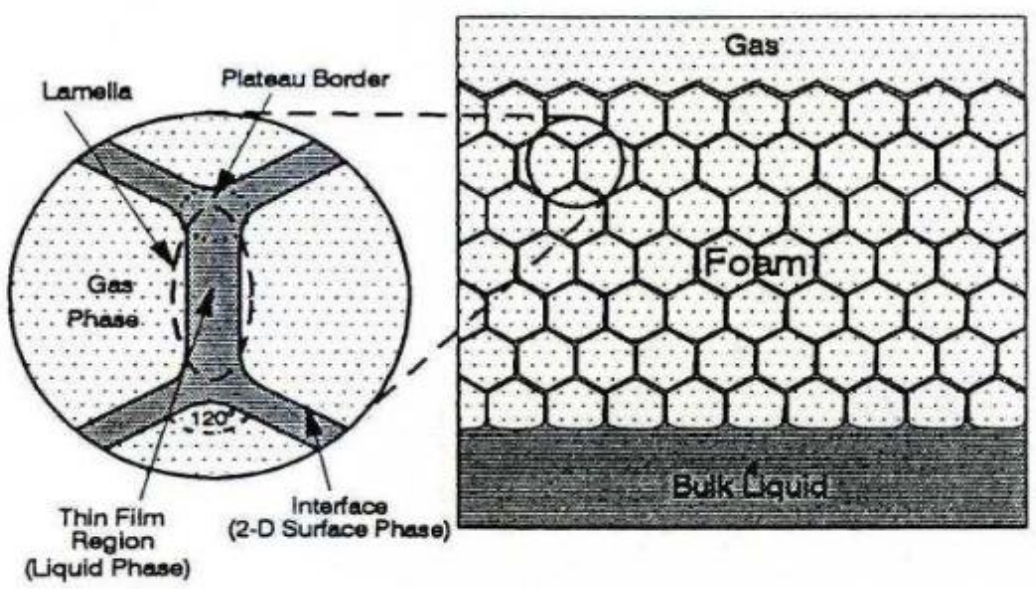

Figure 1.1 Generalized foam system (Schramm, 1994)

1.2 Problem Statement

The residual oil of water flooding is a result of high capillary force of water, viscous forces and reservoir heterogeneities, so EOR methods are the main approach of producing that residual oil. Liquid chemicals such as polymers, surfactants, and hydrocarbon solvents are commonly used in chemical EOR methods. Polymers provide mobility control and drive injection. However, some reservoir conditions are not favorable for the use of polymers. Consequently, for improving the displacement efficiency in chemical-EOR process, foam can be an alternative to polymer as a mobility control agent by reducing gas mobility. Foam can be generated by co-injection or alternate injection of gas and foaming agent (surfactant), ASG process.

In ASG process, reducing gas mobility can be achieved by creating more resistance to gas flow since gas bubbles are surrounded in foam by lamella. Oil displacement by foam is strongly dependent on reservoir temperature, pressure and crude oil composition. As a result, it is important to understand foam performance, foamability and stability of foam.

Despite carbonate reservoirs contains a significant amount of world's oil reserves, there has been only a few studies of ASG process. Most of previous studies about foam flooding achieved on sandstones and dolomite rocks. In this project, systematic laboratory studies on foam flooding for limestone rocks have been performed. Both the optimization of foamability and stability, and the investigation of operating parameters such as foam injection modes and gas liquid ratio (foam quality) are the key factors to ensure high incremental oil recovery.

1.3 Research Objectives

In this study, limestone rocks will be used to investigate the performance of chemical flooding with nitrogen (N_2) through a series of experiments. This investigation will be achieved through the following objectives:

1. To evaluate the effect of surfactant type on the recovery of oil during ASG process of. Five surfactants were selected including three fluorosufactants and two hydrocarbon surfactants.
2. To carry out the aqueous stability and phase behavior tests to determine the stability of chemicals at a given salinity (21,600 ppm)and temperature (60°C)
3. To study the foamability and the stability of the foam and select the favorable surfactant for ASG process.
4. To carry out coreflooding experiments and determine the effectiveness of ASG process as potential EOR technique.
5. Studying the effect of the permeability, alkaline, and type of surfactants on the performance of the ASG process.

CHAPTER 2

LITERATURE REVIEW

2.1 Literature Review of ASG Process

Kamal and Marsden (1973) carried out ASG experiments on high permeability sand packs. A chemical slug was first injected in the sand pack, and then displaced by the foam drive. The size of slugs in that experiments were small, either 0.05 PV or 0.1 PV. The slug was an aqueous solution of a commercially available surfactant, Triton X-100. For the drive, surfactant solution and gas were first mixed in a foam generator and then injected into the sand pack. The sand pack was completely saturated with brine solution, followed by oil injection to bring the sand pack to residual water saturation. From this point, two set of experiments were conducted. In one set, chemical slug and drive fluid were injected into the sand pack at residual water saturation, thus modeling a secondary recovery process. In the second set, the sand pack was first water flooded to residual oil saturation and then slug fluid was injected. Thus, the second set of experiments modeled a tertiary recovery process. In their experiments, oil recovery varied from 60% to 65% of the original oil in place (OOIP). Their work was one of the first demonstrations of successful application of foam in chemical floods.

Lawson and Riseberg's (1980) studied alternate injection of an inert gas and surfactant solution as a method for providing mobility control in chemical floods. In their experiments, chemical slug was displaced by alternate slugs of gas and surfactant. The

slug ratio was kept at 1:1. The size of chemical slug varied from 0.1 PV to 0.25 PV. The size of gas and surfactant slugs in the drive was 0.1 PV. Polymer was not added in the chemical slug to provide mobility control. Their work suggested that as long as gravity segregation and foam drainage is prevented, the performance of alternate slugs of gas and dilute surfactants compares favorably with water-soluble polymers.

Noll et al. (1989) studied the effects of temperature, salinity and wettability on surfactant loss. They concluded that, factors which decrease surfactant solubility generally increase adsorption. Adsorption was also observed to increase up to a maximum with increasing salt concentration and the magnitude of the molar enthalpy of adsorption indicate that surfactant adsorption is a physical process.

French and Burchfield (1990) concluded that a mixture of surfactant and alkaline produces lower interfacial tension (IFT) and sustains low 1FT longer than either reactant alone. This trend was observed with crudes having low and high acid numbers. They also showed that an alkaline preflush protects synthetic surfactants from precipitation by removal of divalent ions and alkali reduces surfactant adsorption. A low-pH alkaline (such as sodium bicarbonate and sodium carbonate) is effective in reducing alkali consumption and scaling in production wells.

Also Later, Rossen and Zhou (1992) studied and modeled the foam diversion in matrix acidizing process on sandstone rocks. Their conclusion was that the greatest diversion could be obtained when foam is preceded by surfactant pre-flush then followed by an acid slug that is compatible with foam. They also concluded that the key to success of

such a process is the ability of surfactant solution to immobilize the gas in previously injected foam.

Wang (2006) conducted ASG experiments on micro-models and sand packs by co-injecting ASP slug and gas. Micro models experiments, although not representative of porous media, provided visual observation of the process. They observed that the co-injection of ASP slug and gas is more effective when the oil saturation is low. This is because foam is more stable at low oil saturations. They found that ASG process is more effective when alkali is added in the slug. Addition of alkali assists in achieving low IFT conditions without adding extra surfactant and reduces surfactant adsorption (Nelson, 1984). Oil-wet conditions reduced the effects of flowing foam, resulting in relatively lower oil recovery compared to water-wet flowing conditions. Wang's work demonstrated that co-injection of ASP slug and gas can be effectively designed to achieve enhancement in oil recovery.

Renjing et al. (2008) studied nitrogen foam flooding efficiencies at Shengli oilfield. They applied experiments, numerical simulation and field tests to optimize the operating conditions and develop a reservoir-condition screening criterion. From their study, it was shown this technique has stronger blocking ability and can channel selectively through high permeability zones under high heterogeneity reservoir condition. Furthermore, they concluded that this technique is more effective for heterogeneous formations rather than homogeneous ones.

Similar to Lawson and Riseberg's work, Li et al. (2008) also tested mobility control in sand packs by alternate injection of surfactant and gas. They carried out alternate

injection in both slug and drive injection phases. A blend of anionic surfactants was used in the slug. Polymer was added to the slug for foam stability, although its concentration was not enough to provide favorable mobility control. Therefore, mobility control in the experiment was provided by foam. In the slug injection phase, alternate cycles of 0.1 PV ASP formulations and 0.1 PV gas were injected. The slug was followed by the drive, which comprised of alternate cycles of 0.1 PV of gas and surfactant. A surfactant with good foaming ability was used in the drive. Almost piston like displacement of oil was observed in the experiments.

Viet et al. (2008) performed a series of experiments on carbonate rocks to study the injection strategy for foam generation. They applied several injection strategies, including conventional SAG (surfactant alternating gas), novel WAGs (water alternating gas with surfactant injected in CO_2), and novel CO_2 (continuous CO_2 injection with dissolved surfactant). The foam was generated in all injection strategies. Moreover, CO_2-dissolved surfactant injection greatly reduced gas mobility compared to conventional injection strategies, which pointed out the potential of foam as mobility control agent.

Mayank et al. (2009) systematically studied the ASG process through corefloods and provided a better understanding of some issues that include the effects of chemicals, rock type, heterogeneity; optimal design of ASG process; and the performance of ASG flooding in comparison with ASP flooding. The performance of ASG process was investigated by evaluating oil recovery, coreflood pressure response, and effluent from coreflood. They performed these coreflood experiments on sandstone and dolomite rock samples where they carried out that oil recovery was greater in dolomite samples than sandstone samples. From ASG pressure data, the pressure drop increased during slug

injection, however, it decreased as soon as the drive injection started. After continued injection, the pressure drop exhibited an increasing trend until it reached steady state pressure drop because of the trapped surfactant. Moreover, from ASG oil recovery data, there was no early breakthrough, thus demonstrating absence of viscous fingering and presence of favorable mobility control in the process. Rock permeability was not the main factor in the oil recovery variation observed in ASG corefloods comparing to these factors are slug size, surfactant type, and rock type.

Farajzadeh et al. (2009) reported an experimental study of CO_2 and N_2 foam flows in natural sandstone cores containing oil with the aid of X-ray Computed Tomography. They partially saturated the cores with oil and brine (half top) and brine only (half bottom). The CO_2 was injected either under subcritical conditions (immiscible) or under super-critical conditions (miscible), whereas N_2 injected under subcritical conditions. The foaming agent, Alpha Olefin Sulfonate (AOS) surfactant, was injected with 1-2 pores. They concluded that increasing the oil recovery when injection of AOS prior to CO_2 injection above its minimum miscibility pressure (MMP) compared to below MMP CO_2. This is due to the fact that the presence of oil does not allow formation of foam in the porous medium. They also observed that it is possible to reduce the mobility of sub- and super-critical CO_2 when there is no oil present. Moreover, they found that N_2 can form weak foam zone in the presence of oil, ahead of which an oil bank moves towards the outlet of the porous medium. In this case, foaming of the gas enhances the oil recovery compared to gas injection.

Also Mayank et al. (2010) conducted a study on the performance of ASG process using carbonate cores. Many parameters in ASG corefloods were studied to show the level of

mobility control achieved by co-injecting gas and liquid during slug and drive injection. By evaluating oil recovery, pressure response, and gas and surfactant breakthrough times, they investigated the effectiveness of ASG process in the carbonate corefloods. First of all, they conducted ASG corefloods on high, medium, and low permeability carbonate cores. They found that the pressure drop increased in slug injection in three cores due to mobilization of trapped oil. On the other hand, the pressure drop increased in drive injection due to the increase in foam propagation in the cores except the lower permeability where the pressure drop decreased because of the weak foam. From the production data, it was indicated that the displacement of mobilized oil was most efficient in high permeability ASG coreflood, as the size of oil bank was largest in that coreflood. Furthermore, another parameter was conducted to study the performance of ASG process was gas and chemical injection rate (injection foam quality). Based on pressure drop and production data from the corefloods, it can be concluded that lower gas velocity results in more stable foam and thus better foam propagation. Also, the size of chemical slug is an important factor in chemical flooding where it should be maintained in order to achieve low IFT conditions. Finally, gas and surfactant breakthrough occurred approximately at the same time if the stable displacement front and absence of gas fingering through the oil bank is achieved.

Liu et al. (2010) carried out nitrogen foam injection to control fingering of heterogeneous reservoir and enhance oil recovery rate after water flooding. They developed three sets of foam system, 0.3% foaming agent with 30 mg/L foaming stabilizer, 0.3% foaming agent with 700 mg/L foaming stabilizer, and 0.5% foaming agent with 1500 mg/L

foaming stabilizer. From evaluation experiments, they concluded that these three set were suitable for the oil reservoir with temperature of 50°C and salinity less than 10,000 mg/L.

Farajzadeh et al. (2010) and Andrianov et al. (2012) provided tangible evidence that foam could be adequately stable in the presence of oil, leading to the recovery of a significant fraction of oil remaining in the core after water flooding. This was performed by using sandstone cores were only partially saturated with oil, leaving the other part free of oil so that it could serve as a 'foam generation chamber'. It was clearly demonstrated that foam which was generated in that 'chamber' did not completely decay upon coming in contact with oil.

Hou et al. (2012) have performed systematic laboratory studies on foam flooding for highly heterogeneous conglomerate rocks. They apply nitrogen foam formulas which had good performance of foamability and stability. By using stirring method, the foamability was characterized by the initial foam volume (V_i), and the stability of bulk foam was evaluated by the time for dewater 100 ml from foam ($t_{1/2}$). At reservoir conditions (T = 28.7°C, P = 9.4 MPa, and TDS = 9038 mg/l), many parameters such as foam injection modes and gas liquid ratio were investigated. They concluded that the direct injection of foam is better than co-injection of gas and surfactant solution.

Haugen et al. (2012) studied N_2 foam flow mechanistically in fractured, oil-wet limestone rocks. They performed many experiments on foam flow in fractured cores (obtained from the Edwards outcrop formation in west Texas) where the fractures are in contact with a porous matrix (rather than using glass or micro models). The maximum oil recovery was

obtained at very large numbers of pore volume (PV) injected, for one case (95.4 PV N_2.and 8.4 PV surfactant solution)

Simjoo et al. (2012) investigated the effects of oil on foam stability and oil recovery by foam through systematic laboratory study with the aid of X-ray Computed Tomography. Foam was generated by co-injecting nitrogen gas and either AOS or mixtures of AOS and a polymeric fluorocarbon (FC) esther at a fixed foam quality of 91% into water-flooded Bentheimer sandstone cores. It was noted that two main oil displacement regimes, the first oil recovery arises from the formation of an oil bank, and the second one regime corresponds to oil displacement as a dispersed phase that is transported by foam lamellae. Moreover, higher mobility reduction factors and longer breakthrough time, consequently a higher incremental oil recovery obtained, were obtained for foam injected under gravity stable conditions. From the 3D CT images, the mobility reduction factor (MRF) increases steeply as foam crosses consecutive core segments consistently.

2.2 Surfactants

The surfactant term is a contraction of “surface active agent”, where are chemical substances that adsorb on or concentrate at a surface or phases interface. Sulfonated hydrocarbons are the most common surfactants used in surfactant flooding. Significantly, the surfactants decrease the interfacial tension, IFT. A typical surfactant monomer consists of two portions; a head witch is the polar (hydrophilic) group, and a tail witch is the nonpolar (hydrophobic) group, Figure 2.2.

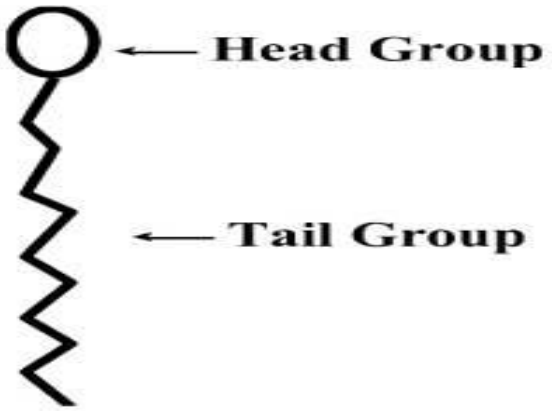

Figure 2.1 Representation of a linear surfactant molecule

2.2.1 Surfactants Classification

The ionic nature of the head group classifies the surfactants into four types namely:

Anionic. The anionic surfactant has negative charge on its head group. For instant, sodium dodecyl sulfate, SDS, ($C_{12}H_{25}SO_4^-Na^+$) which has been widely used in enhanced oil recovery (EOR) applications since it has low adsorption on rock surface (especially in sandstone reservoirs), relatively stable, and it can be produced economically.

Cationic: The cationic surfactant; for example, dodecyltrimethylammonium bromide ($C_{12}H_{25}N^+Me_3Br^-$); has positive charge on its polar moiety. Cationic surfactants are rarely used due to strong adsorption on rock surface.

Nonionic: Nonionic surfactants mainly used as cosurfactants to improve phase behavior of micro emulsion system. The role of nonionic surfactants to reduce IFT is not as good as anionic surfactants although they are more tolerant of high salinity. In addition, they do not ionize when they are dissolved in aqueous solution, and their head group is larger than the tail group. Dodecylhexaoxyethlene glycol mono ether ($C_{12}H_{25}[OCH_2CH_2]OH$) is one of the nonionic surfactants.

Amphoteric (Zwitterionic): This class of surfactants such as 3-dimethyldodecylamine propane sulfonate, contains aspects of two or more of the other classes, opposite charges, where the ionic character or the polar group depends on the pH of the solution.

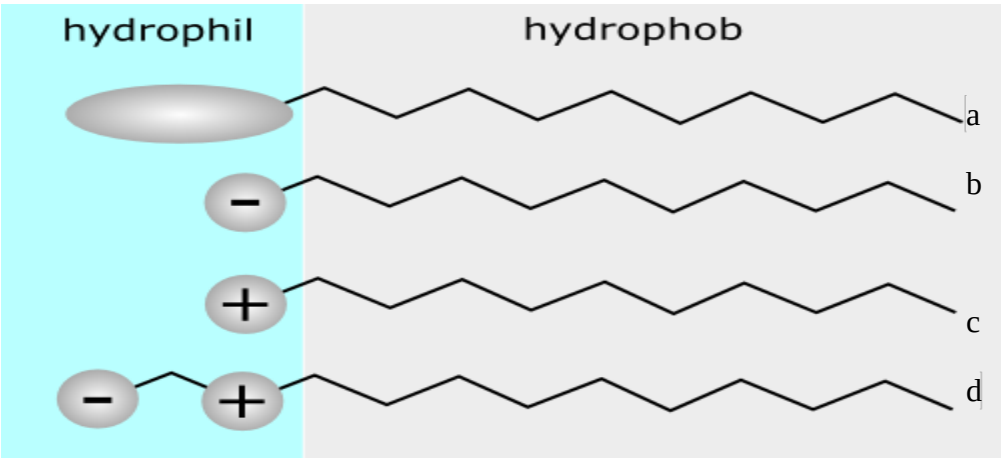

Figure 2.2 Surfactants classification, (a) nonionic, (b) Anionic, (c) Cationic, (d)Zwitterionic

2.2.2 Surfactants Characterization

Hydrophile–Lipophile Balance (HLB) is a number used to indicate the relative tendency to form water-in-oil or oil-in-water emulsions by solubilizing in oil or water. The HLB value can be used to predict the following surfactant properties (Sheng 2011):

Table 2.1 Surfactant Property based on HLB

HLB	Surfactant Property
0 - 3	antifoaming agent
4 - 6	W/O emulsifier
7 - 9	wetting agent
8 - 18	O/W emulsifier
13 - 15	Typical of detergents
10 - 18	A solubilizer or hydrotrope

*Critical Micelle Concentration (*CMC) *and Kraff Point.* CMC is defined as the concentration of surfactants above which micelles are spontaneously formed as presented in Figure 2.3. Before reaching the CMC, the surface tension decreases sharply with the concentration of the surfactant. After reaching the CMC, the surface tension stays more or less constant. Krafft Point or temperature is the minimum temperature at which surfactants form micelles. Below the Krafft temperature, there is no value for the critical micelle concentration; that is, micelles cannot form. For a nonionic surfactant, containing

polyoxyethylene chains, cloud point is, the temperature at which phase separation occurs, thus becoming cloudy.

Solubilization Ratio. Solubilization ratio for oil or water is defined as the ratio of the solubilized oil or water volume to the surfactant volume in the micro emulsion phase. Solubilization ratio is closely related to IFT, as formulated by Huh (1979). When the solubilization ratio for oil is equal to that for water, the IFT reaches its minimum.

$$SR_o = {}^{V_o}/_{V_s} = \frac{volume\ of\ oil\ in\ microemulsion\ phase}{volume\ of\ surfactant\ in\ microemulsion\ phase} \quad (2.\ 1)$$

$$SR_w = {}^{V_w}/_{V_s} = \frac{volume\ of\ water\ in\ microemulsion\ phase}{volume\ of\ surfactant\ in\ microemulsion\ phase} \quad (2.2)$$

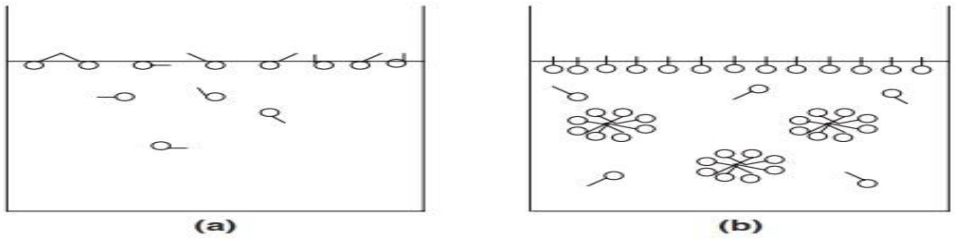

Figure 2.3 Distribution of surfactant molecules in solution at concentrations (a) below and (b) above CMC

2.2.3 Phase behavior of Micro Emulsions

The phase behavior of micro emulsions is a complex system and dependent on a number of parameters. These parameters are the types and concentrations of the surfactants, cosurfactants, hydrocarbons, brine, and temperature and pressure.

Brine salinity has a significant effect on phase behavior where increasing the salinity of an aqueous phase decreases the solubility of an ionic surfactant. According to the terminology of Windsor, the micro emulsions classified to three types based on salinity changes, as following:

- *Windsor Type I Behavior*. This type (oil-in-water micro emulsion) formed at low salinity where surfactant stays in the aqueous phase. Thereby, it is difficult to achieve ultra-low interfacial tensions
- *Windsor Type II Behavior*. This type (water-in-oil microemulsion) formed at high salinity where surfactant lost to the oil and observed as surfactant retention.
- *Windsor Type III Behavior*. This type (Separate micro emulsion) formed as bi-continuous layers of water and dissolved hydrocarbons at optimum salinity. In this form an ultra-low interfacial tensions ~ 0.001 dynes/cm achieves and it is desirable for EOR.

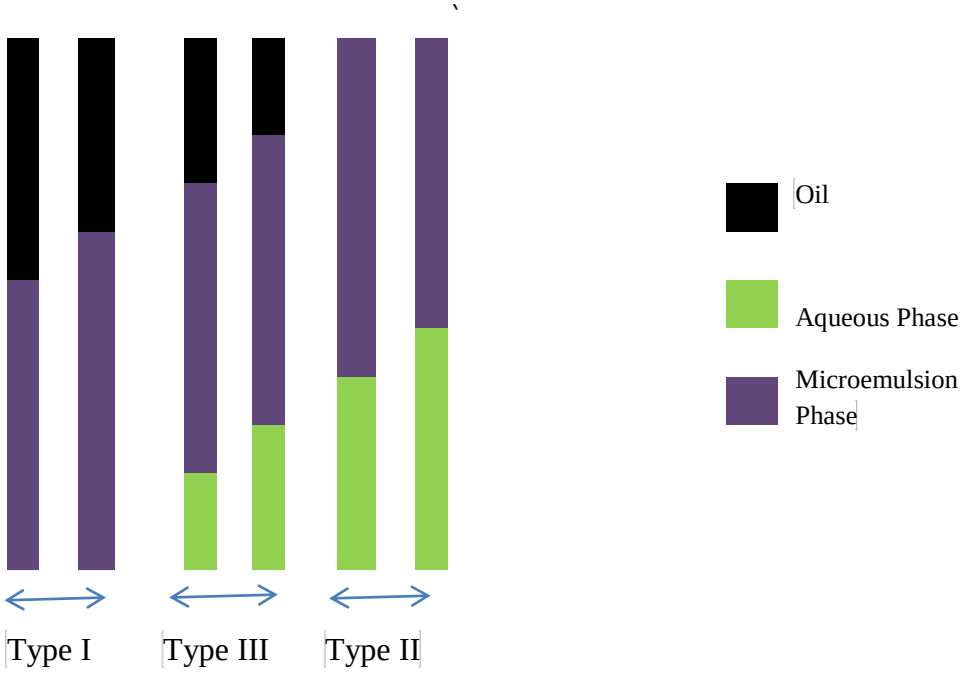

Figure 2.4 Phase behavior of microemulsions

2.3 Alkaline

Generally, the alkaline are chemically defined by Bronsted-Lowery as substances that are able to accept hydrogen ions from other chemicals,. Many alkalis are used in chemical EOR applications such as sodium hydroxide (NaOH), sodium carbonate (Na_2CO_3) and sodium metaborate (Na_2B_2O).

The use of alkali achieves many functions such as reducing the adsorption of anionic surfactants (Wesson and Harwell, 2000), and sequester divalent cations. In additions, the soap can be generated in-situ due to the reaction of alkali and naphthenic acid in reactive crude oil. Moreover, the use of alkali is very important in making an effective EOR process for fractured oil-wet reservoirs where the alkali has ability of changing rock wettability [24] (Nguyen, 2010).

2.4 Limestone Rocks

Limestone is a sedimentary rock composed primarily of calcium carbonate ($CaCO_3$) in the form of the mineral calcite. It most commonly forms in clear, warm, shallow marine waters or through evaporation. It is usually an organic sedimentary rock that forms from the accumulation shell, coral, algal and fecal debris. Some limestone rocks can form by direct precipitation of calcium carbonate from marine or fresh water. Limestone rocks formed this way are chemical sedimentary rocks. They are thought to be less abundant than biological limestone. There are many different names, based upon their appearance or their composition and other factors, used for limestone such as chalk, coquina, fossiliferous limestone, lithographic limestone, oolitic limestone, and travertine.

2.5 Fundamentals and Concepts of Foam Flooding

As mention in chapter 1, foam in porous media as “a dispersion of a gas in a liquid such that the liquid phase is continuous (i.e. connected) and at least some part of the gas phase is made discontinuous by thin liquid films called lamellae.

2.5.1 Foam Generation Mechanisms

2.5.1.1 Capillary snap-off

Capillary snap-off can repeatedly occur during multiphase flow in porous media regardless of the presence or absence of surfactant, Figure 2.5. It is recognized as a mechanical process. In the presence of surfactant, three sets of capillary snap – off exist, depending upon the liquid saturation and the pore-body to pore-throat aspect ratio (Chambers and Radke, 1991). These categories are pre-neck snap–off, rectilinear snap–off, and neck snap – off (or roof snap–off)

2.5.1.2 Lamella division

This mechanism contains the breaking-up of a bubble into two smaller ones when stretching around a branch point of a flow channel, Figure 2.6. The most important factors that govern lamella division are the pressure gradient, pore geometry and bubble size[9] (Yan, 2006).

2.5.1.3 Leave-behind

The left behind mechanism formed when two gas fingers invade adjacent liquid-filled pore bodies Figure 2.7. First, a lens is left behind as two menisci converge downstream

and the lens may drain to a thin film (lamella) later (Owete and Brigham, 1987). Leave-behind mechanism can generate weak foam compared to snap-off and lamella division where they can generate strong foam.

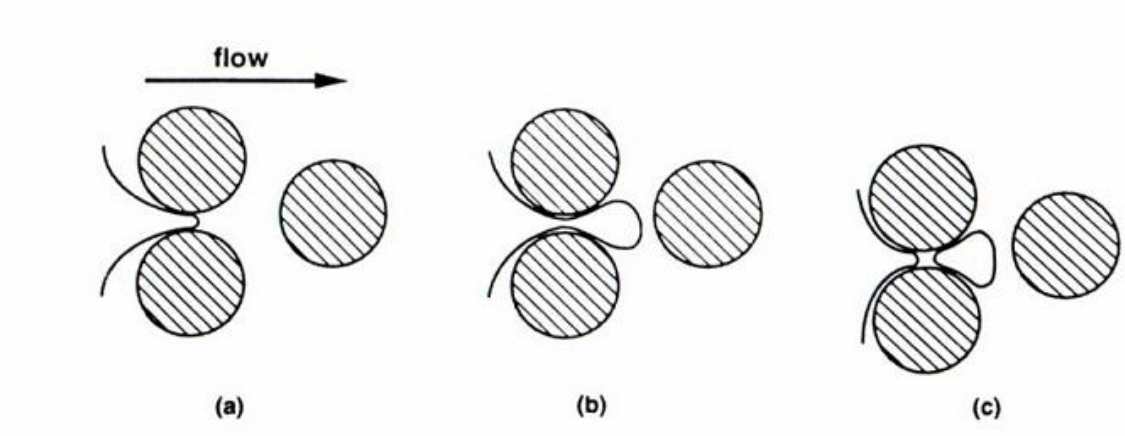

Figure 2.5 Schematic of capillary snap-off mechanism, (Yan, 2006)

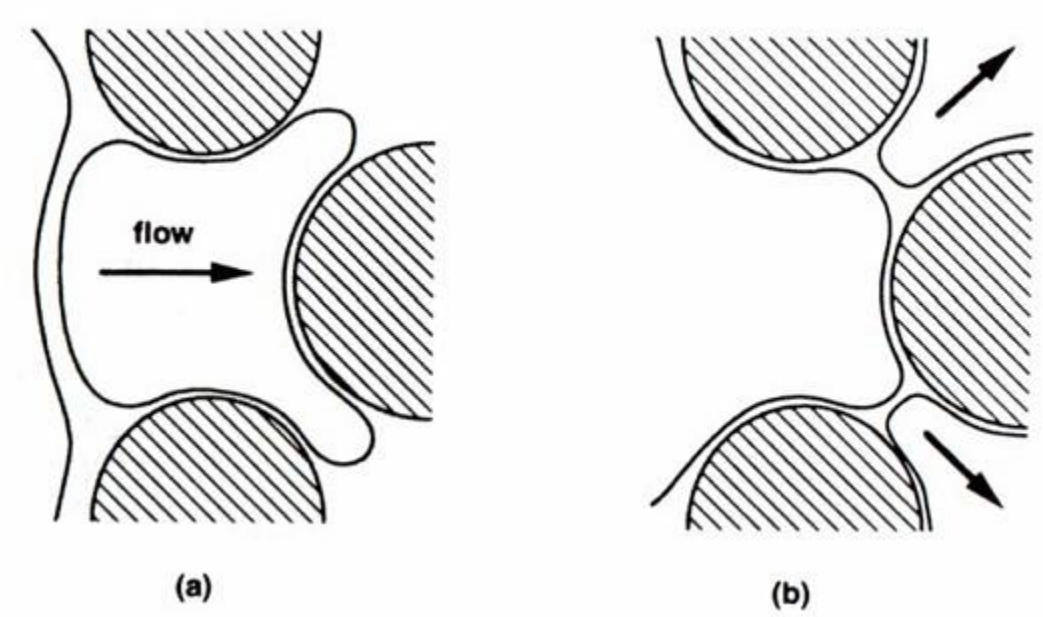

Figure 2.6 Schematic of lamella division mechanism, (Yan, 2006)

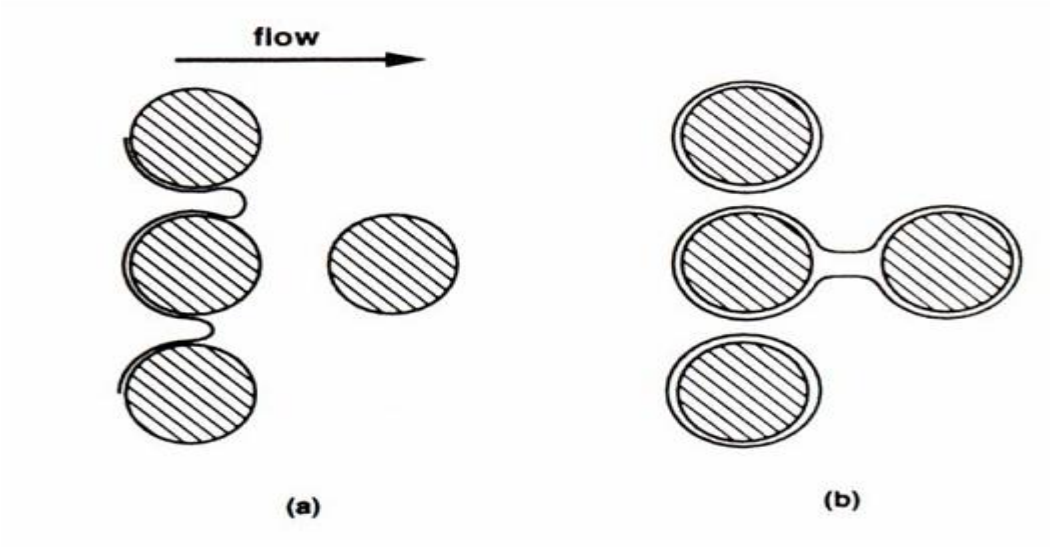

Figure 2.7 Schematic of leave-behind mechanism, (Yan, 2006)

2.5.2 Classification of Foam

2.5.2.1 Bulk Foam

The bulk foam formed when the characteristic length scale of the pore space is much greater than the size of individual foam bubbles (Yan, 2006)[9]. Bulk foam can be treated a single homogeneous phase where the velocities of gas and liquid phases are considered similar since bubbles in bulk foam are relatively small compared to flow channel (Calvert, 1989). When the gas fraction is low, the bulk foam is "spherical foam" which consists of well-separated, spherical bubbles. When the gas fraction is high, the bulk foam is called the half-life time of bulk foam is sometimes used to evaluate the forming ability of surfactants

2.5.2.2 Foam in Porous Media

In contrast, foam in porous media is characterized by the distribution of pore size and pore throat (Yan, 2006). According to Ettinger and Radke (1992), an individual bubble occupies one or several pores, thus foam does not behave as a continuous and homogeneous phase within porous media. In fact, foam in porous media is a discontinuous phase in which gas are separated from each other by lamella.

2.5.3 Foam Properties

2.5.3.1 Foam Quality

The quality of foam represents the gas volume in the foam and it is expressed in coreflood experiment as:

$$Foam\ quality\ (\%) = \frac{Foam\ quality\ (\%)}{Foam\ quality\ (\%) + Foam\ quality\ (\%)} \times 100 \qquad (2.3)$$

The foam is classified based on foam quality to either too wet (foam quality < 25%) or too dry (foam quality > 98%) (Srivastava et al, 2009). In addition, Bullen et al. (1975) stated that mobility reduction cannot be accomplished at low (<40%) or extreme high quality (>95%) since foams are unstable at these conditions.

2.5.3.2 Texture

Foam texture can be described in bubble size where it is one of parameters influencing stability of foam. The foam with narrow bubble size distribution (40-90 μm) is more stable compared to wide size distribution (28-205 μm) (Friedman and Jensen, 1986). Also the foam texture can be termed of average bubble radius (or diameter) or a distribution of radii (Stenuf et al., 1953). When average bubble diameter is much smaller than the pores diameter, foam flow as dispersed bubbles in pore channels. However, if average bubble size is much larger than pores diameter, foam flow as progression of films separating individual bubbles (Lake, 1989). As a result, foam can be trapped in small pore channels where low capillary pressure or pressure gradient occurs.

In general, foam texture depends on type and concentration of surfactants, pore geometry, pressure, and foam quality.

2.5.3.3 Rheology

Foam rheology studies showed that foams are frequently pseudo plastic, which means foam has shear-dependent viscosity, or shear thinning properties. Thus foam apparent viscosity is measured instead of true foam viscosity. Results have shown that foam apparent viscosity decreases with increasing shear-rate and with decreasing foam quality (Marsden, 1964).

2.5.4 Effect of Foam on Gas and Liquid Mobilities

In the presence of foams in porous media, gas mobility can be reduced drastically with two different mechanisms. The first one is where stationary lamellae traps the gas and makes it immobilized by decreasing gas relative permeability. Moreover, in the second mechanism, the moving lamellae cause a resistance to gas flow due to increasing gas apparent viscosity, Figure 2.8. On the other hand, in the presence of foam there is no effect in a liquid relative permeability by neither gas saturation nor the foaming agent, (Bernard et al, 1965).

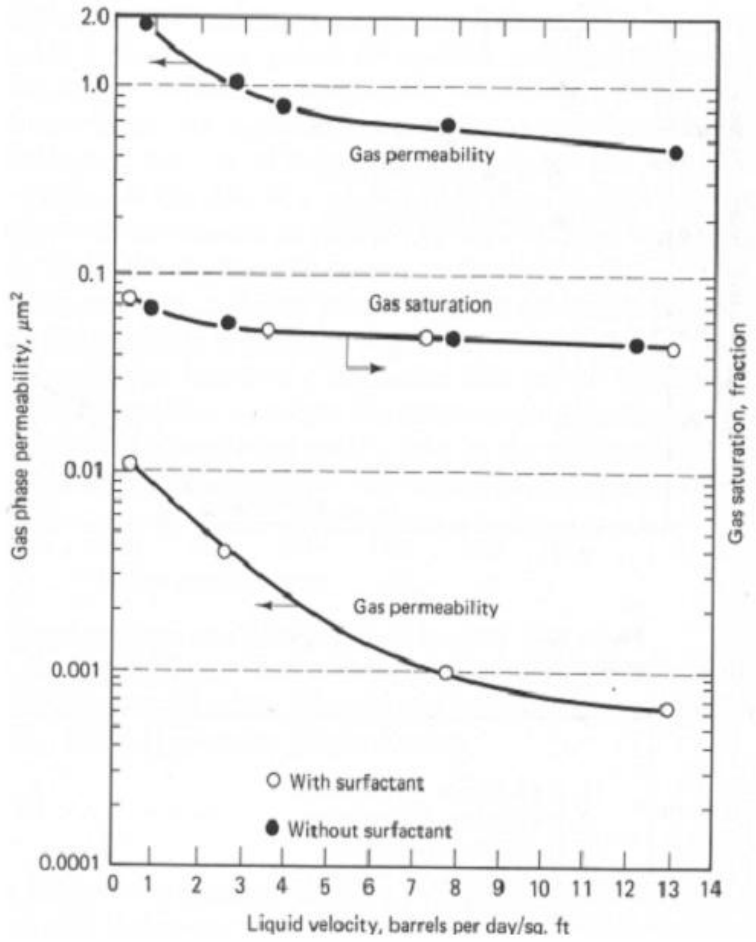

Figure 2.8 Effect of liquid rate and gas saturation on gas permeability with and without surfactant (Bernard and Holm, 1964)

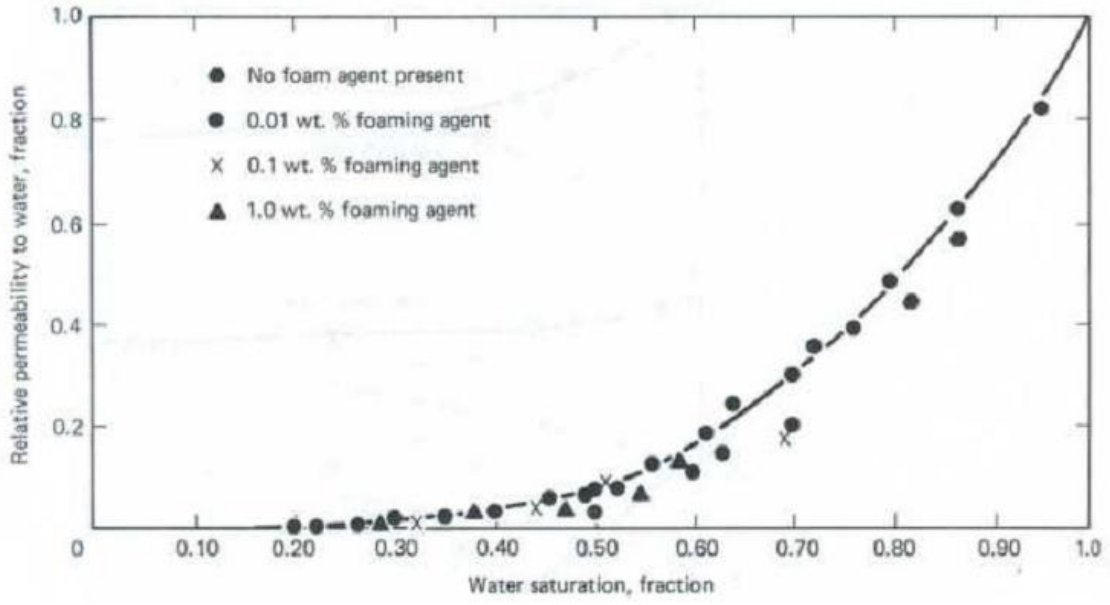

Figure 2.9 Effect of foam on liquid relative permeability (Bernard et al., 1965)

2.5.5 Foam Stability

Foam stability test is considerable as an initial indicator of surfactant's ability to provide stability to foam. However, in porous media, the actual ability of surfactant may differ from the results of foam stability tests due to adsorption, presence of capillary forces, foam interactions with micro-emulsions.

The foam stability mechanisms can be understood based on the structure and stability of liquid films (lamellae). The more stable the lamellae, the more stable the foam. However, destruction of lamellae leads to foam coalescence. The parameters that govern lamellae destruction are film drainage, gas diffusion, oil effect, surfactant concentration temperature (Yan, 2006).

The main mechanisms that manage the film drainage are gravity that usually observed in thick lamellae and capillary drainage due to capillary pressure (or suction at Plateau borders), (Rossen, 2004). In addition, gas diffusion is generated from the trapped bubbles in porous media. Oil has opposite effects on foam stability where adsorption of surfactant into oil phases cause the liquid depletion in lamellae. Also, foam generation is hard when rock wettability is changed by oil.

CHAPTER 3

RESEARCH METHODLOGY

3.1 Materials

3.1.1 Limestone Samples

Two limestone core plugs obtained from Indiana limestone cores. The plugs were named as IL-005 and IL-013. Both samples IL-005 IL-013 have length of 25.336 cm and 25.401 cm, and diameter of 3.709 cm and 3.733 cm, respectively. The porosity of the cores was measured by mass balance method where the plugs were subjected under 2000 psi to fully saturate by brine of 21,600 ppm (reservoir brine). The properties of each plug are shown in Table 3.1

Table 3.1 Limestone core plugs properties

The property	Sample IL-005	Sample IL-013
Length, L,(cm)	25.336	25.401
Diameter, d, (cm)	3.709	3.733
Porosity, ϕ, %	19.28	12.0

Figure 3.1 Limestone core plugs

3.1.2 Synthetic Brine

Two types of brine were used in the experiments, hard brine and soft brine. The composition of hard brine is shown in Table 3.2. In addition, composition of the soft brine that used in phase behavior test with different concentrations is presented in Table 3.3.

Table 3.2 Brine Composition

The salt	Composition, ppm
NaCl	16,700
$CaCl_2$	1,280
$MgCl_2$	3,620
Total Dissolve Solids (TDS)	21,600

Table 3.3 Soft Brine (NaCl)

Sample No.	NaCl (ppm)	NaCl (%wt)
1	4000	0.4
2	8000	0.8
3	12000	1.2
4	16000	1.6
5	20000	2
6	24000	2.4
7	28000	2.8
8	32000	3.2
9	36000	3.6
10	40000	4

3.1.3 Dead Oil

The crude oil used in this study is from one of the field in Saudi Arabia. The composition of the oil is shown Table 3.4

Table 3.4 Dead Oil Components

Components	Mole%
C5	3.30
C6	6.64
C7	12.47
C8	19.00
C9	21.37
C10	16.92
C11	9.03
C12+	11.26
Total	100

3.1.4 Surfactants

Five sets of surfactants were used in this project. The product names are Capston FS-50, Capston FS-51, Capston FS-61 fluorosurfactant from DuPont, Tergitol NP-9 from Dow Chemical Company, and Triton X-100 from and Segma-Aldrich. The Characteristics of these products are shown in Appendix C.

3.2 Phase Behavior Tests

3.2.1 Concentration of surfactant in foam solution

Two approaches were applied to determine the favorable concentration of each surfactant. The first approach; aqueous stability test, is to investigate of the solubility and

stability of surfactant mixture in electrolyte solution by changing the salinity. The second one was the evaluating of the stability of bulk foam to determine the concentration of each surfactant.

3.2.1.1 Aqueous stability test

This test is to investigate the solubility as well as stability of surfactant mixture in electrolyte solution, at different salinities encountered during corefloods and phase behavior. As previously mention 3.1.4, the surfactants that were selected in this study were Capston FS-50, Capston FS-51, Capston FS-61, Tergitol NP-9, and Triton X-100 and tested for aqueous stability test. The procedures of the experiment included the following steps:

1. The salinity of hard brine was changed by adding different amounts of sodium chloride solution to the base brine (4,900 ppm), as well as, the salinity of soft brine was changed by adding different amount of sodium chloride, Table 3.3.
2. Different concentrations of each surfactant were mixed with brine (2 ml of surfactant solutions in plexiglass bottle, Figure 3.2, to see the stability of the solution.
3. Each plexiglass bottle was shaken by using Multi-Wrist Shaker, to test the foamability and settle for one hour (at room temperature), see Figure 3.2.

Figure 3.2 Stability test using Triton X-100 as foam agent

3.2.1.2 Stability of bulk foam test

Four sets of surfactants were tested as foaming agent in this study, Capston FS-50, Capston FS-51, Tergitol NP-9 and Triton X-100 surfactants. By stirring method with Mammonlex Blender (Figure 3.3), the stability of bulk foam was measured to determine the concentration of each surfactant. 200 ml surfactant solutions were prepared with different concentrations (0.1 %wt to 1 %wt) and 21,600 ppm hard brine. After foam generation, the stability of bulk foam was characterized by the initial foam volume (V_i) and the time for dewater 100 ml from foam ($t_{1/2}$). Higher initial foam volume and half-time for dewater indicate favorable foamability and stability of examined bulk foam system. Thereby, from this evaluation, the concentration that provides higher initial foam volume and half-time for dewater was selected as favorable concentration of each surfactant and used in the following experiments.

3.2.2 Phase Behavior Tests

Phase behavior tests include the aqueous stability test, salinity scan, and oil scan. The objective of aqueous stability test is to investigate the solubility and stability of surfactant mixture in electrolyte solution. In addition, both salinity scan and oil scan are applied to determine the optimal salinity, where the highest solublization ratios was observed in the optimal salinity.

Phase behavior tests or pipette tests were conducted in 5 ml-glass pipettes with inner diameter of 0.581 cm and 0.05 ml markings. The pipettes were sealed by plastic rubber from the bottom and covered by the plastic rubber from the top as well.

Figure 3.3 Stability of bulk foam test of 1 %wt Tergitol NP-9

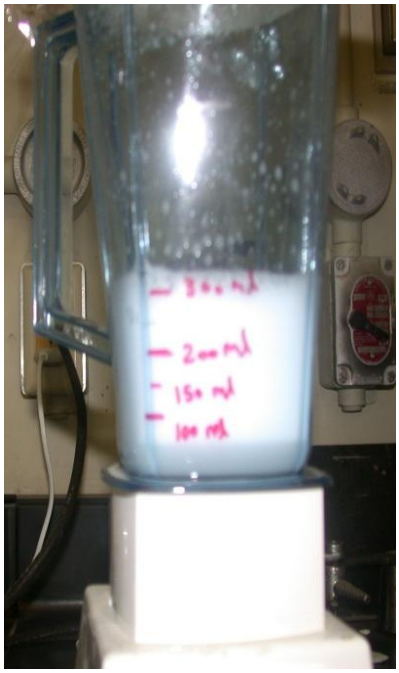

Figure 3.4 Stability of bulk foam test of 0.1 %wt Tergitol NP-9

Figure 3.5 Phase behavior test by using pipette tests

3.3 Core Flooding Approach

From the core flooding results, we studied the performance of the foam flooding (alternating of N_2 gas and surfactant) with nitrogen (N_2) as mobility controller in limestone carbonate rocks. The success of the process was determined by evaluation of oil recovery, coreflood pressure response and effluent from coreflood experiments. We studied the effect of the permeability, adding alkaline, and type of surfactants on the performance of the ASG process. Four experimental flooding (ASG1, ASG2, ASG3, and ASG4) were conducted to study the effect of these parameters. The experiments were performed on fixed parameters such as temperature of 60^0C, back pressure of 1050 psi, flow rate of 0.1 ml/min, and injected brine of 21,600 ppm. The description and the details of the other parameters will be illustrated in section 4.2.

3.3.1 Core Flooding Experimental Set-up

The diagram of the core flooding experimental setup is shown in Figure 3.6. A brief description of the experimental setup and its main components is given below.

High Pressure Fluid Injection System: The high pressure fluid injection system is composed of a dual cylinder positive displacement ISCO pump. This pump can inject fluids precisely at high pressure into the composite core at various flow rates. The dual cylinder pump is required for continuous flow and pump cylinders are controlled by a controller for automatic operation.

Core Holder: The stainless steel hassler core holder was used to perform various experiments. It can accommodate about 30 cm long cores and the maximum working pressure of the core holder is 10,000 psig.

Overburden Pressure (OBP) Pump: A high-pressure pump manufactured by BECKMAN is used to apply and maintain required overburden pressure (OBP) on the core holder.

Back Pressure Regulator: A dome shaped back pressure regulator was employed to apply and control the back pressure. Nitrogen was used as a medium for back pressure application.

Oil and Gas Measurement System: The produced fluids were passed through an oil and gas separator at atmospheric conditions. The oil and gas were separated under gravity in the separator and gas produced was passed through the gas meter.

Accumulators: Three one liter accumulators were used for dead oil, brine, and surfactant solution.

Nitrogen supply: One cylinder for nitrogen with maximum pressure 2000 psig connected to the system flooding through mass flow controller.

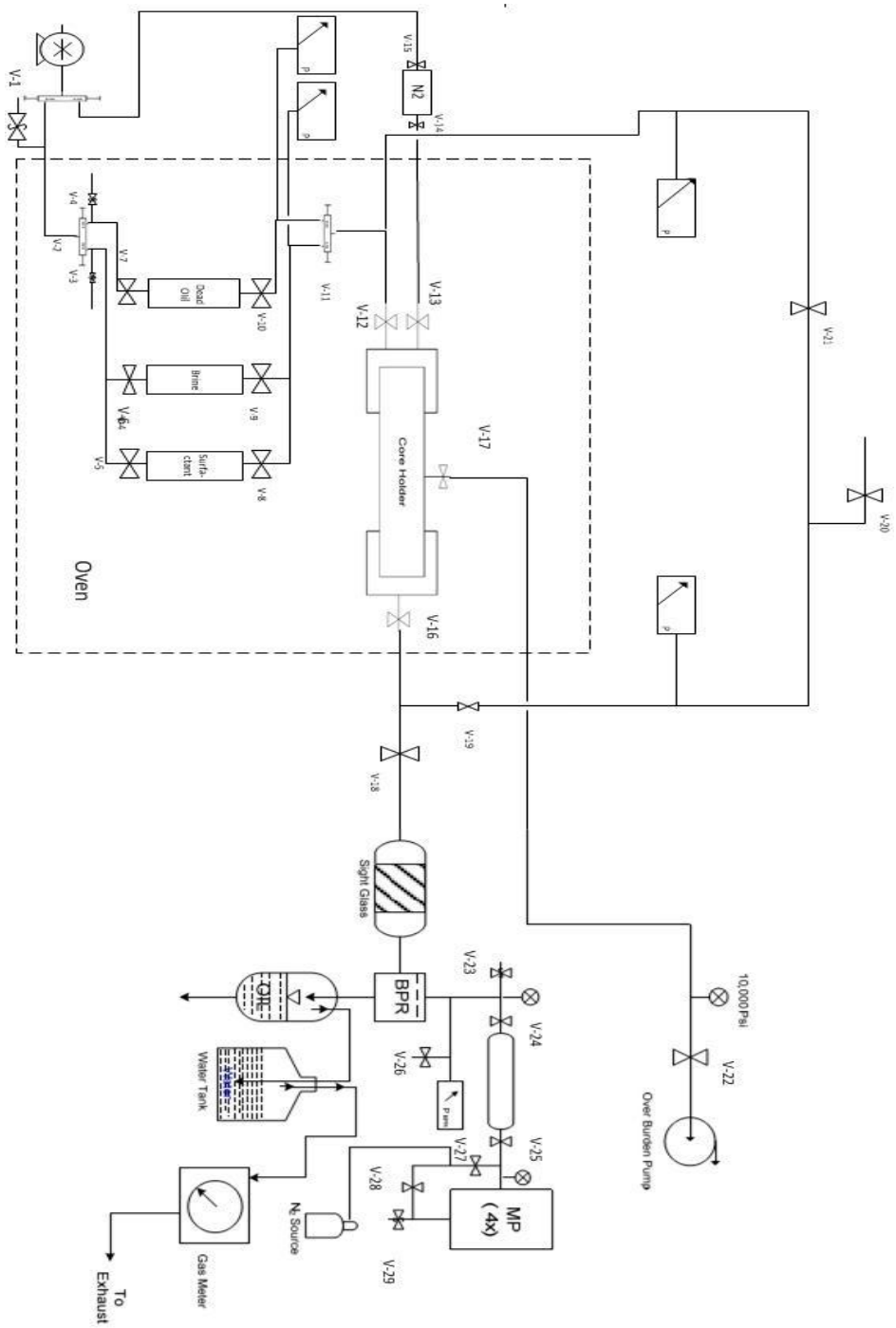

Figure 3.6 diagram of the core flooding experiment

3.3.2 Core Flooding Experimental Procedure

3.3.2.1 Core Samples Preparation and Loading

The core samples were from Indiana field, see 3.1.1. The plugs were cleaned and dried in a vacuum oven. We recorded the dry weights core samples and effective porosity was measured after saturating the core by brine using mass balance method. Then the cores were loaded in the flooding setup and we started flooding.

$$PV = \frac{M_{sat.} - M_{dry}}{\rho_{brine}} \quad (3.1)$$

$$\phi = \frac{\text{interconnected PV}}{V_{bulk}} = \frac{PV}{\pi D^2 L/4} \quad (3.2)$$

Where:

PV= Pore volume of the core, cm^3

$M_{sat.}$ =Weight of the saturated core by brine, gm

M_{dry}= Weight of the dry core, gm

ρ_{brine} = Density of the core, gm/ cm^3

V_{bulk}= Bulk volume of the core, cm^3

D = Core diameter, cm

L = Core length, cm

3.3.2.2 Brine Flooding

We started flooding with brine of compositions similar to reservoir brine, Table 3.2. The core is injected at different rates while recording pressure drop along the core and collecting fluid at effluent. From this procedure, we determined absolute permeability to brine of the core using Darcy's law by injecting at different rates and recording steady pressure of each rate

$$k_{abs}=\frac{Q\mu_{brine}L}{A\Delta P}=\frac{Q\mu_{brine}L}{\pi\left(D^2/_4\right)\Delta P} \quad (3.3)$$

Where:

K_{abs} = absolute permeability (Darcy)

Q= brine rate (cm^3/sec)

μ_{brine} = brine viscosity (cP)

ΔP= steady state pressure along the core (atm)

3.3.2.3 Oil Saturation

Crude oil was injected into the core at a fixed rate until producing 100% oil to determine initial oil saturation (S_{oi}) and oil effective permeability (k_o). The following equations were used for calculating S_{oi} and k_o:

$$S_o = \frac{V_{injected} - V_{produced}}{PV} \quad (3.4)$$

$$S_o = \frac{\Delta Q_o \mu_o L}{\pi\left(D^2/4\right)\Delta P} \quad (3.5)$$

$$k_o = \frac{Q\mu_o L}{A\Delta P} = \frac{Q\mu_o L}{\pi\left(D^2/4\right)\Delta P} \quad (3.6)$$

$$k_{ro} = \frac{k_o}{k_{abs}} \quad (3.7)$$

Where

$V_{injected}$ = Volume of oil injected into the core, cm^3

$V_{produced}$ = Volume of oil collected at effluent, cm^3

PV = Pore volume, cm^3

Q_o= Oil rate, cm^3/sec

S_o = Initial oil saturation (%)

μ_o = Oil viscosity (cP)

k_o = Effective oil permeability (md)

k_{ro} = end – point oil relative permeability (md)

3.3.2.4 Water Flooding

The same brine as in brine saturation, 21,600 ppm, was used for water flood. Brine is injected at fixed rate of 2.5 PV/day until no more oil is coming. In this step, residual oil

saturation S_{ro}, water effective permeability k_w and end – point water relative permeability k_{rw} were calculated.

$$S_{ro} = \frac{V_o - V_{produced}}{PV} \times 100 = \frac{(S_o \times PV) - V_{produced}}{PV} \times 100 = \left(S_o - \frac{V_{produced}}{PV}\right) \times 100 \quad (3.8)$$

$$k_w = \frac{Q_w \mu_{brine} L}{\pi\left(D^2/_4\right)\Delta P} \quad (3.9)$$

$$k_{rw} = \frac{k_w}{k_{abs}} \quad (3.10)$$

Where:

V_o = Initial volume of oil in the core, cm^3

$V_{produced}$ = Volume of oil produced at effluent, cm^3

PV = Pore volume, cm^3

Qw= Brine rate, cm^3/min

S_{ro} = Residual oil saturation (%)

μ_{brine} = Brine viscosity (cP)

k_w = Effective water permeability (md)

k_{rw} = End – point water relative permeability (md)

3.3.3 Foam Injection

We applied the strategy of foam injection that was alternative injection of surfactant and nitrogen as showing in Figure 3.7.

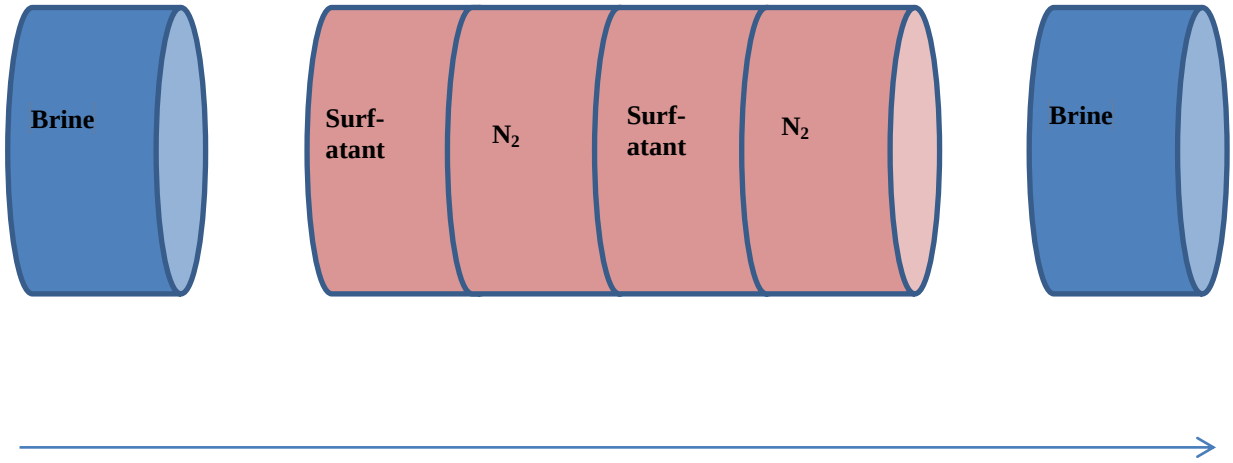

Figure 3.7 The strategy of foam injection

CHAPTER 4

RESULTS AND DISCUSION

4.1 Phase Behavior Results

From phase behavior tests, we determine the optimal salinity, where the highest oil solubilization ratios were obtained.

4.1.1 Surfactant concentration in foam

Figure 4.1 shows aqueous stability test of Capstone FS-61 Fluorosurfactant. Five different concentrations (0.01, 0.02, 0.03, 0.04, 0.05) wt% of Capstone FS-6 were prepared. Then each concentration was mixed with different salinities of hard brine where the base brine was 4,900 ppm of $CaCl_2$ and $MgCl_2$ and changing the salinity of NaCl from (4,000-40,000) ppm. Each solution in the plexiglass bottle consists of 2 ml of surfactant solution. The solutions were shaken by the Multi-Wrist Shaker for 1 hr settled for 1 hr. We observed that no foam generated, and precipitation as in Figure 4.2 with visible signs of cloudiness. We conclude that Capstone FS-61 is not soluble in brine at low concentrations of hard brine and soft brine. Thereby, this surfactant was not included in phase behavior test by adding crude oil to the aqueous solution.

The same procedure of Capstone FS-61 was conducted for Tergitol NP-9 and Triton X-100 surfactants. Ten different concentrations (0.1, 0.2…..1.0) wt% of both Tergitol NP-9 and Triton X-100 were prepared. Then, each concentration was mixed with different

salinities of hard brine where the base brine was 4,900 ppm of $CaCl_2$ and $MgCl_2$ and changing the salinity of NaCl from (4,000-40,000) ppm. The solutions were shaken by the Multi-Wrist Shaker for 1 hr and settle for 1 hr. Figure 4.4 and Figure 4.3 shows the aqueous solution test of both Tergitol NP-9 and Triton X-100 respectively. It was observed that the generated foam was strong and stable for more than 1 hr. In addition, no precipitation or visible signs of cloudiness was observed through this range of concentrations. In relation to the previous observations, Tergitol NP-9 and Triton X-100 were selected for phase behavior test by adding crude oil to the aqueous solution. The favorable concentration of both Tergitol NP-9 and Triton X-100 as foam agent was 1.0 wt%.

The aqueous test of both Capston FS-50, Capston FS-51 was conducted in the pipettes with of 5 ml volume. Six different concentrations (0.1, 0.2, 0.4, 0.6, 0.8, and 1.0) wt% of both Capston FS-50, Capston FS-51 were prepared. Then, each concentration was mixed with different salinities of hard brine of 21,600 ppm of $CaCl_2$ and $MgCl_2$ and NaCl. The solutions were shaken by hand for 3 minutes and settled for 1 hr. We noted that foam generation is strong and the foam was stable for more than 1hr. In addition, no precipitation or visible signs of cloudiness was observed through this range of concentrations. Therefore, both Capston FS-50, Capston FS-51 were selected for phase behavior test by adding crude oil to the aqueous solution.

The foam ability and the stability of four surfactants, Tergitol NP-9, Triton X-100, Capston FS-50, and Capston FS-51 will be discussed in section 4.1.2.

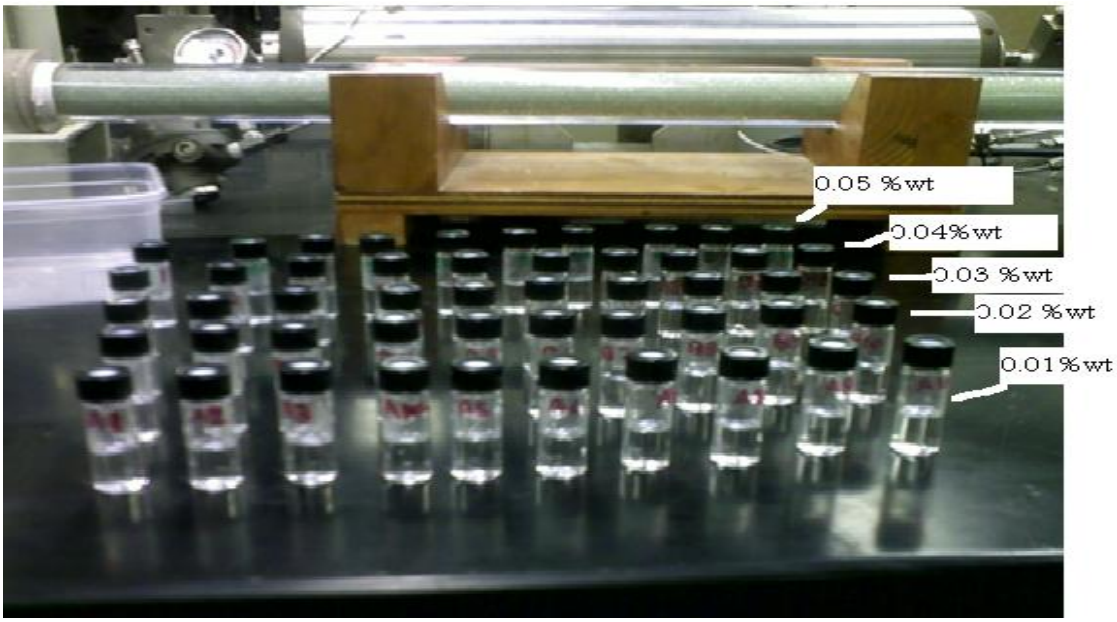

Figure 4.1 Capstone FS-61 (0.01 - 0.05 wt%) with hard brine

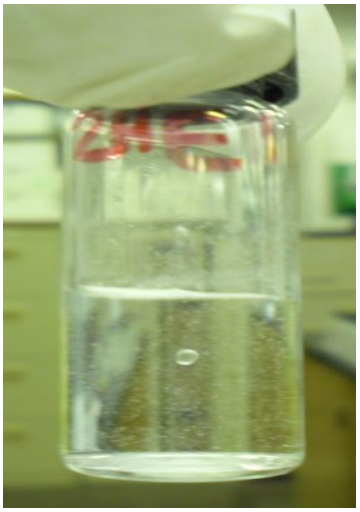

Figure 4.2 Precipitation of 0.05 wt% of Capstone FS-61 with 4,900 ppm

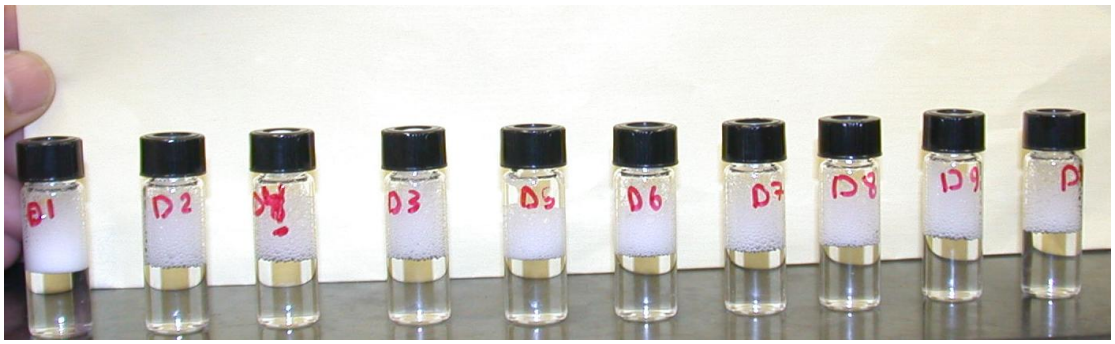

Figure 4.3 Tergitol NP-9 (0.4 wt%) with hard brine

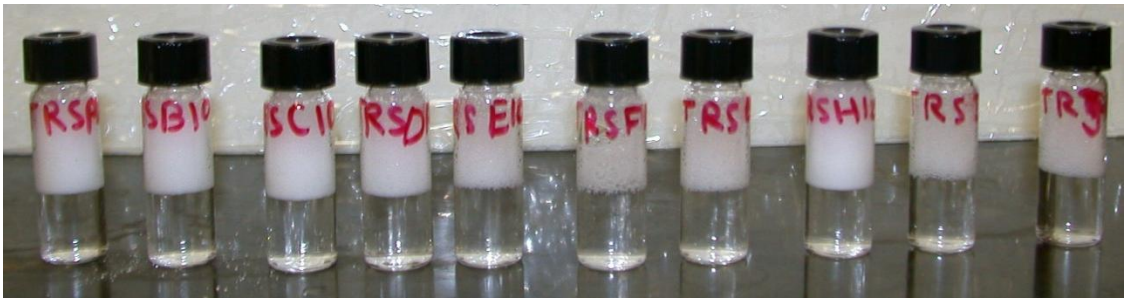

Figure 4.4 Triton X-100 (0.1 – 1 wt%) with soft brine of 40,000 ppm

4.1.2 Stability of bulk foam test

For Tergitol NP-9, Triton X-100 surfactants, the foamability and the stability of bulk foam were measured by stirring method with Mammonlex Blender, Figure 3.3. Furthermore, from this step we determined the favorable concentration of each surfactant. 200 ml surfactant solutions were prepared with different concentrations (0.1 to 1 wt%) and 21600 ppm hard brine. After foam generation, the stability of bulk foam was characterized by the initial foam volume (V_i) and the time for dewatering 100 ml from foam ($t_{1/2}$). Table 4.1 and Table 4.2 summarize the result of stirring method for both Tergitol NP-9, Triton X-100 surfactants, respectively. In addition, from Figure 4.5 and Figure 4.6 we conclude that by increasing the concentration of surfactant, foamability and the stability of bulk foam would increase. Higher initial foam volume and half-time for dewater indicated favorable foamability and stability of examined bulk foam system. Thereby, from this evaluation, the concentration that provided higher initial foam volume and half-time for dewater was selected as favorable concentration of each surfactant and used in the following experiments. We note that at 1 wt%of surfactants, foamability and the stability of bulk foam is strong.

Table 4.1 Bulk foam Stability for Tergitol NP-9

wt%	V_i, ml	$t_{1/2}$, sec
0.1	300	35
0.2	345	40
0.3	360	47
0.4	400	55
0.5	450	66
0.6	490	82
0.7	520	101
0.8	630	136
0.9	680	179
1	750	235

Table 4.2 Bulk foam stability for Triton X-100

%wt	V_i, ml	$t_{1/2}$, sec
0.1	325	49
0.2	370	59
0.3	417	73
0.4	470	89
0.5	519	105
0.6	593	130
0.7	655	163
0.8	710	205
0.9	760	240
1	820	289

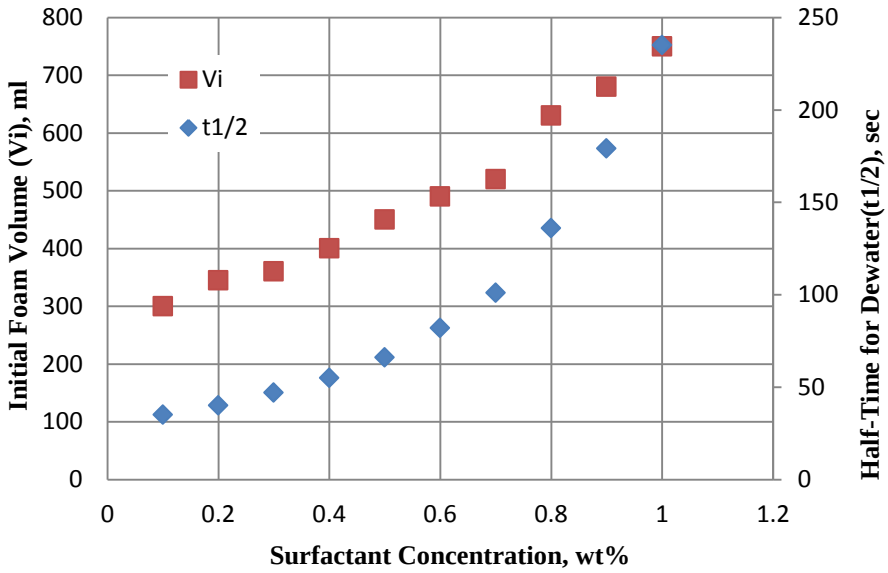

Figure 4.5 Effect of surfactant concentration on initial foam and half time for Tergitol NP-9

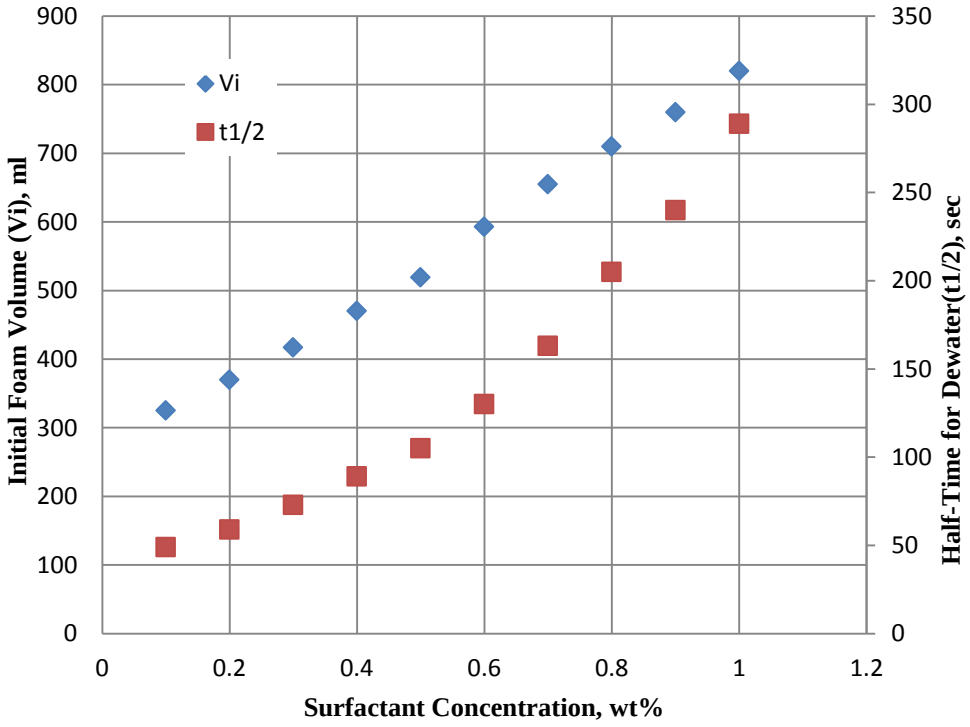

Figure 4.6 Effect of surfactant concentration on initial foam and half time for Triton X-100

For Capston FS-50, Capston FS-51, the foamability and the stability of bulk foam were conducted by pipettes of 5 ml volume. Six different concentrations (0.1, 0.2, 0.4, 0.6, 0.8, 1.0) wt% of surfactants were prepared. Then, each concentration was mixed with different salinities of hard brine of 21600 ppm of $CaCl_2$ and $MgCl_2$ and NaCl. The solutions were shaken by hand and settled for 1 hr. We determined the foamability of each type of surfactant by calculating the initial volume of foam. Foam stability was determined by calculating the half time for dewatering 1 ml of the foam, Table 4.3 and Table 4.4. Figure 4.7 and Figure 4.8 explain the foamability and the stability of bulk foam of and Capston FS-51, respectively. For Capston FS-50, It is observed from Figure 4.7 that the initial foam volume increases by increasing surfactant concentration and reach the maximum at 0.6 wt%. In addition, the foam stability increases by increasing the surfactant concentration and become constant from 0.4 to 0.8 wt%. On other hand, for Capston FS-51, Figure 4.8 shows that no clear trend of the initial foam but the maximum initial foam is at 0.6 wt%. From these figures, the optimum concentration of both Capston FS-50 and Capston FS-51 is 0.6 wt%.

Table 4.3 The foamability and the stability of bulk foam of Capston FS-50

wt%	2 ml Stock Sol., ml	ml Brine, ml	Initial Volume of Foam, V_i , cc	Half Time, $t_{1/2}$ sec
0.1	0.0071	1.99	5	87
0.2	0.0143	1.98	5.1	83
0.4	0.0287	1.97	5.2	137
0.6	0.0431	1.95	5.35	140
0.8	0.0575	1.94	5.15	140
1	0.0719	1.92	5.3	168

Table 4.4 The foamability and the stability of bulk foam of Capston FS-51

%wt	2 ml Stock Sol., ml Sol.,	ml Brine, ml	Initial Volume of Foam, V_i , ml	Half Time, $t_{1/2}$ sec
0.1	0.004673	1.995327	4.5	93
0.2	0.009346	1.990654	4.7	107
0.4	0.018692	1.981308	4	79
0.6	0.028037	1.971963	3.3	163
0.8	0.037383	1.962617	3.9	115
1	0.046729	1.953271	3.9	122

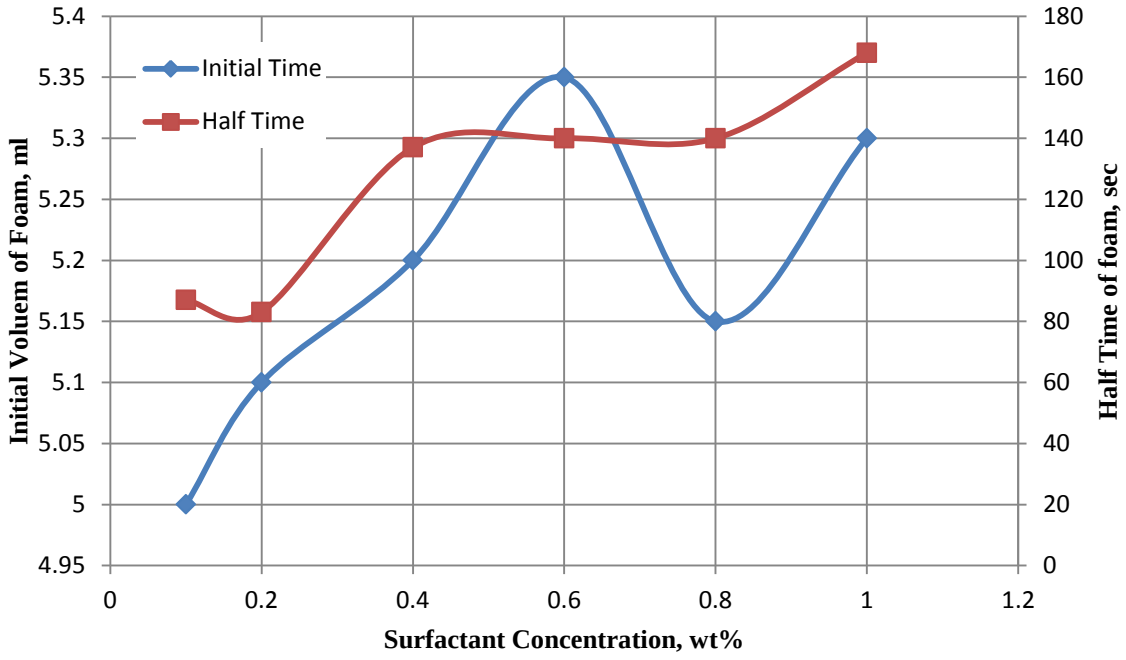

Figure 4.7 The foamability and the stability of bulk foam for Capston FS-50

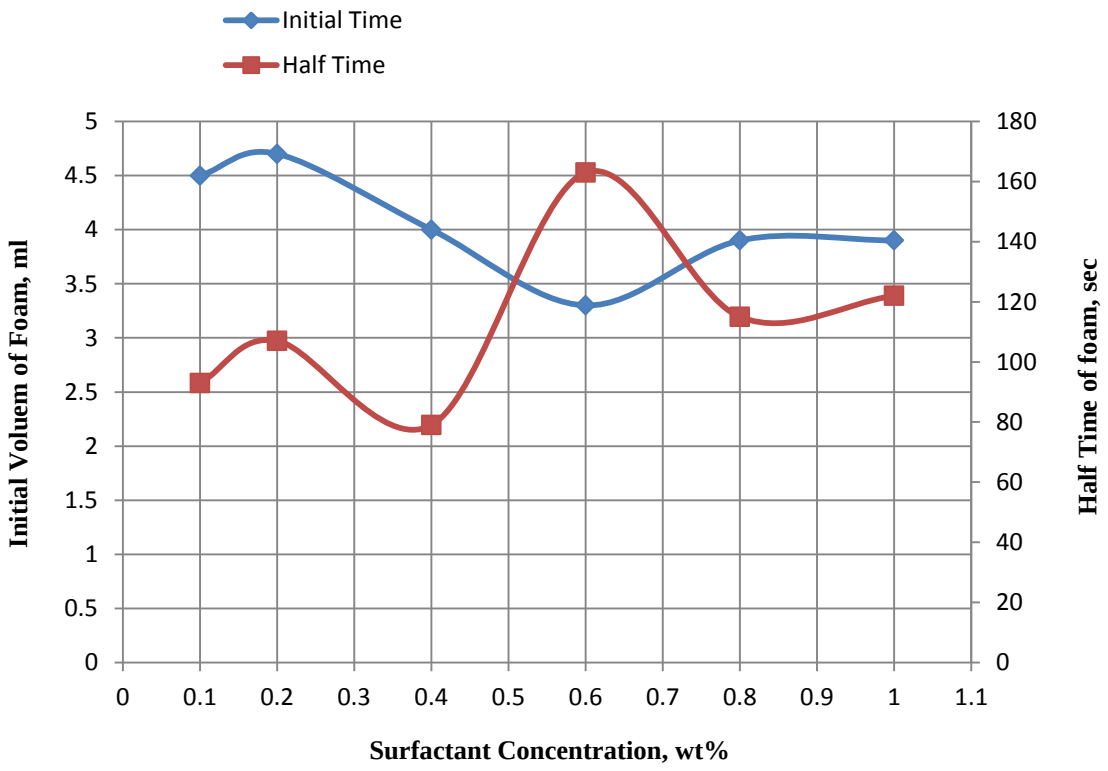

Figure 4.8 The foamability and the stability of bulk foam for Capston FS-51

4.1.3 Optimum Salinity Determination

The phase behavior test was conducted at atmospheric pressure and different temperatures (50, 60, 87, and 97°C). At 97 °C, the maximum oil solublization ratio for Tergitol NP-9 was 15.78 ml/ml while at 85 °C, the maximum oil solublization ratio in Triton X-100 was 18.518 ml/ml, Figure 4.11 and Figure 4.14, respectively. In addition, there is no clear trend of oil solublization by increasing salinity. Micro-emulsion phase behavior of both surfactants is oil-in-water micro-emulsion (Winsor Type I Behavior) because there are two phases formed (oil phase and emulsion phase), Figure 4.9 and Figure 4.13. Capston FS-51 provides good oil solublization comparing to Capston FS-50, Figure 4.15 and Figure 4.16. Figure 4.17 shows the favorable salinity with provide high oil solublization is 36,000ppm. In addition, because there are two phases formed (oil phase and emulsion phase), micro-emulsion phase behavior of both surfactants is oil-in-water micro-emulsion (Winsor Type I Behavior), Figure 4.15 and Figure 4.16.

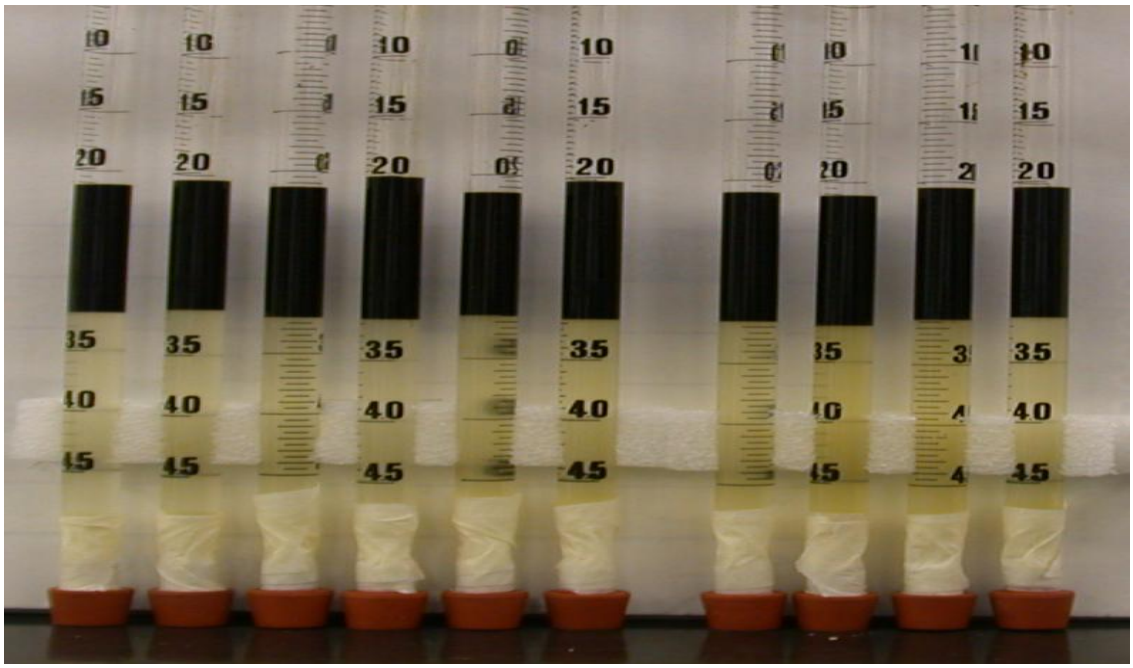

Figure 4.9 Phase behavior for Tergitol NP-9 (1 %wt) with (4,000-40,000) ppm NaCl at 25^{o}C

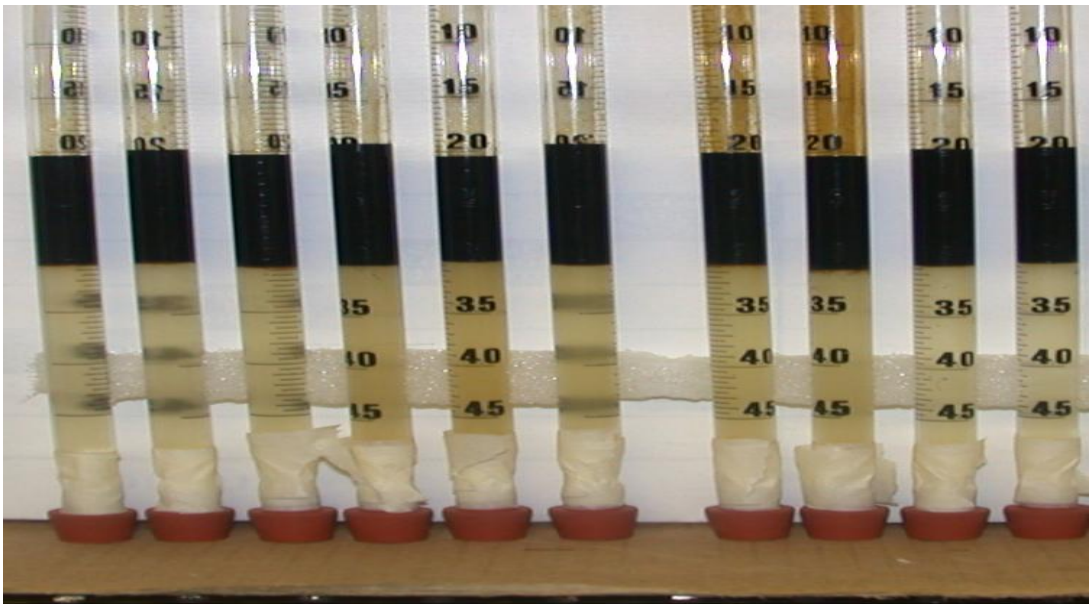

Figure 4.10 Phase behavior for Tergitol NP-9 (1 wt%) with (4,000-40,000) ppm NaCl at 97 ^{o}C

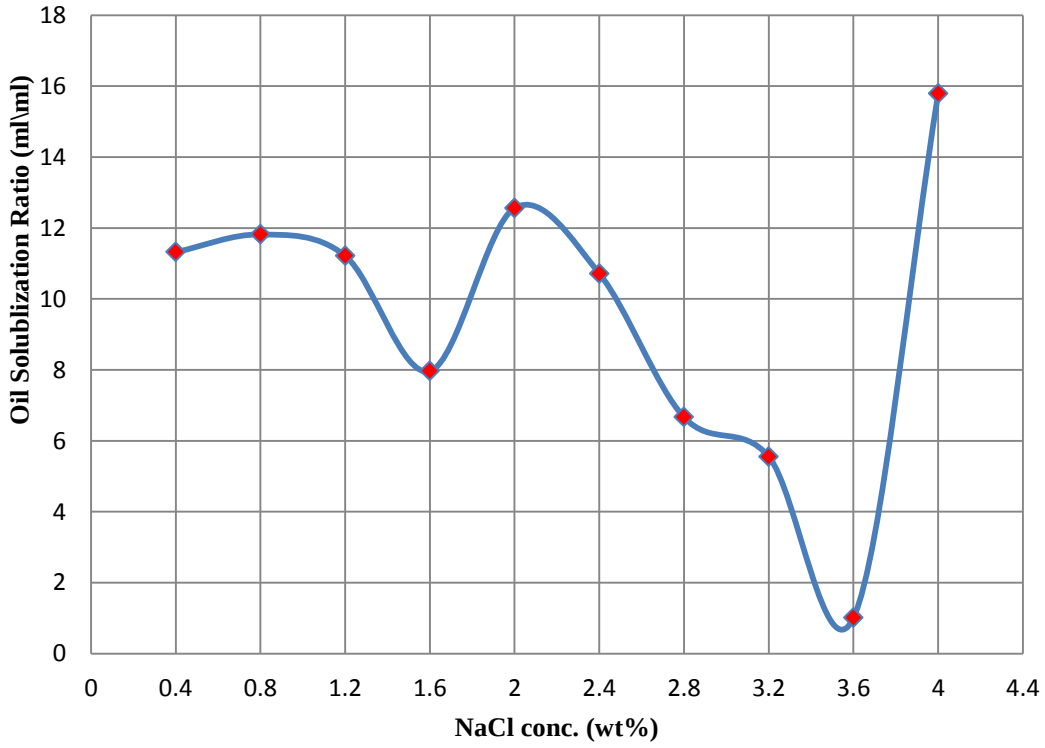

Figure 4.11 Phase behavior of Tergitol NP-9, 1 wt% at 97 ^{0}C

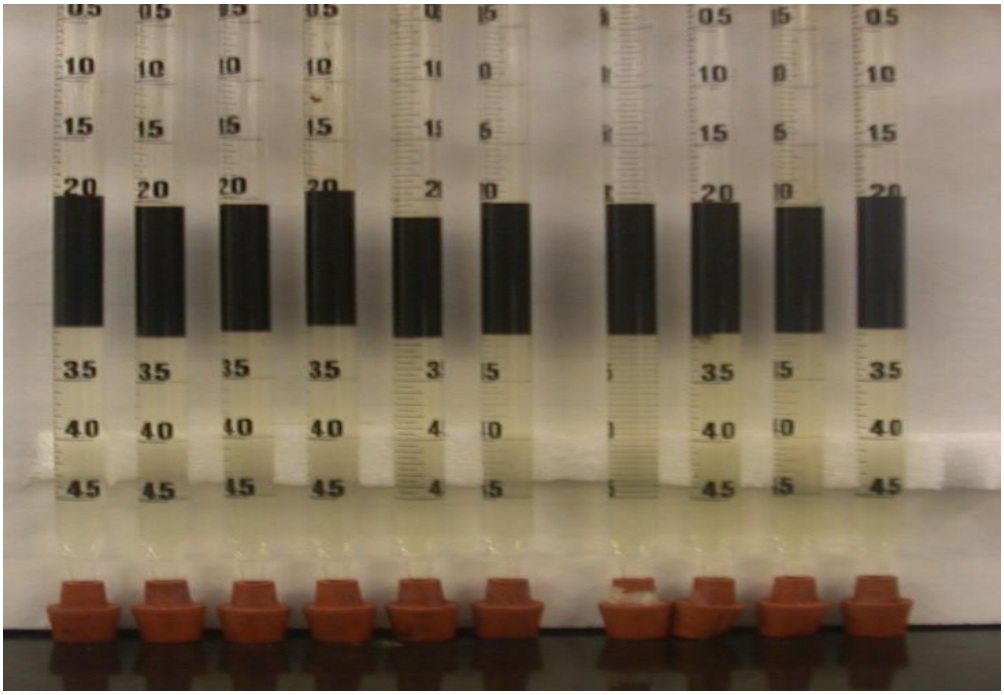

Figure 4.12 Phase behavior for Triton X-100 (1 wt%) with (4,000-40,000) ppm NaCl at 25 ^{0}C

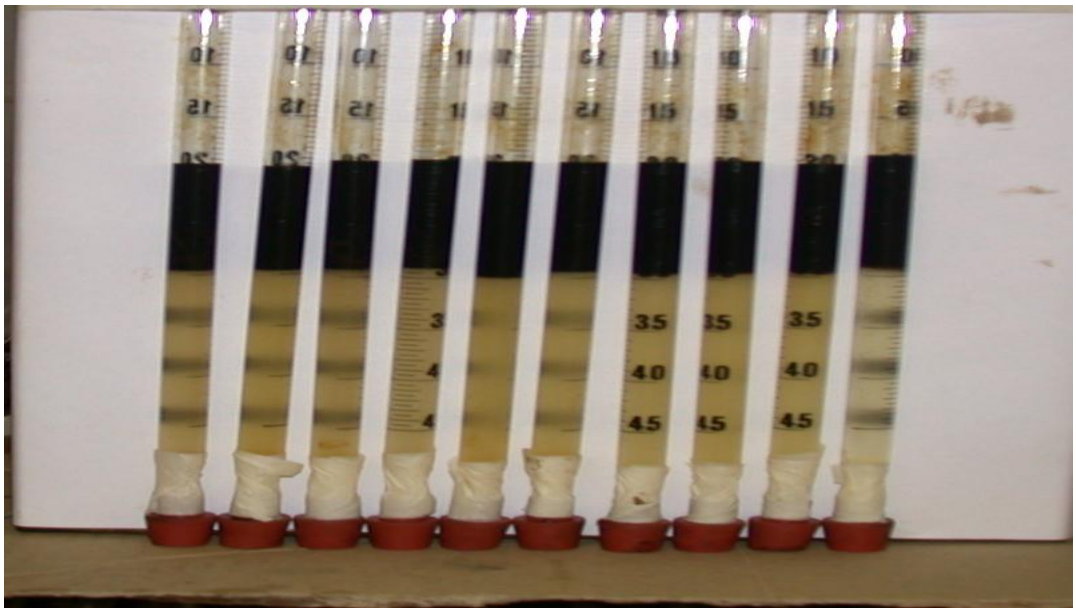

Figure 4.13 Phase behavior for Triton X-100 (1 wt%) with (4,000-40,000) ppm NaCl at 85 ^{o}C

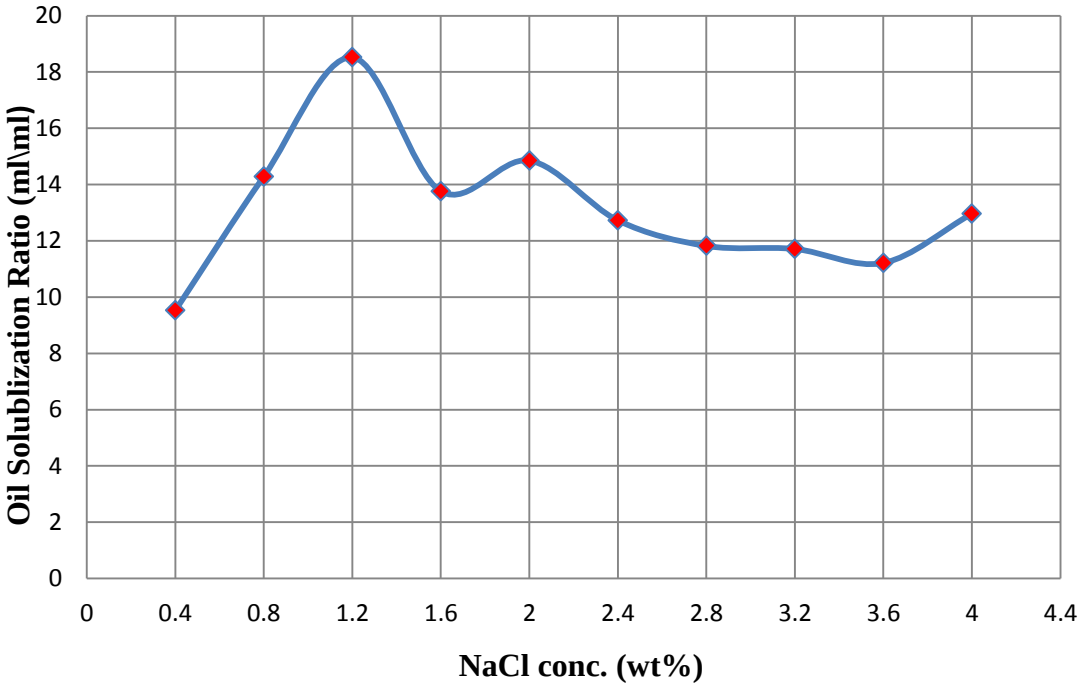

Figure 4.14 Phase behavior for Triton X-100 (1 wt%) at 85 ^{0}C

Figure 4.15 Phase behavior for Capstone FS-50 (0.6 wt%) at 60 ^{0}C

Figure 4.16 Phase behavior for Capstone FS-51 (0.6 wt%) at 60 ^{0}C

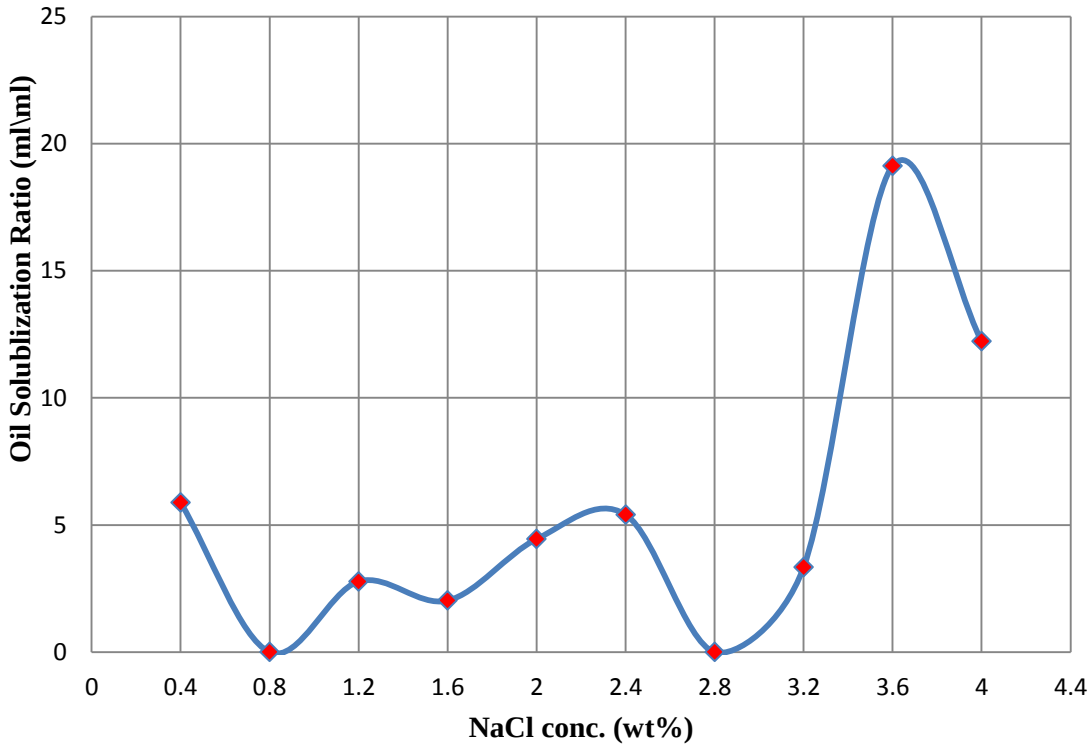

Figure 4.17 Phase behavior of Capstone FS-51(0.6 wt%) at 60 ^{o}C

4.2 Core Flooding

From the core flooding results, we studied the performance of the foam flooding (alternating of N_2 gas and surfactant) with nitrogen (N_2) as mobility controller in limestone carbonate rocks. Four experimental flooding (ASG1, ASG2, ASG3, and ASG4) were conducted to evaluate of oil recovery and coreflood pressure response, thereby, to realize the performance of the ASG process. In addition, we studied the effect of the permeability, adding alkaline, and type of surfactants on the performance of the ASG process. The experiments were performed on fixed parameters such as temperature of 60^0C, back pressure of 1050 psi, flow rate of 0.1 ml/min, and injected brine of 21,600 ppm. The description and the details of the parameters will be illustrated as following.

4.2.1 ASG 1

In this ASG flooding experiment, we investigate the performance of the ASG process by using high permeability limestone core (IL-005). FS-51 was used as a foam agent with a concentration of 0.6 wt%. The reservoir conditions are temperature of 60 °C and pressure of 1050 psi.

4.2.1.1 Water Flooding

Before starting core flooding the effective porosity of the core was determined by mass balance method. The core was saturated by brine using the reservoir brine of salinity 21,600 ppm. From equations (3.1) and (3.2) and Table 3.1, we calculated the porosity as following:

$L = 25.336$ cm

M_{dry} = 599.4 gm

$M_{sat.}$ = 652.9 gm

ρ_{brine} = 1.0135 gm/cc at room conditions, 22 °C and 14.7 psi

$V_{bulk} = 273.74$ cm^3

Then

$$PV = \frac{652.9 - 599.4}{1.0135} = 52.78 \text{ cm}^3$$

$$\phi = \frac{52.78}{273.74} = 19.283\ \%$$

By determining the effective porosity of the core, the core was ready to be uploaded in the core holder and placed on flooding setup. Also the accumulators were filled by dead oil, surfactant and brine and placed on the flooding system. The flooding system was set at 60 °C and left for 12 hr to ensure that the system was well heated. The back pressure was set at 1050 psi.

We started brine flooding at fixed rate of 0.5 cm^3/min to build the pressure of the core for simulating reservoir conditions. 2 PV of brine was injected at the same rate, and then we changed the flow rate and recorded pressure drop along the core, Table 4.5, to calculate the absolute permeability by using Darcy's law, equation (3.3). From data on Table 4.5, we generated the relation between flow rates and the pressure drops by drawing them on Cartesian graph, as in Figure 4.19, the slope was calculated to be 5.74 psi/(cc/min). The viscosity of the brine at reservoir conditions was calculated by Meehan's correlation (1980), equation (4.1). The brine viscosity was 0.571 cp. From the calculations by applying Darcy's law, we got the absolute permeability of 202.38 md.

$$\mu w = \mu wD\,[1 + 3.5 \times 10 - 2p2(T - 40)] \qquad (4.1)$$

With $\mu_{wD} = A+B/T$

$A = 4.518\times10^{-2}+9.313\times10^{-7}\times Y - 3.93\times10^{-12}\times Y^2$

$B= 70.634+9.576\times10^{-10}\times Y^2$

Where

μ_w = Brine viscosity at p and T, cp

μ_{wD} = Brine viscosity at p = 14.7, T, cP

p = Pressure of interest, psia

T = Temperature of interest, ^{0}F

Y = Water salinity, ppm

After that, we injected crude oil into the core at a fixed rate of 0.1 cc/min until 100% oil cut to determine initial oil saturation (S_{oi}), equation (3.4).

$$S_o = \frac{142.4\text{ cc} - 98\text{ cc}}{52.78\text{ cc}} = 0.757 = 75.7\ \%$$

Then

S_{wi} = 1-So =0.2423 = 24.23 %

We repeated the procedure of determining the absolute permeability to estimate the effective oil permeability. We changed the flow rate and recorded pressure drop along the core, Table 4.6. By using Darcy's law, and from data on Table 4.5, we generated the

relation between flow rates and the pressure drops by drawing them on Cartesian graph, as in From Figure 4.19, the slope was calculated to be 90.52 psi/(cc/min). The viscosity dead oil at reservoir conditions was calculated by Glaso's Correlation (1980), equation (4.2). The dead oil viscosity was 1.99 cp. From the calculations by applying Darcy's law, we got the effective oil permeability of 51.81 md.

$$\mu od = [3.141(1010)]\,(T - 460) - 3.444\,[\log(API)]a \qquad (4.2)$$

Where the coefficient is given by:

a=13.313[log(T-460)]-36.447

API of dead oil = 37.74

We calculated the relative oil preameability as below:

$k_{ro} = k_o/k_{abs}$=51.81/202.38=0.256

The saturated core was aged 24 hrs before water flooding. Initially, we started oil production by water flooding where the same brine as in brine saturation was used for water flood. Brine was injected at fixed rate of 2.5 PV/day until 100% water cut is obtained. We can see from Figure 4.20 that pressure drop is almost 3 psi. Figure 4.24 shows that most of initial oil in place (IOIP), (50 %) was produced by injecting 1.5 PV of brine. However, about 15 % of IOIP was produced by injecting 6 PV of brine. In this step, we calculated residual oil saturation $S_{ro,}$ equation (3.8), water effective permeability k_w, equation (3.9), and end point water relative permeability, k_{rw}, equation (3.10) as following:

$$S_{ro} = \frac{39.99-25.52}{52.78} \times 100 = 27.40\ \%$$

For calculating k_w, we changed the flow rate and recorded pressure drop along the core, Table 2.1. By using Darcy's law, and from data on Table 4.7, we generated the relation between flow rates and the pressure drops by drawing them on Cartesian graph, Figure 4.21. From Figure 4.21, the slope is 25.076 psi/(cc/min). From the calculations by applying Darcy's law, we got the absolute permeability of 46.338 md. So, the relative permeability, k_{rw}, was calculated as below:

$$k_{rw} = \frac{46.338}{202.38} = 0.229$$

Table 4.5 Flow rate and pressure drop of brine injection for ASG1 Expermint

q, cc/sec	P_1, atm	P_2, atm	ΔP, atm
0.008333	72.29252	72.22449	0.068027
0.016667	72.4966	72.36054	0.136054
0.025	72.56463	72.36054	0.204082
0.041667	72.70068	72.42857	0.272109
0.05	72.83673	72.4966	0.340136
0.066667	72.90476	72.4966	0.408163

Table 4.6 Flow rate and pressure drop of oil for ASG1 Expermint

q, cc/sec	P_1, atm	P_2, atm	ΔP, atm
0.001667	72.29252	72.08844	0.204082
0.008333	73.31293	72.56463	0.748299
0.016667	74.12925	72.70068	1.428571
0.033333	76.03401	72.97279	3.061224

Table 4.7 Flow rate and pressure drop of brine injection after water flooding for ASG1 Expermint

q, cc/sec	P_1, atm	P_2, atm	ΔP, atm
0.008	72.224	71.816	0.190
0.017	72.565	71.884	0.462
0.025	73.041	72.156	0.667
0.042	73.313	72.224	0.871
0.050	73.925	72.361	1.347
0.067	74.333	72.429	1.687

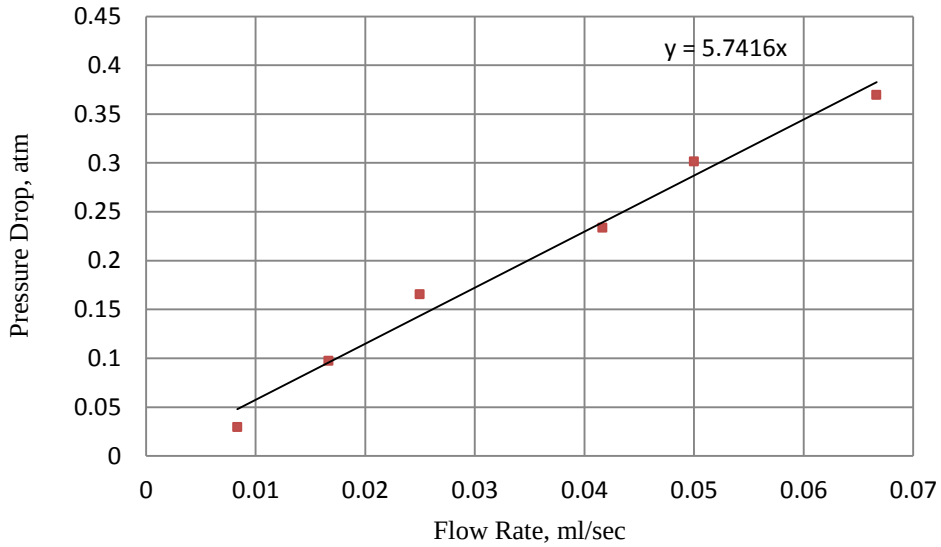

Figure 4.18 The relation between flow rates and the pressure drops of brine injection for ASG1 experiment

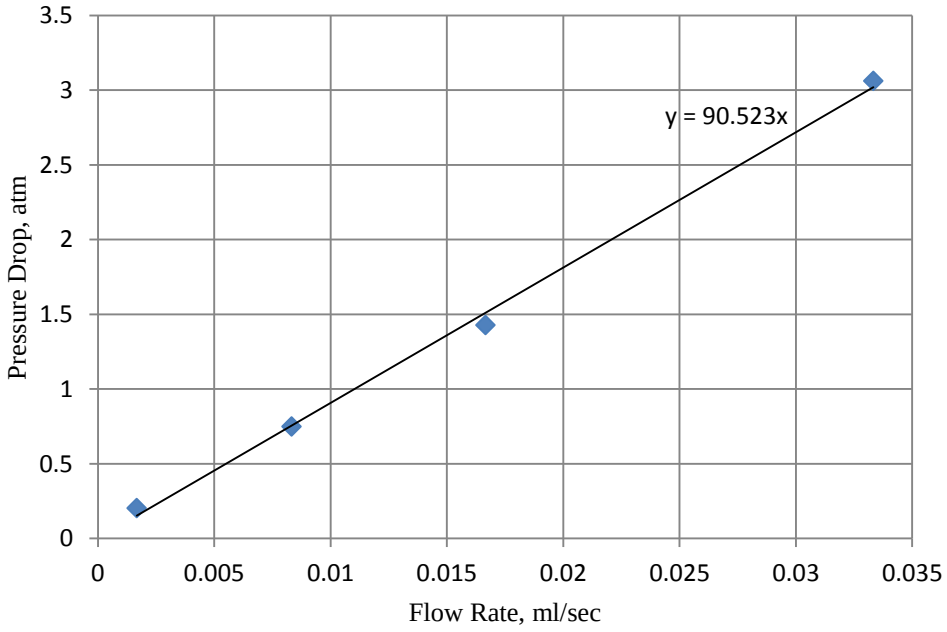

Figure 4.19 The relation between flow rates and the pressure drops of oil injection for ASG1 experiment

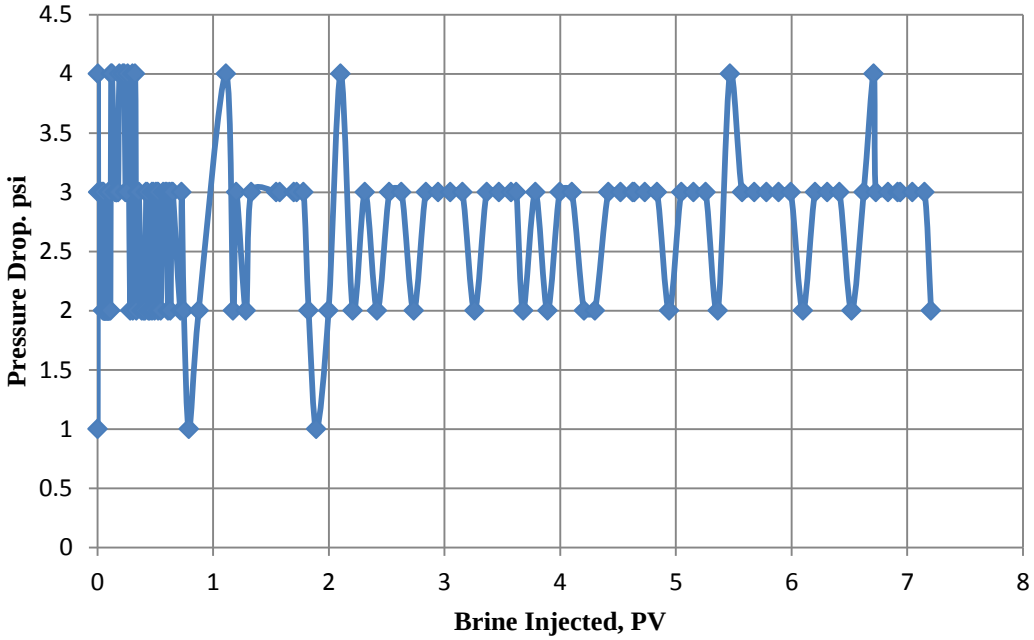

Figure 4.20 Pressure drop during water flooding for ASG1 experiment

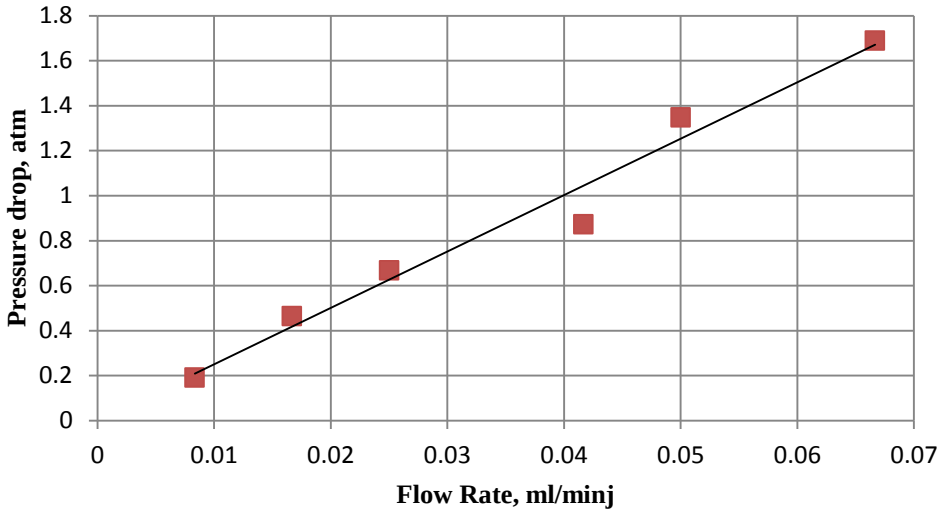

Figure 4.21 The relation between flow rates and the pressure drops of brine injection after water flooding for ASG1 experiment

4.2.1.2 Foam Injection

By injecting 7.2 PV brine during water flooding we got about 63 % of OOIP, where no more oil was produced. Thus, we started foam injection to produce more oil. We selected Capstone FS-51 as a foam agent to see the production performance by foam. The strategy of foam injection was alternative injection of surfactant and nitrogen.

Firstly, we injected 0.2 PV slug of surfactant with fixed rate of 2.5 PV/day. Then, 0.1PV of N_2 was injected at the same rate of surfactant slug followed up with 0.2PV of surfactant slug injected after N_2 injection. We observed that the pressure drop was the almost the same as water flooding, Figure 4.22. This indicated that no foam generation. As a result, we increased the injected volume of gas to 0.2 PV followed the second surfactant slug. After that, 0.2 PV FS-51slug was injected at rate of 2.5 PV/day. From Figure 4.22, we noted that the pressure drop increased comparing to previous slugs. We concluded that the foam was generated and it was stable while the injecting surfactant. 0.2 PV of N_2 was injected followed by 0.2 PV slug of surfactant. The same observation that pressure drop increased during surfactant injection.

In addition, the progression of pressure drop during ASG slug due to mobilization of trapped oil that forms an oil bank (containing both oil and water) ahead of the slug. Then, when oil bank breaks through on the outlet during ASG drive, the pressure drop decrease and gradually stabilizes to pseudo steady state value, 10 psi. From Figure 4.24, we noted the oil recovery was increased by foam injection from 63 % to 75 % of OOIP. The increase in oil recovery (12 %) represents 43 % of residual oil in place.

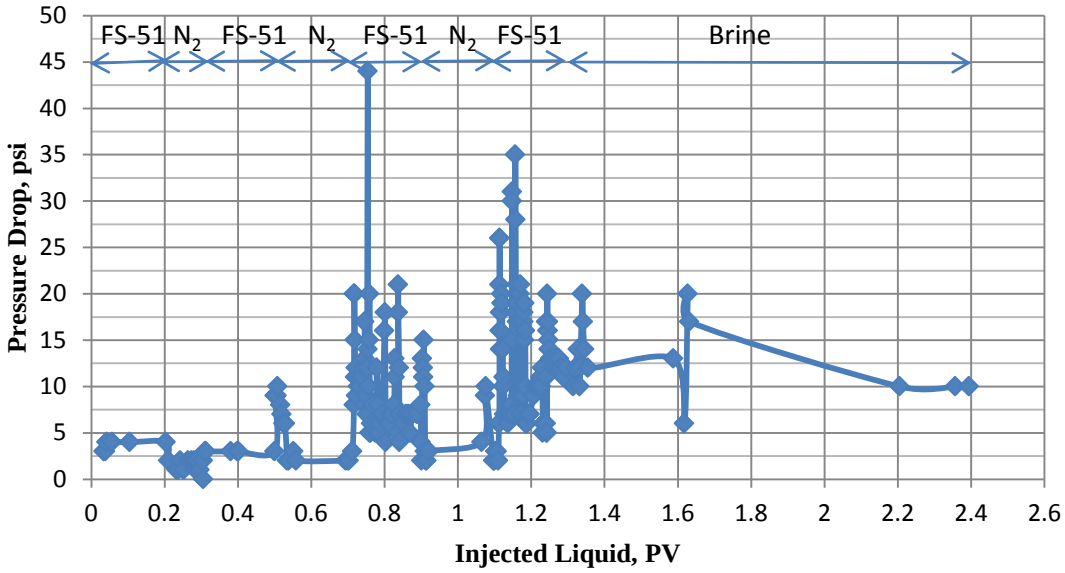

Figure 4.22 Pressure drop during foam injection for ASG1 experiment

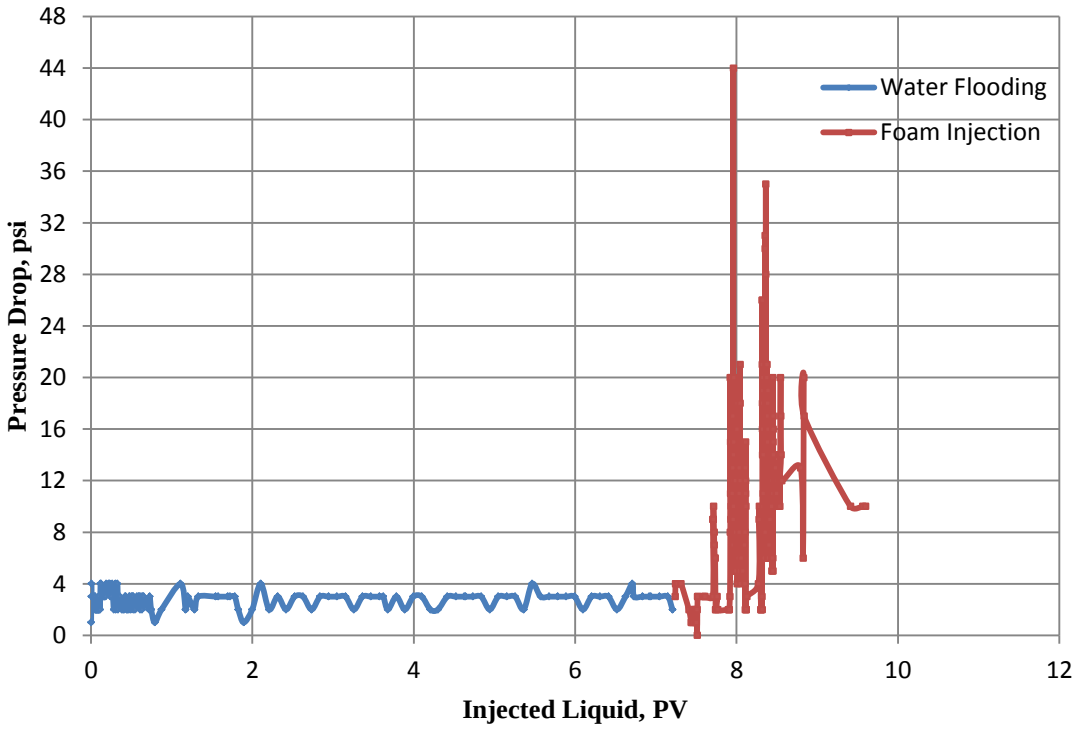

Figure 4.23 Pressure drop during production by water flooding and foam injection for ASG1 experiment

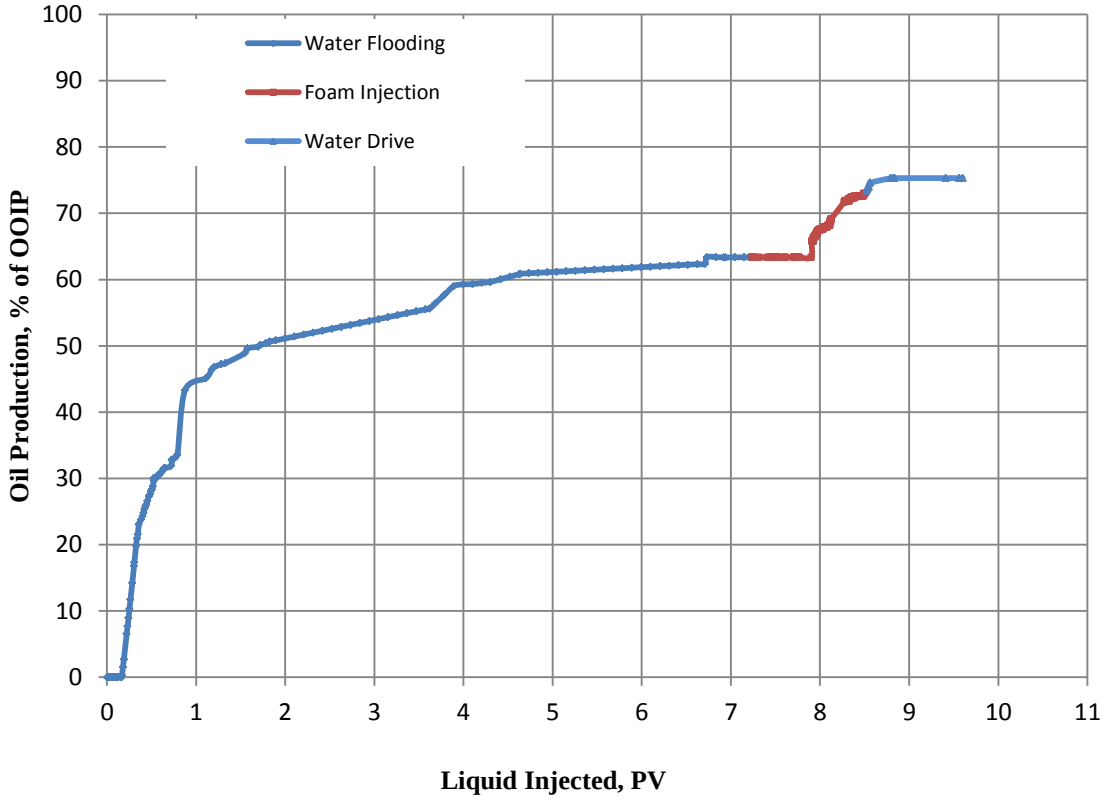

Figure 4.24 Oil recovery by water flooding and foam injection for ASG1 experiment

4.2.2 ASG 2

In this ASG flooding experiment, we investigate the performance of the ASG process by using low permeability limestone core (IL-013). FS-51 was used as a foam agent with a concentration of 0.6 wt%. The reservoir conditions are temperature of 60 °C and pressure of 1050 psi.

4.2.2.1 Water Flooding

Before starting core flooding the effective porosity of the core was determined by mass balance method. The core was saturated by brine using the reservoir brine of salinity 21600 ppm. From equations (3.1) and (3.2) and Table 3.1, we calculated the porosity as following:

$L = 25.401$ cm

M_{dry} = 654.2gm

$M_{sat.}$ = 688 gm

ρ_{brine} = 1.0135 gm/cc at room conditions, 22 °C and 14.7 psi

$V_{bulk} = 278.0076$ cm^3

Then,

$PV = \frac{688 - 654.2}{1.0135} = 33.349$ cm^3

$\phi = \frac{52.78}{273.74} = 11.99$ %

By determining the effective porosity of the core, the core was ready to be uploaded in the core holder and placed on flooding setup. Also the accumulators were filled by dead oil, surfactant and brine and placed on the flooding system. The flooding system was set at 60 °C and left for 12 hr to ensure that the system was well heated. The back pressure was set at 1050 psi.

We started brine flooding at fixed rate of 0.1 cc/min to build the pressure of the core for simulating reservoir conditions. 2 PV of brine was injected at the same rate, and then we changed the flow rate and recorded pressure drop along the core, Table 4.7, to calculate the absolute permeability by using Darcy's law, equation (3.3). From data on Table 4.7, we generated the relation between flow rates and the pressure drops by drawing them on Cartesian graph, as in. From Figure 4.25, the slope was calculated to be 567.35 psi/(cc/min). From the calculations by applying Darcy's law, we got the absolute permeability of 2.05 md.

After that, we injected crude oil into the core at a fixed rate of 0.05 cc/min until no more oil coming out, to determine initial oil saturation (S_{oi}), equation (3.4). We got S_{oi} of 77.5 % and S_{wi} of 22.5 %.

By using Darcy's law, and from data on Table 4.9, we generated the relation between flow rates and the pressure drops by drawing them on Cartesian graph, as in Figure 4.26. From Figure 4.19, the slope was calculated to be 10671 psi/(cc/min). From the calculations by applying Darcy's law, we got the absolute permeability of = 0.440 md.

The saturated core was aged 24 hrs before water flooding. Initially, we started oil production by water flooding where the same brine as in brine saturation was used for

water flood. Brine was injected at fixed rate of 0.1 cm^3/min until 100% water cut is obtained. We can see from Figure 4.28 pressure drop range is between a maximum value of 190 psi and a minimum of 47 psi. In addition, Figure 4.29 show that 68 % of OOIP was produced by injecting 2 PV brine, and the maximum oil recovery by water flooding was 69 % of OOIP. From equation (3.8), the residual oil saturation (S_{ro}) after water flooding was 23 %. Moreover, we got the water effective permeability k_w of 0.473 md, Table 4.10 and equation (3.9), and end point water relative permeability, k_{rw}, of 0.231, equation (3.10).

Table 4.8 Flow rate and pressure drop of brine injection for ASG2 Expermint

q, cc/sec	P_1, atm	P_2, atm	ΔP, atm
0.0017	71.136	70.048	1.088
0.0033	72.429	70.456	1.973
0.0050	73.857	70.864	2.993
0.0067	75.014	71.068	3.946
0.0083	75.966	71.136	4.830

Table 4.9 Flow rate and pressure drop of oil for ASG2 Expermint

q, cc/sec	P_1, atm	P_2, atm	ΔP, atm
0.00017	72.497	70.456	2.041
0.00033	74.810	71.136	3.673
0.00050	76.578	71.068	5.510
0.00083	79.980	70.864	9.116

Table 4.10 Flow rate and pressure drop of brine injection after water flooding for ASG1 Expermint

q, cc/sec	P_1, atm	P_2, atm	ΔP, atm
0.002	75.354	70.184	5.170
0.003	79.367	69.367	10.000
0.005	84.129	70.320	13.810
0.007	88.075	70.524	17.551

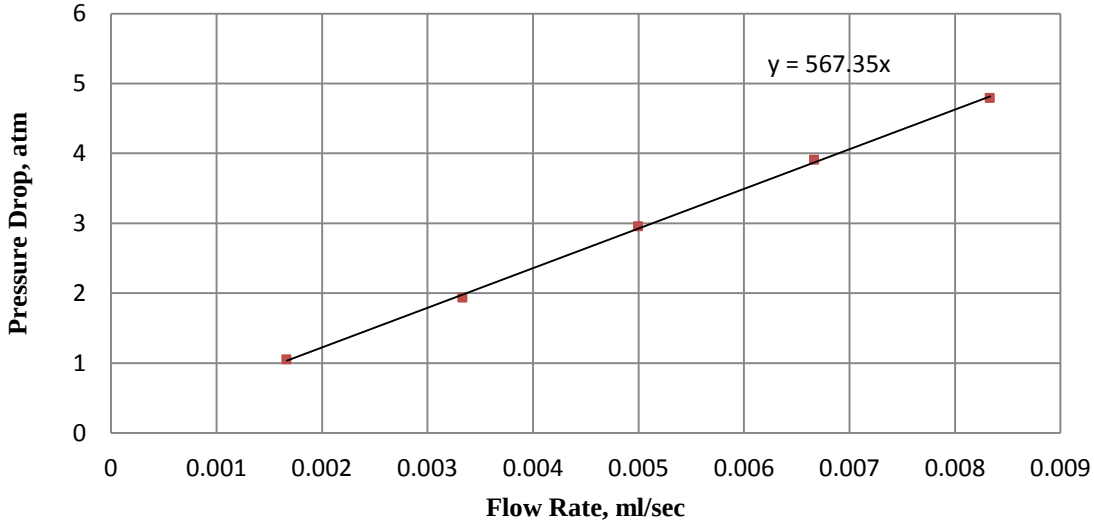

Figure 4.25 The relation between flow rates and the pressure drops of brine injection forASG2 experiment

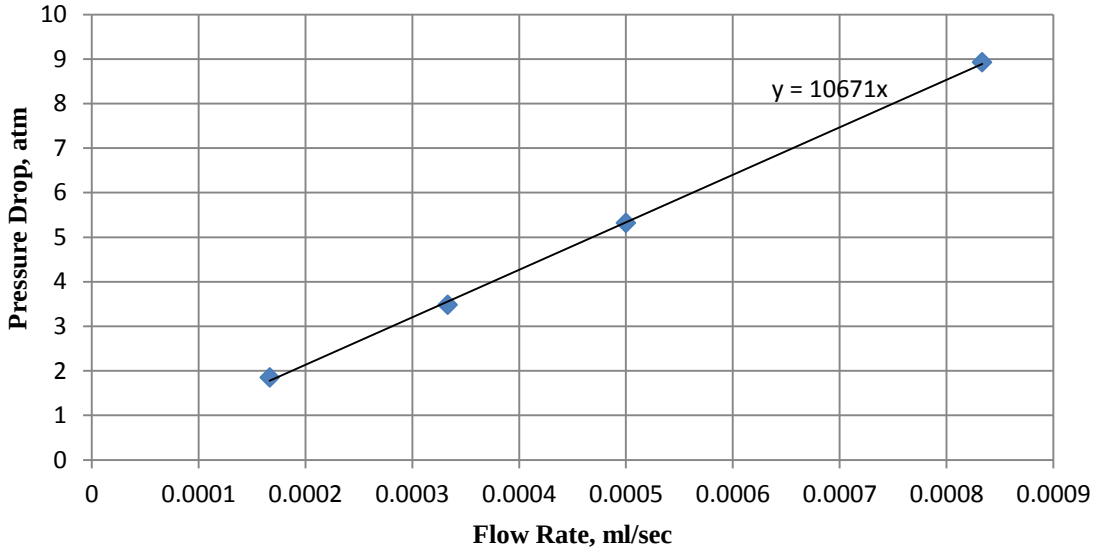

Figure 4.26 The relation between flow rates and the pressure drops of oil injection for ASG2 experiment

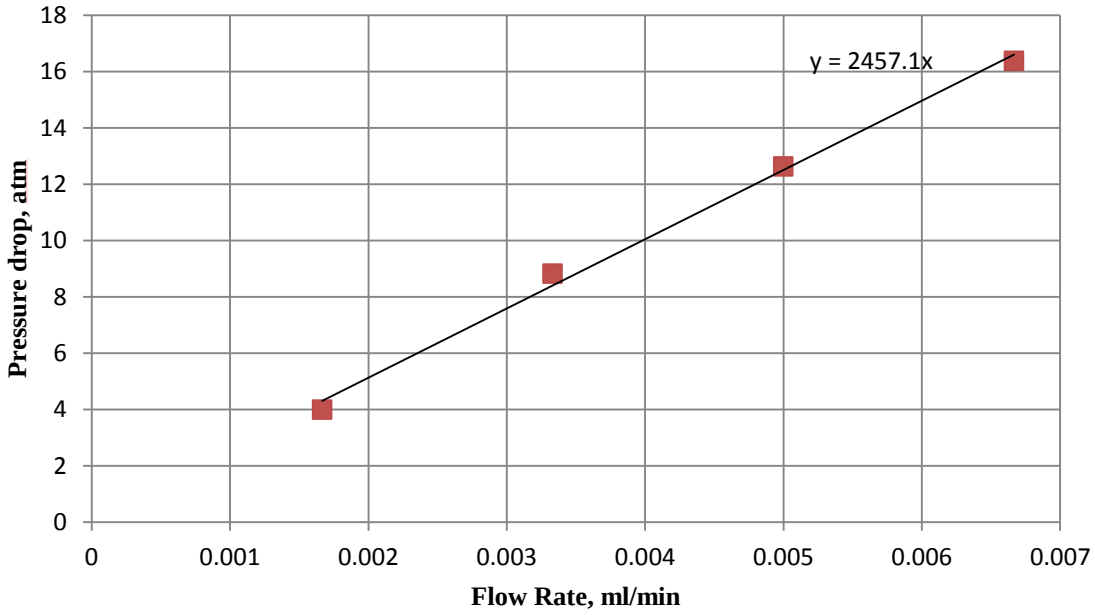

Figure 4.27 The relation between flow rates and the pressure drops of brine injection after water flooding for ASG2 experiment

4.2.2.2 Foam Injection

As mentioned previously, by water flooding we got about 69 % of OOIP, where no more oil was produced. Thus, we started foam injection to produce more oil. We selected Capstone FS-51 as a foam agent to see the production performance by foam. The selected surfactant concentration was 0.6 %wt and the solution salinity was 36,000 ppm NaCl. The strategy of foam injection was alternative injection of surfactant and nitrogen.

Firstly, we injected 0.2 PV slug of surfactant with fixed rate of 0.1 cc/min. Then, 0.2 PV of N_2 was injected at the same rate of surfactant slug. After that, 0.2 PV of surfactant slug was injected followed by 0.2 PV of N_2. Next, 1.2 PV of brine was injected to drive the foam and produce more oil.

From Figure 4.28, we observed that the pressure drop increased comparing to pressure drop during water flooding. We can see from Figure 4.28 pressure drop range is between a maximum value of 426 psi and a minimum of 43 psi. We concluded that the foam was generated and it was stable while the injecting surfactant.

From Figure 4.29, we noted the oil recovery was increased by foam injection from 69% to 82 % of OOIP. The increase in oil recovery (13 %) represents 47.7 % of residual oil in place.

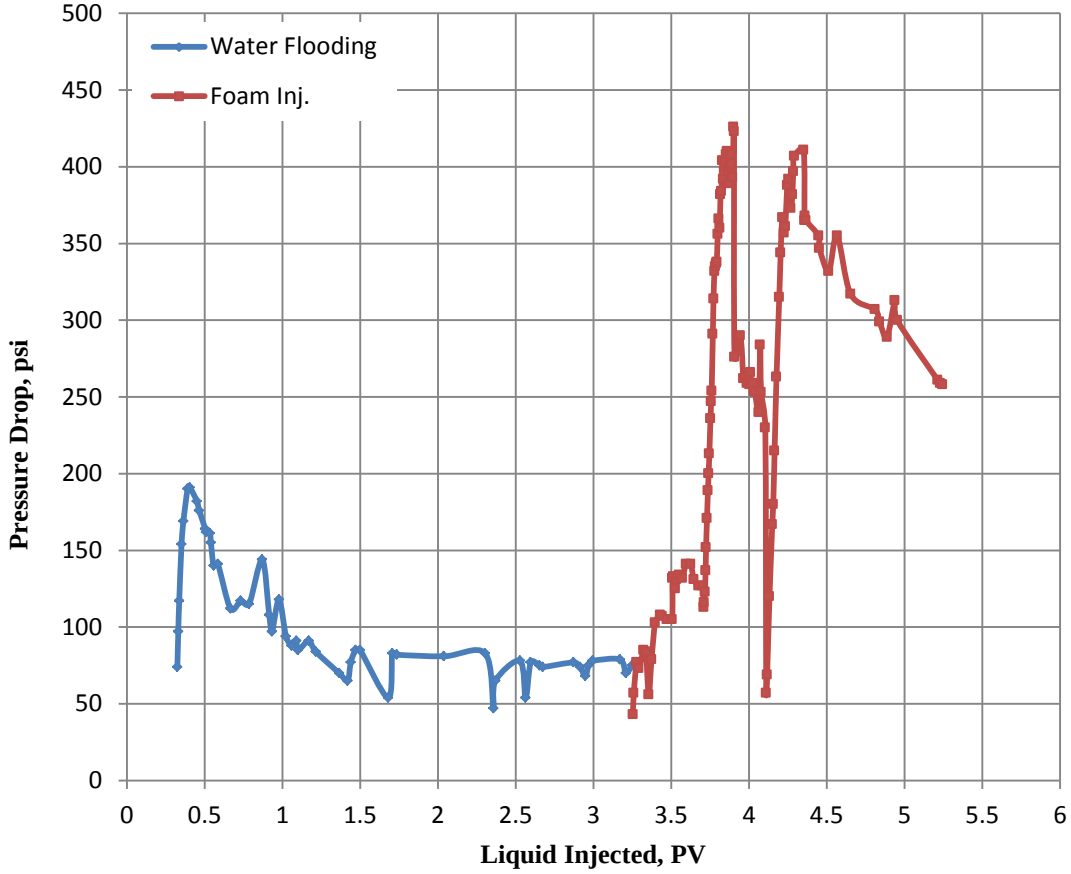

Figure 4.28 Pressure drop during production by water flooding and foam injection for ASG2 experiment

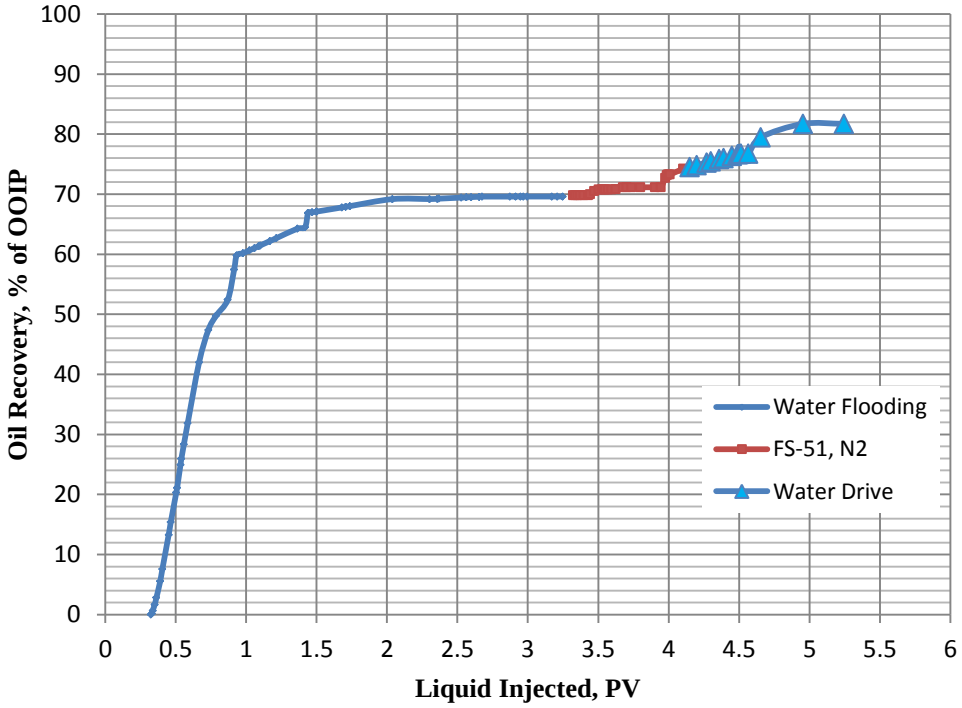

Figure 4.29 Oil recovery by water flooding and foam injection for ASG2 experiment

4.2.3 ASG 3

In this ASG flooding experiment, we investigate the performance of the ASG process by using high permeability lime stone core (IL-005). FS-51 was used as a foam agent with a concentration of 0.6 wt%. We add NaOH with concentration of 0.31 %wt to see the effect of alkaline.

In general, there many roles for using alkaline in ASG process such reducing the adsorption of anionic surfactants (Wesson and Harwell, 2000), sequester divalent cations and generating soap in-situ due to the reaction of alkali and naphthenic acid in reactive crude oil. Moreover, the use of alkali is very important in making an effective EOR process for fractured oil-wet reservoirs where the alkali has ability of changing rock wettability [24](Nguyen, 2010).

4.2.3.1 Water Flooding

As mention previously, firstly we determine the effective porosity of the core was by mass balance method. Form the calculations; the core effective porosity of was 19.35 %. By determining the effective porosity of the core, the core was ready to be uploaded in the core holder and placed on flooding setup and set the system temperature.

By using Darcy's law, equation (3.3) and Figure 4.30, the absolute permeability was 202.07 md. After that we injected crude oil into the core at a fixed rate of 0.05 cm^3/min until no more oil coming out, to determine initial oil saturation (S_{oi}), equation (3.4). We got S_{oi} of 67.07 % and S_{wi} of 32.93 %.

We repeated the procedure of determining the absolute permeability to estimate the effective oil permeability. By using Darcy's law and Figure 4.31, the effective oil permeability was 51.83 md.

The saturated core was aged 24 hrs before water flooding. Initially, we started oil production by water flooding where the same brine as in brine saturation was used for water flood. Brine is injected at fixed rate of 0.1 ml/min until 100% water cut is obtained. We can see from Figure 4.33that pressure drop range is between a maximum value of 3 psi and a minimum of 1 psi. In addition, Figure 4.34 shows that 64 % of OOIP was produced by injecting 1.6 PV brine, and the maximum oil recovery by water flooding was 68 % of OOIP. From equation (3.8), the residual oil saturation (S_{ro}) after water flooding was 22.55 %. Moreover, we got the water effective permeability k_w of 0.473 md.

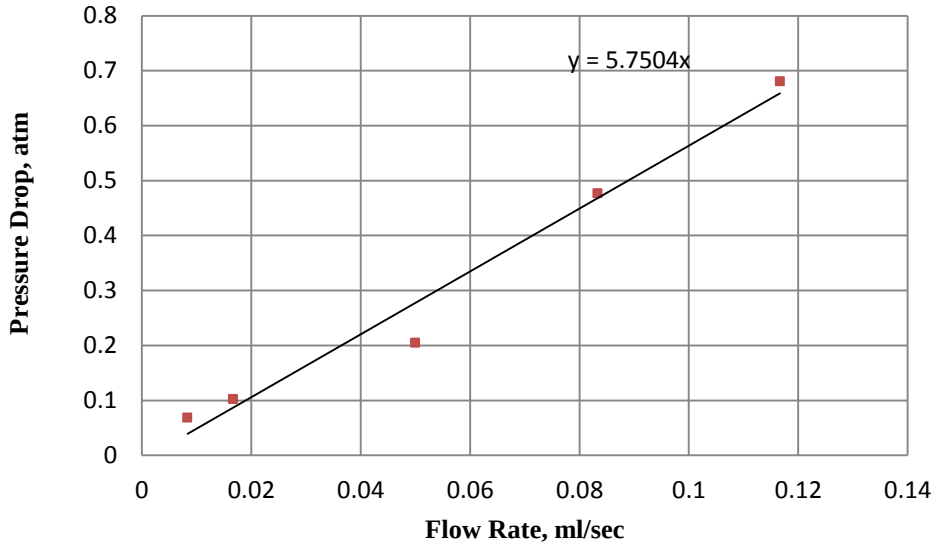

Figure 4.30 The relation between flow rates and the pressure drops of brine injection for ASG3 experiment

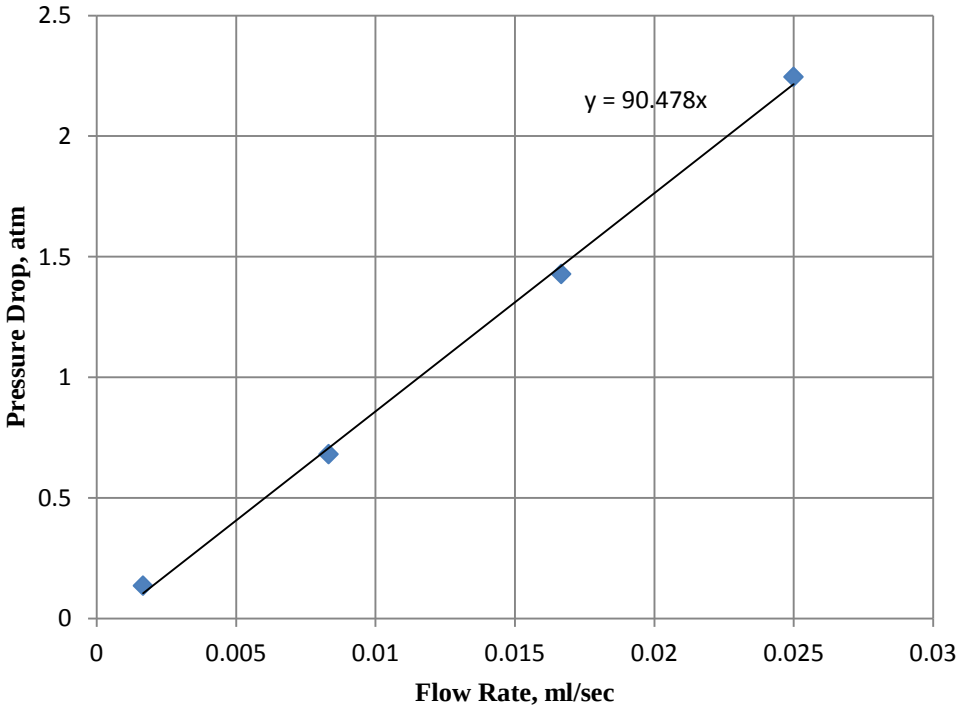

Figure 4.31 The relation between flow rates and the pressure drops of oil saturation for ASG3 experiment

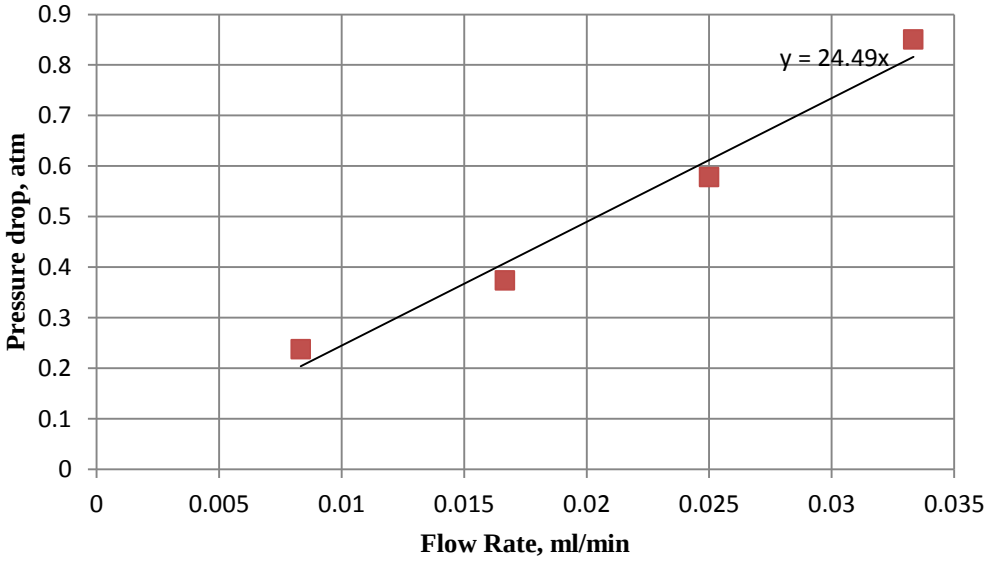

Figure 4.32 The relation between flow rates and the pressure drops of brine after water flooding for ASG3 experiment

4.2.3.2 Foam Injection

As mentioned previously, by water flooding we got about 68 % of OOIP, where no more oil was produced. Thus, we started foam injection to produce more oil.

Firstly, we injected 0.2PV slug of surfactant with fixed rate of 0.1 cm^3/min. Then, 0.2 PV of N_2 was injected at the same rate of surfactant slug. After that, 0.2 PV of surfactant slug was injected followed by 0.2 PV of N_2. Next, 1 PV of brine was injected to drive the foam and produce more oil.

From Figure 4.33, we observed that the pressure drop increased comparing to pressure drop during water flooding. We can see from Figure 4.33 pressure drop range is between a maximum value of 24 psi and a minimum of 1 psi. We concluded that the foam was generated and it was stable while the injecting surfactant.

From Figure 4.34, we noted the oil recovery was increased by foam injection from 68 % to 75.6 % of OOIP. The increase in oil recovery (7.4 %) represents 41.2 % of residual oil in place.

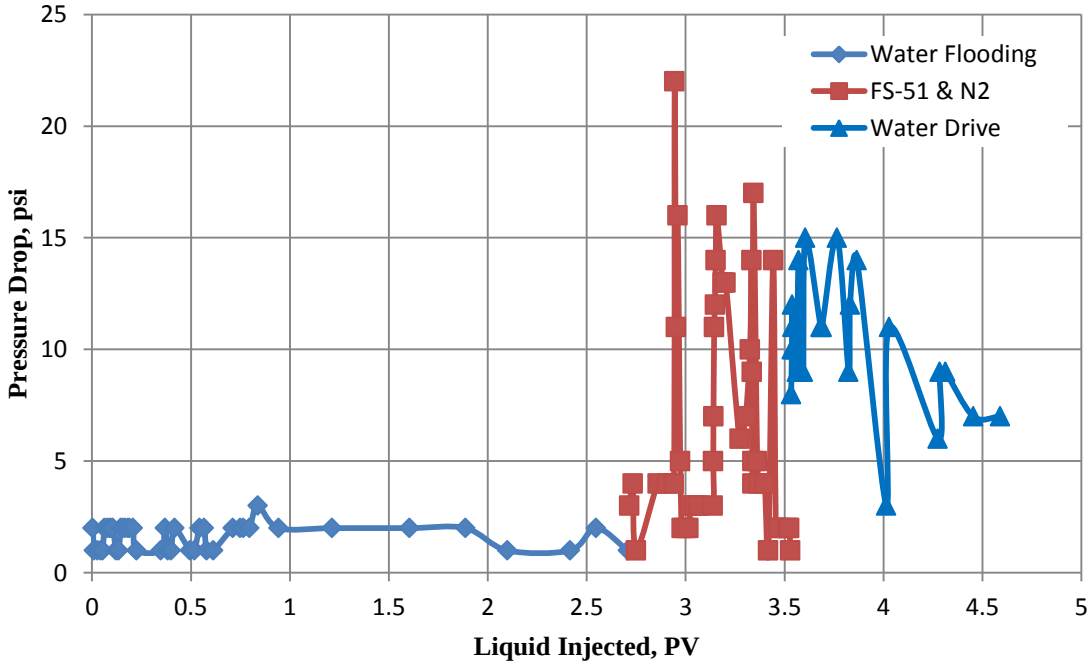

Figure 4.33 Pressure drop during production by water flooding and foam injection for ASG3 experiment

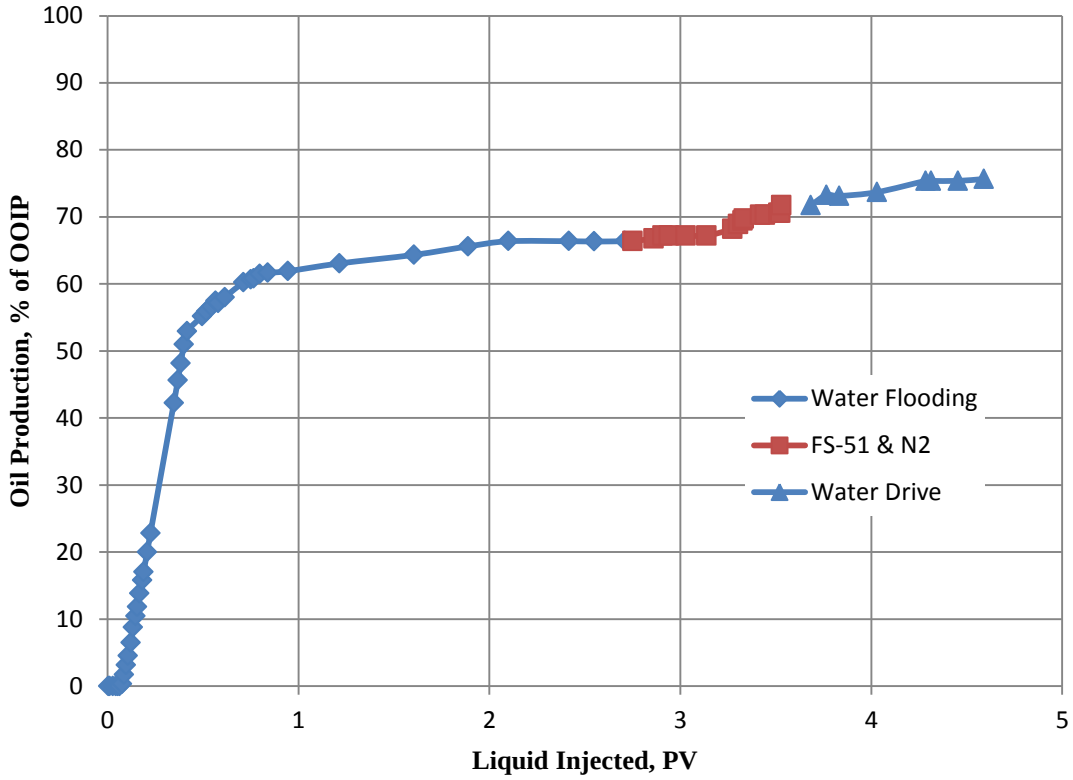

Figure 4.34 Oil recovery by water flooding and foam injection for ASG3 experiment

4.2.4 ASG 4

In this ASG flooding experiment, we investigate the performance of the ASG process by using low permeability lime stone core (IL-013). FS-50 was used as a foam agent with a concentration of 0.6 wt%.

4.2.4.1 Water Flooding

Form mass balance method, the core effective porosity of was 11.92 %. Then the core was ready to be uploaded in the core holder and placed on flooding setup and set the system temperature.

From Darcy's law, equation (3.3) and Figure 4.35, the absolute permeability was 1.65 md. By applying equation (3.4), we got S_{oi} of 73.9 % and S_{wi} of 26.1 %. Also from Darcy's law and Figure 4.36, the effective oil permeability was 0.340 md. Then the saturated core was aged 24 hrs before water flooding. Initially, we started oil production by water flooding at fixed rate of 0.1 ml/min until 100 % water cut is obtained.

We can see from Figure 4.38 that pressure drop range is between a maximum value of 320 psi and a minimum of 87 psi. In addition, Figure 4.39 shows that 68 % of OOIP was produced by injecting .87 PV brine, and the maximum oil recovery by water flooding was 71 % of OOIP. From equation (3.8), the residual oil saturation (S_{ro}) after water flooding was 20.8 %. Moreover, we got the water effective permeability, k_w, of 0.187 md.

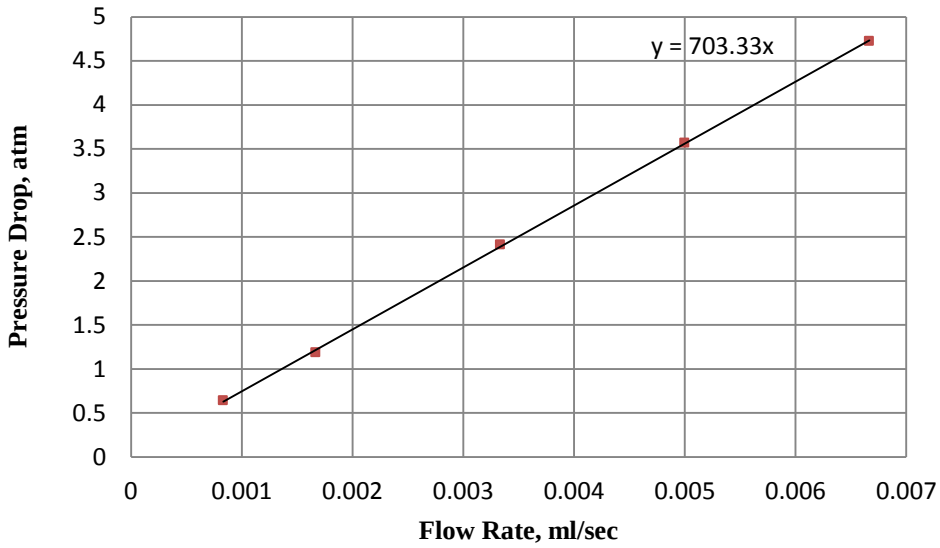

Figure 4.35 The relation between flow rates and the pressure drops of brine injection for ASG4 experiment

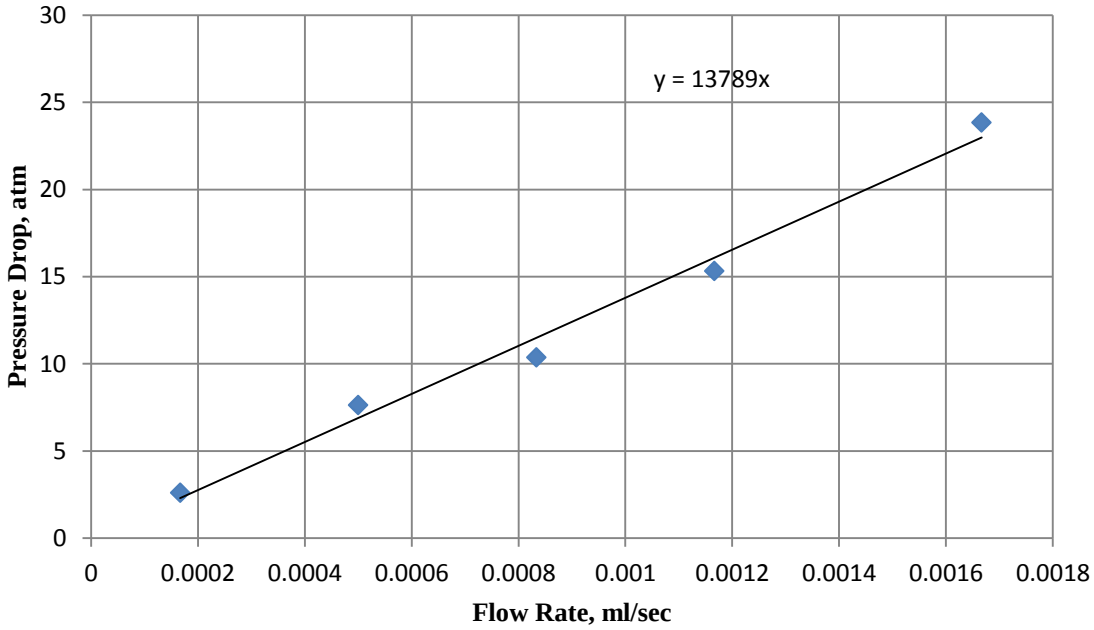

Figure 4.36 The relation between flow rates and the pressure drops of oil saturation for ASG4 experiment

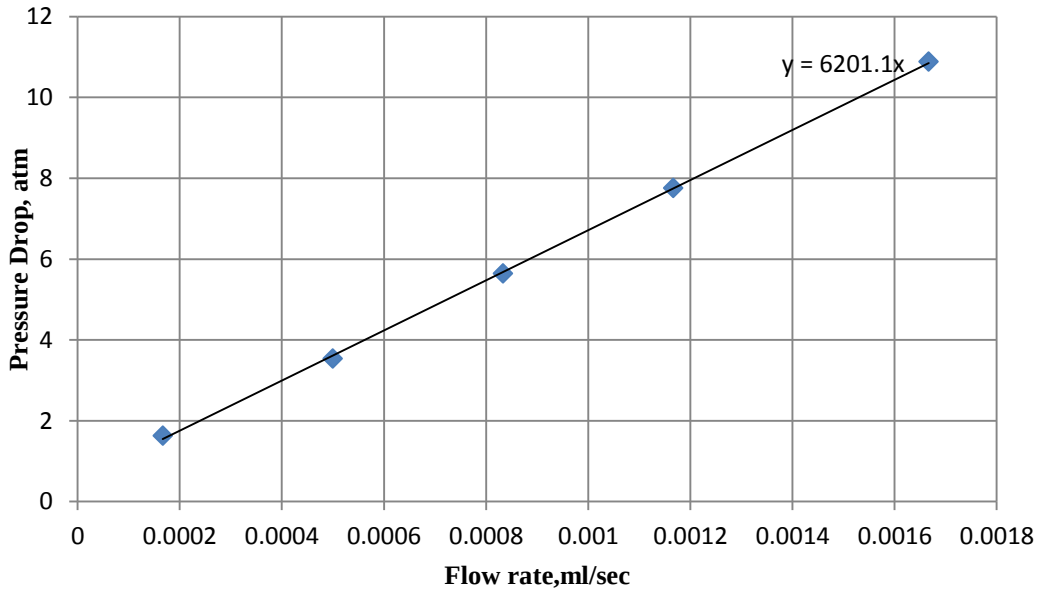

Figure 4.37 The relation between flow rates and the pressure drops of brine after water flooding, ASG4

4.2.4.2 Foam Injection

As mentioned previously, by water flooding we got about 72 % of OOIP, where no more oil was produced. Thus, we started foam injection to produce more oil.

Firstly, we injected 0.2 PV slug of surfactant with fixed rate of 0.1 cm^3/min. Then, 0.2 PV of N_2 was injected at the same rate of surfactant slug. After that, 0.2 PV of surfactant slug was injected followed by 0.2 PV of N_2. Next, 1 PV of brine was injected to drive the foam and produce more oil.

From Figure 4.38, we observed that the pressure drop increased comparing to pressure drop during water flooding. We can see from Figure 4.38 pressure drop range is between a maximum value of 491 psi and a minimum of 81 psi. We concluded that the foam was generated and it was stable while the injecting surfactant.

From Figure 4.39, we noted the oil recovery was increased by foam injection from 71.8 % to 77.5 % of OOIP. The increase in oil recovery (5.7%) represents 21 % of residual oil in place.

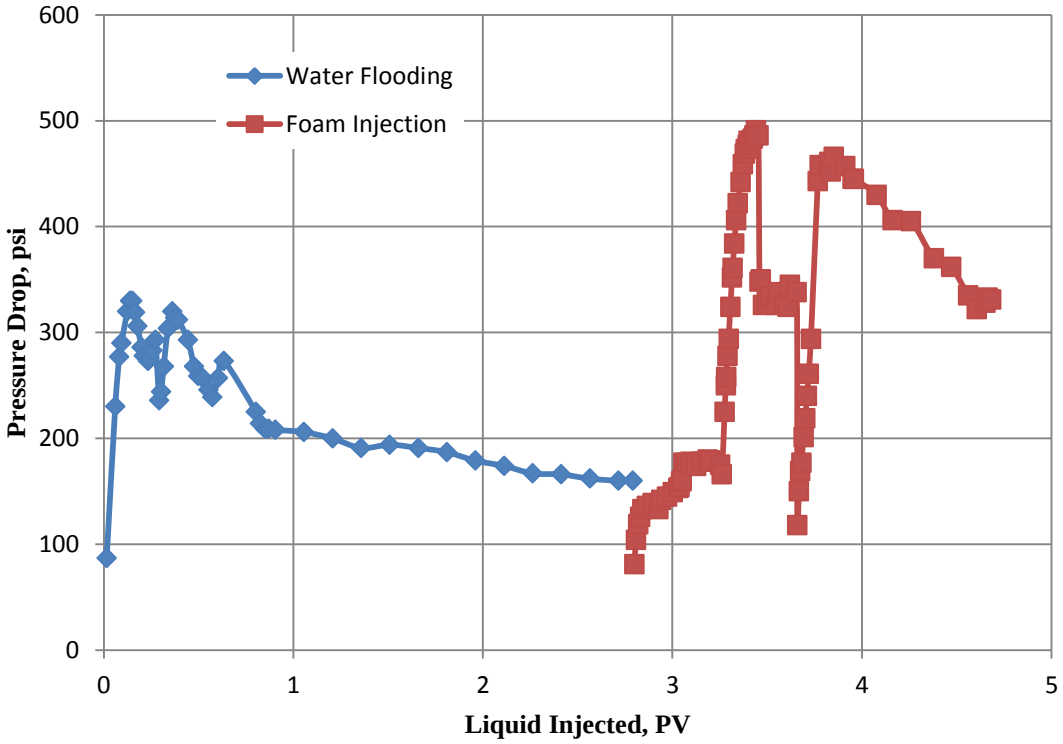

Figure 4.38 Pressure drop during production by water flooding and foam injection for ASG4 experiment

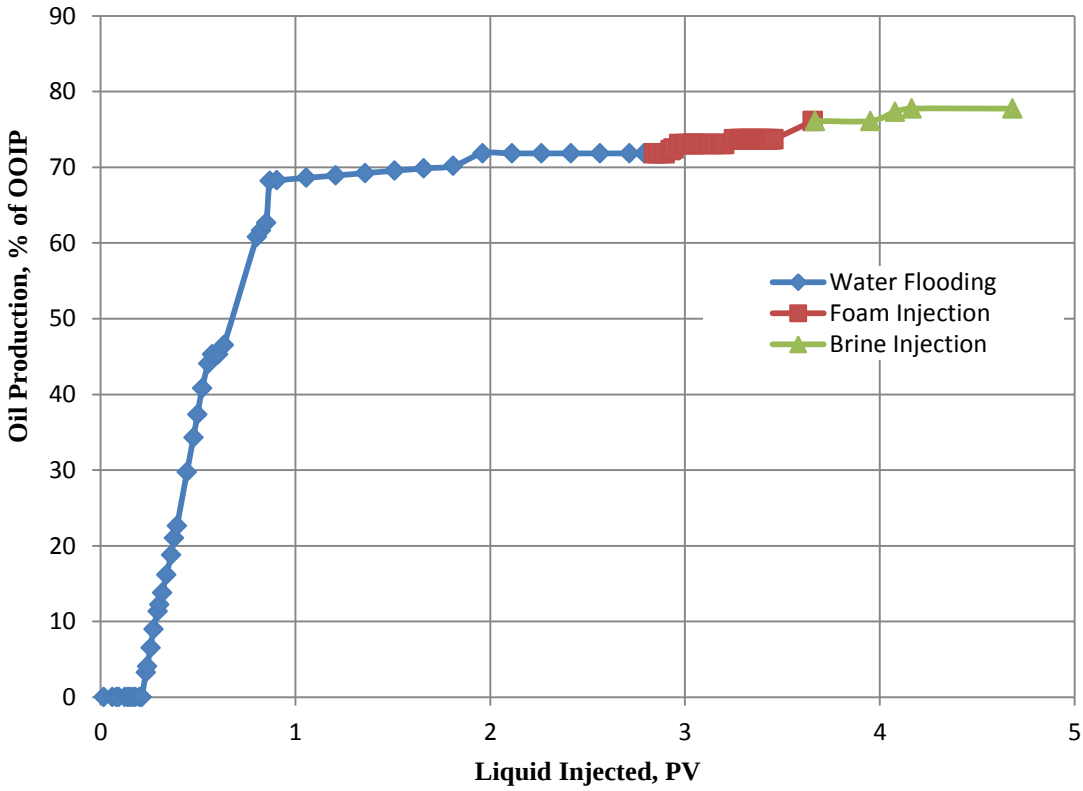

Figure 4.39 Oil recovery by water flooding and foam injection for ASG4 experiment

Table 4.11 Summary of ASG experiments

	ASG1	ASG2	ASG3	ASG4
Core Sample	IL-005	IL-013	IL-005	IL-013
Porosity, %	19.28	12.00	19.36	11.93
Permeability to brine, md	202.38	2.05	202.07	1.65
Initial oil Saturation, %	75.77	77.54	67.08	73.90
Residual Oil Saturation, %	27.76	23.57	22.55	20.82
Liquid rate for water flooding, foam injection, and water drive, ml/min	0.1	0.1	0.1	0.1
Gas rate during foam injection, ml/min	0.1	0.1	0.1	0.1
Foam quality (%)	50	50	50	50
Liquid slug for ASG process (each cycle), PV	0.2×4	0.2×2	0.2×2	0.2×2
Gas slug for ASG process, PV	0.2×4	0.2×2	0.2×2	0.2×2
FS-50 concentration in slug, wt%	-	-	-	0.6
FS-51 concentration in slug, wt%	0.6	0.6	0.6	-
NaOH concentration in slug, wt%	-	-	-	0.31
Slug NaCl salinity, ppm	36,000	36,000	36,000	36,000
Oil recovery (% of ROIP), %	43.04	47.74	41.17	21.01
Oil recovery (% of OOIP), %	12	13	7.4	5.7

4.3 Studying ASG Performance by some parameters

In this section, we studied the effect of the permeability, adding alkaline, and type of surfactants on the performance of the ASG process.

4.3.1 Permeability effect

From the results of ASG1 and ASG2 experiments, we study the effect of permeability on ASG performance. ASG1 was conducted on a core with high permeability (202.38 md), however ASG2 was conducted on a core with low permeability (2.04 md). From Figure 4.40, we note that the performance of ASG2 is better for the core with low permeability when using the same surfactant FS-51. For the low permeability core, 47.7 % of the residual oil was produced comparing to the high permeability core, 43%. The foam plays as a good mobility controller in a very low permeability core The foam plays as a good mobility controller in a very low permeability core so the oil bank formed ahead of the slug by the mobilization of trapped oil can be moved easily. The foam did not cause plugging in a very low permeability core highlights the potential of ASG process in very low permeability rocs comparing to polymer application that may cause formation plugging.

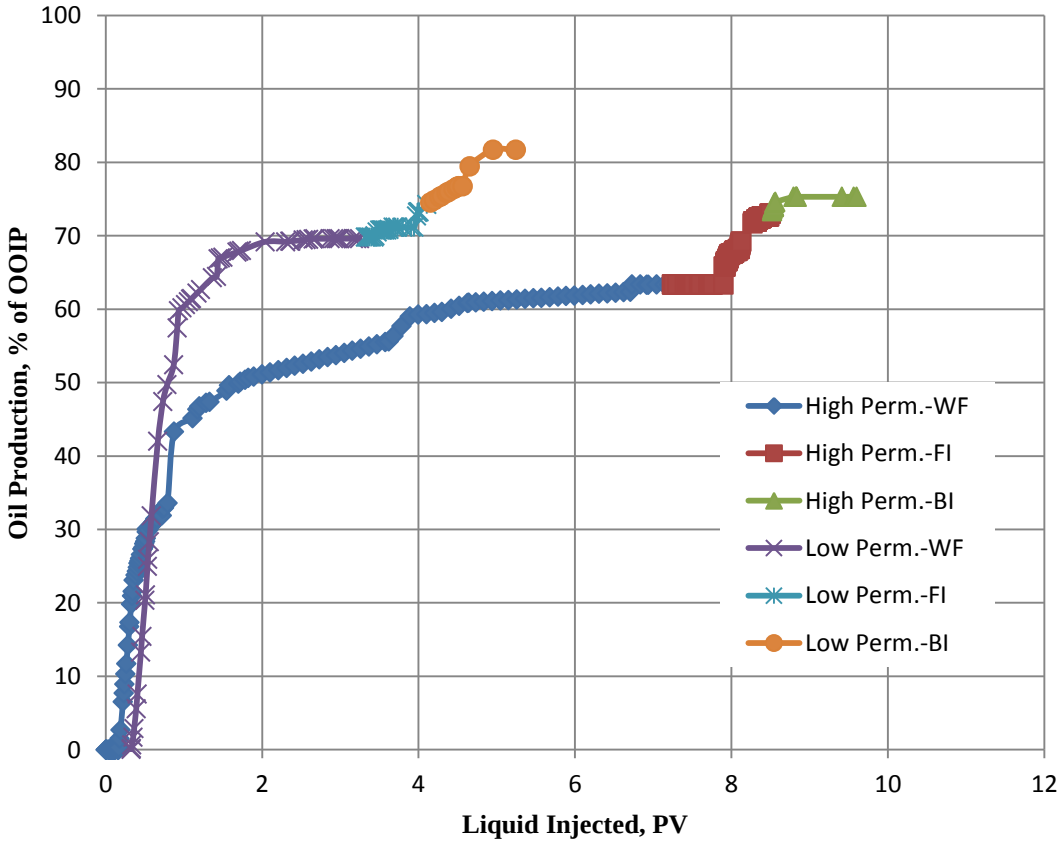

Figure 4.40 Effect of Permeability on ASG Performance

4.3.2 Alkaline effect

From the results of ASG1 and ASG3 experiments, we study the effect of alkaline (NaOH) on ASG performance. In ASG1 the foam agent (FS-51) was used only as a chemical, however in ASG2 we added NaOH to the slug solution with concentration of 0.31 %wt. From Figure 4.41, we observe that 43 % of the residual oil was produced in ASG1 without alkaline comparing to ASG3 with alkaline, 41.1%. As a result, no need for adding alkaline (NaOH) to the chemical slug.

As mentioned previously, section 4.2.3, the alkaline functions are to reduce the adsorption of anionic surfactants, sequester divalent cations, and generate soap in-situ due to the reaction of alkali and naphthenic acid in reactive crude oil. In this case, the role of alkaline is to see foam generation when adding alkaline. From the pressure drop result, Figure 4.23 and Figure 4.33, it is observed that foam generated in ASG1 with alkaline is stronger than in ASG3 without alkaline.

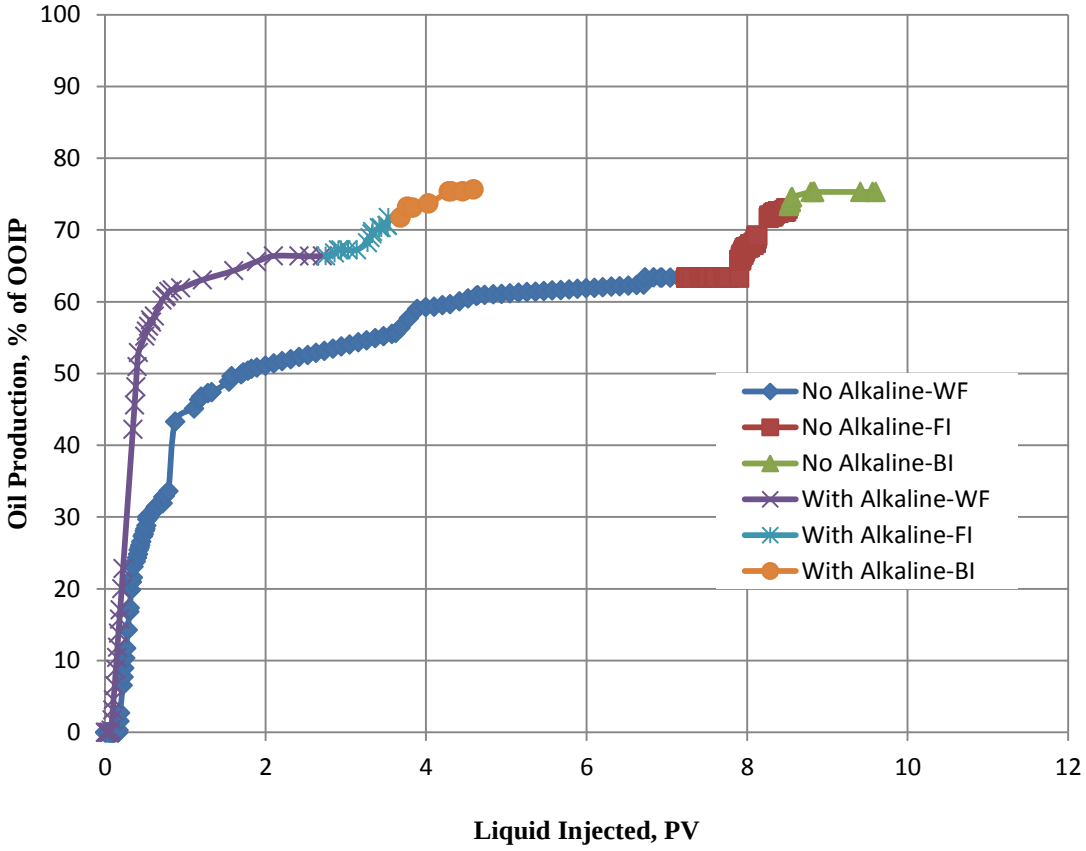

Figure 4.41 Effect of Alkaline on ASG Performance

4.3.3 Surfactant Type effect

From the results of ASG2 and ASG4 experiments, we study the effect of surfactant type (FS-50 and FS-51) on ASG performance. In ASG2, FS-51 was used as a foam agent, however in ASG4 the FS-50 was the foam agent. From Figure 4.42, we observe that 47.7 % of the residual oil was produced in ASG2 comparing to ASG4, 21%. Thus, FS-51 is better for ASG performance than FS-50.

From the phase behavior test, section 4.1.3, it was observed that FS-51 Capston provides better solublization than FS-50 at reservoir conditions, T = 60 °C, P = 1050 psi, and salinity of 21600 ppm. Thus, FS-51 forms micro-emulsion at ultra-low oil-water interfacial tension (IFT)

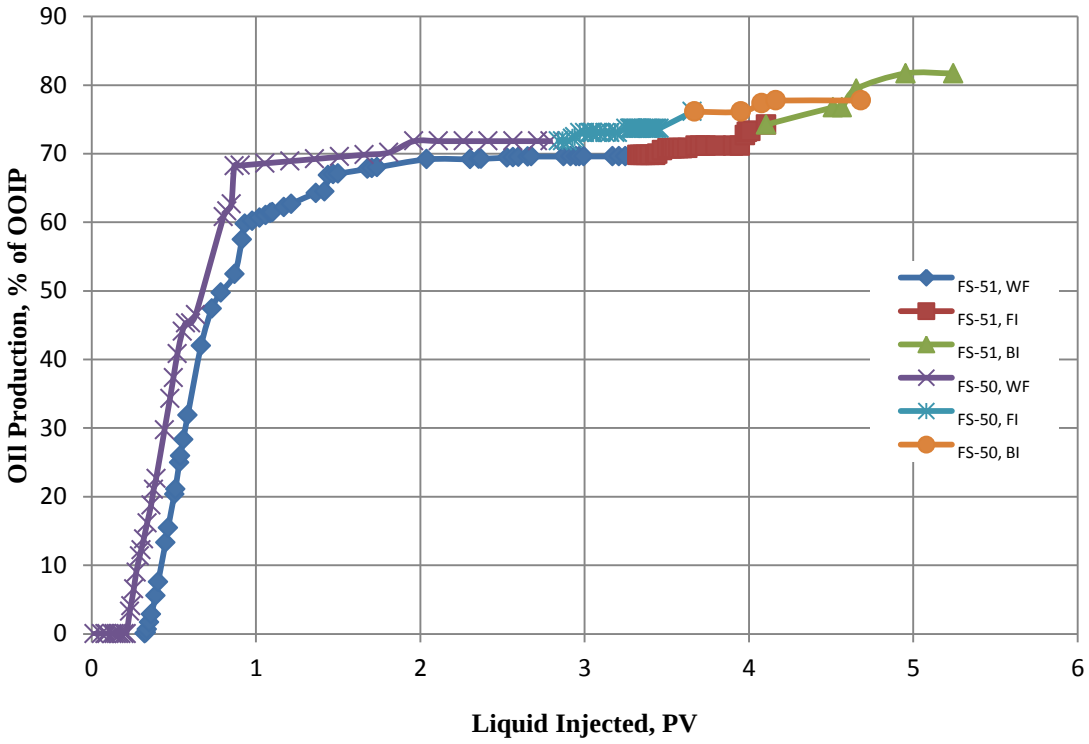

Figure 4.42 Effect of surfactant type on ASG Performance

CHAPTER 5

CONCLUSION AND RECOMMENDATIONS

5.1 Conclusions

- From aqueous stability test and phase behavior test, Capston FS-61 fluorosurfactant provides precipitation and signs of cloudiness, and there was no foam generation.
- Tergitol NP-9 and Triton X-100 provide strong foam generation and the foam was stable for more than 1 hr. In addition, neither precipitation nor visible signs of cloudiness was observed the favorable concentration of both Tergitol NP-9 and Triton X-100 as foam agent was 1.0 wt%.
- From aqueous stability test, no precipitation nor visible signs was observed for Capston FS-50, Capston FS-51. The foam generation is strong and the foam was stable for more than 1 hr.
- The concentration that provides higher initial foam volume and half-time for dewater was 1 wt% of Tergitol NP-9 and Triton X-100 surfactants. However, 0.6 wt% of Capston FS-50, Capston FS-51 is the favorable concentration.
- Micro-emulsion phase behavior of all surfactants is oil-in-water micro emulsion (Winsor type I Behavior).
- Capston FS-51 provides good oil solublization comparing to Capston FS-50 at 36,000 ppm and 40,000 ppm of NaCl.

- In ASG1, the increase of pressure drop by increasing the PVs injected of N_2 from 0.1 PV to 0.2 PV, indicates to the good foam generation.
- The oil recovery was increased by foam injection from 63 % to 75 % of OOIP. The increase in oil recovery (12 %) represents 43 % of residual oil in place.
- In ASG2, the oil recovery was increased by foam injection from 69 % to 82 % of OOIP. The increase in oil recovery (13 %) represents 47.7 % of residual oil in place.
- In ASG3, the oil recovery was increased by foam injection from 68 % to 75.6 % of OOIP. The increase in oil recovery (7.4 %) represents 41.2 % of residual oil in place.
- In ASG4, the oil recovery was increased by foam injection from we noted the oil recovery was increased by foam injection from 71.8 % to 77.5 % of OOIP. The increase in oil recovery (5.7 %) represents 21 % of residual oil in place.
- The performance of ASG2 is better for the core with low permeability when using the same surfactant FS-51.
- The oil produced of the residual oil was more when using comparing ASG1 without alkaline comparing to ASG3 with alkaline, 41.1 %. As a result, no need for adding alkaline (NaOH) to the chemical slug.
- We observe that 47.7 % of the residual oil was produced in ASG2 comparing to ASG4, 21 %. Thus, FS-51 is better for ASG performance than FS-50.

5.2 Recommendations

In this study, we would suggest the following future works on ASG

- Using the same parameters that we use in the research to see the recovery performance of the live oil.
- Studying the adsorption and reactions of the surfactants with the rock.
- Carrying out of the performance of the selected foam agents with sandstone rocks.
- Studying the aqueous stability and the phase behavior tests of the selected surfactants on higher salinities and temperatures.
- Carrying out of the performance of the selected foam agents with heavy oil.
- Carry out experiment to study the effect of aging on recovery.

REFERENCES

[1] Medhat Kamal and S.S Marsden Jr.: "Displacement of a Micellar Slug Foam in Unconsolidated Porous Media," SPE 4584 presented at SPE Fall Meeting of the Society of Petroleum Engineers of AIME, held in Las Vegas, Nevada, 1973

[2] Lawson, J. B. and Reisberg, J.: Alternate Slugs of Gas and Dilute Surfactant for Mobility Control during Chemical Flooding. SPE 8839 presented at the First Joint SPE/DOE Symposium on Enhanced Oil Recovery, held in Tulsa, Oklahoma, 20-23 April, 1980

[3] D.O Shah: surface phenomena in Enhanced Oil Recovery, plenum Press 1981

[4] W. R Rossen: "Theories of Foam Mobilization Pressure Gradient," SPE 17358 presented at SPE Enhanced Oil Recovery Symposium, held in Tulsa, Oklahoma, 1988

[5] Laurier L. Schramm: "Foams: Fundamentals and Applications in the Petroleum Industry", published by American Chemical Society, Washington, DC 1994, 47-107.

[6] Eme V. O. 1994: Design of an Alkaline/Surfactant/Polymer Enhanced Oil Recovery Scheme for a Saudi Arabian Limestone Reservoir. MS thesis, King Fahd University of Petroleum & Minerals, Dhahran, Saudi Arabia (July 1994)

[7] W. R Rossen et al: "Injectivity and Gravity Override in Surfactant-Alternating-Gas Foam Processes," SPE 30753 presented at SPE Annual Technical Conference and Exhibition, held in Dallas, Texas, 1995

[8] Green, Don W. and Willhite, G. Paul 1998: Enhanced Oil Recovery. Texas: Richardson

[9] Yan, Wei.(2006): Foam for Mobility Control in Alkaline/Surfactant Enhanced Oil RecoveryProcess.Ph.D.thesis.http://scholarship.rice.edu/bitstream/handle/1911/18997/3216802.PDF?sequence=1

[10] Don W. Green, G Paul Willhite (1998) Enhanced Oil Recovery. Richardson, Texas.

[11] William Richard Rossen and Wietse Joost Renkema: "Success of Foam SAG Processes in Heterogeneous Reservoirs," SPE 110408 presented at SPE Annual Technical Conference and Exhibition, held in Anaheim, California, U.S.A, 2007

[12] Li, R. et al.: “Foam Mobility Control for Surfactant Enhanced Oil Recovery,” SPE 113910, 2008

[13] Shunhua Liu et al.: “Favorable Attributes of Alkaline-Surfactant-Polymer Flooding,” SPE 99744, 2008

[14] Renjing Liu et al: “The Reservoir Suitability Studies of Nitrogen Foam Flooding in Shengli Oilfield,” SPE 114800 presented at the SPE Asia Pacific Oil & Gas Conference and Exhibition held in Perth, Australia, 20–22 October 2008

[15] David Levitt et al: “Identification and Evaluation of High-Performance EOR Surfactants,” SPE 100089, 2009

[16] Adam Flaaten et al: “A Systematic Laboratory Approach to Low-Cost, High-Performance Chemical Flooding,” SPE113469, 2009

[17] Mayank Srivastava et al: “A Systematic Study of Alkaline-Surfactant-Gas Injection as an EOR Technique,” SPE 124752 presented at SPE Annual Technical Conference and Exhibition, held in New Orleans, Louisiana, 2009

[18] Aziz Arshad et al: “Carbon Dioxide (CO_2) Miscible Flooding in Tight Oil Reservoirs: A Case Study,” SPE 127616 presented at SPE Kuwait International Petroleum Conference and Exhibition, held in Kuwait City, Kuwait, 2009

[19] R. Farajzadeh et al: “Foam Assisted Enhanced Oil Recovery at Miscible and Immiscible Conditions,” SPE 126410 presented at SPE Kuwait International Petroleum Conference and Exhibition, held in Kuwait City, Kuwait, 2009

[20] Robert Feng Li et al.: “Foam Mobility Control for Surfactant Enhanced Oil Recovery,” SPE 113910, 2010

[21] Mayank Srivastava and Quoc Phuc Nguyen: “Application of Gas for Mobility Control in Chemical EOR in Problematic Carbonate Reservoirs,” SPE 129840 presented at SPE Improved Oil Recovery Symposium, held in Tulsa, Oklahoma, USA, 2010

[22] Liu He et al: “Application of Nitrogen Foam for Profile Modification in a Heterogeneous Multi-layer Sandstone Oilfield,” SPE 130767 presented at the SPE Asia Pacific Oil & Gas Conference and Exhibition held in Brisbane, Queensland, Australia, 18–20 October 2010

[23] Eduardo Jose Manrique et al: “EOR: Current Status and Opportunities,” SPE 130113 presented at SPE Improved Oil Recovery Symposium, held in Tulsa, Oklahoma, USA, 2010

[24] Nguyen, N. M. 2010: Systematic Study of Foam for Improving Sweep Efficiency in Chemical Enhanced Oil Recovery. MS thesis, Texas University, Austin (December 2010)

[25] Monika Santa et al: "Sustainable Surfactants in Enhanced Oil Recovery," SPE145039 presented at SPE Enhanced Oil Recovery Conference, held in Kuala Lumpur, Malaysia, 2011

[26] James J. Sheng. 2011: Modern Chemical Enhanced Oil Recovery, Theory and Practice

[27] [http://geology.com/rocks/limestone.shtml

[28] http://www.livestrong.com/article/279352-definitions-of-alkaline/

[29] Haugen et al: "Experimental Study of Foam Flow in Fractured Oil-Wet Limestone for Enhanced Oil Recovery," SPE 129763, 2012

[30] Chen et al: "Ethoxylated Cationic Surfactants for CO2EOR in High Temperature, High Salinity Reservoirs," SPE 154222 presented at the Eighteenth SPE Improved Oil Recovery Symposium held in Tulsa, Oklahoma, USA, 14–18 April 2012

[31] Hou Qingfeng et al: "Studies On Nitrogen Foam Flooding For Conglomerate Reservoir," SPE 152010 presented at the SPE EOR Conference at Oil and Gas West Asia held in Muscat, Oman, 16–18 April 2012

[32] Simjoo et al: "A CT Scan Study of Immiscible Foam Flow in Porous Media for EOR," SPE 155633 presented at the SPE EOR Conference at Oil and Gas West Asia held in Muscat, Oman, 16–18 April 2012

APPENDICES

Appendix A **Apparatuses**

Figure A.1 Flooding setup

Figure A.2 Isco pump used for flooding process

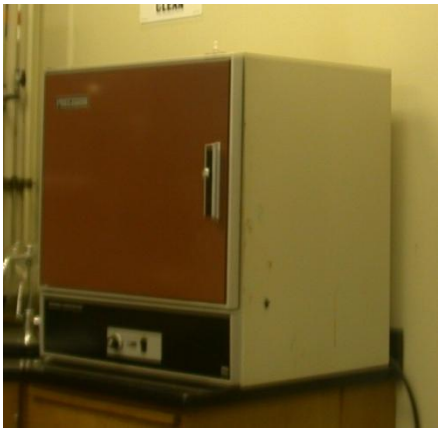

Figure A.3 Oven

Figure A.4 Vacuumed Oven

Figure A.5 Prepared brine

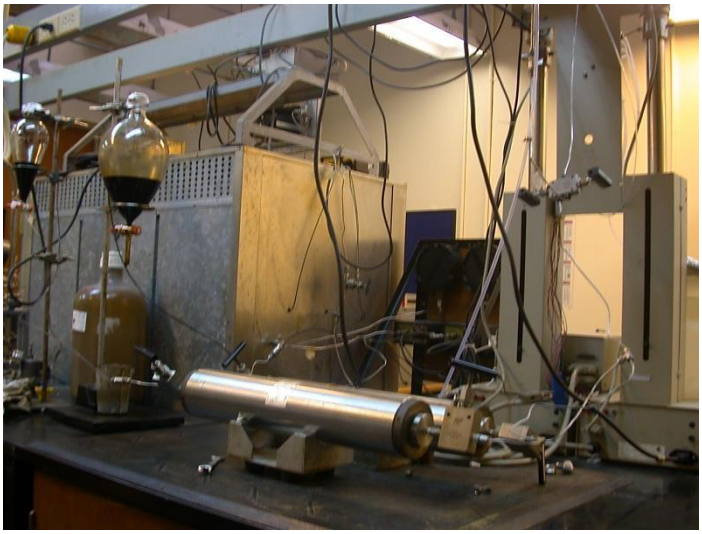

Figure A.6 Setup for filtering oil

Appendix B **Phase Behavior Tests**

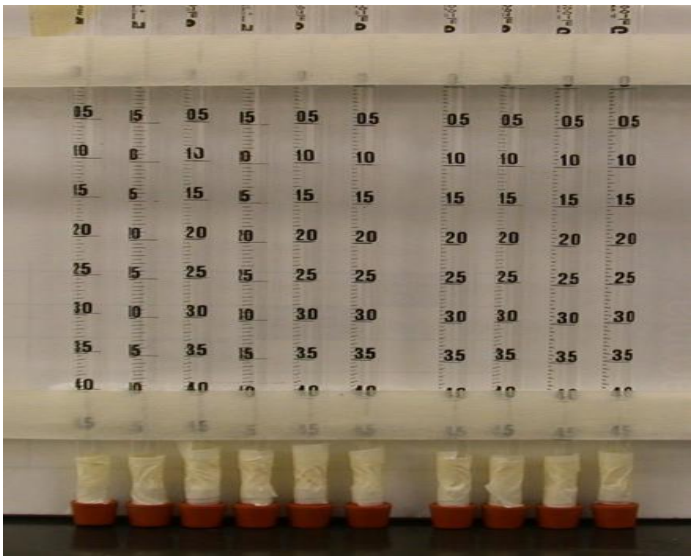

Figure B.1 Pipettes used for phase behavior test

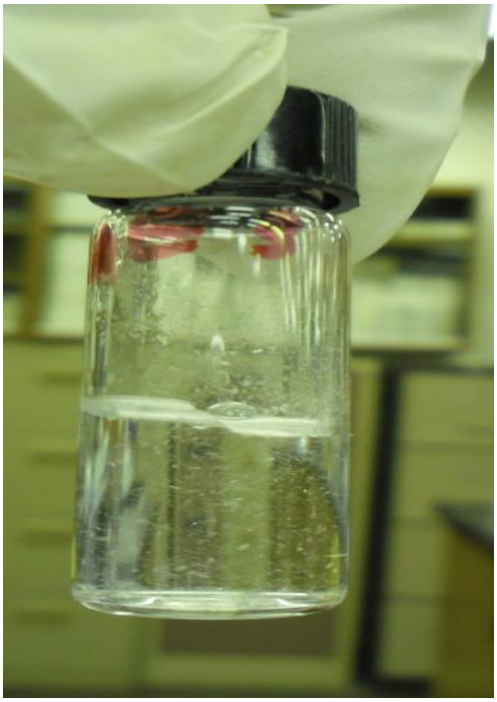

Figure B.2 Precipitation of 0.05 wt% of FS-61 with 12,900 ppm

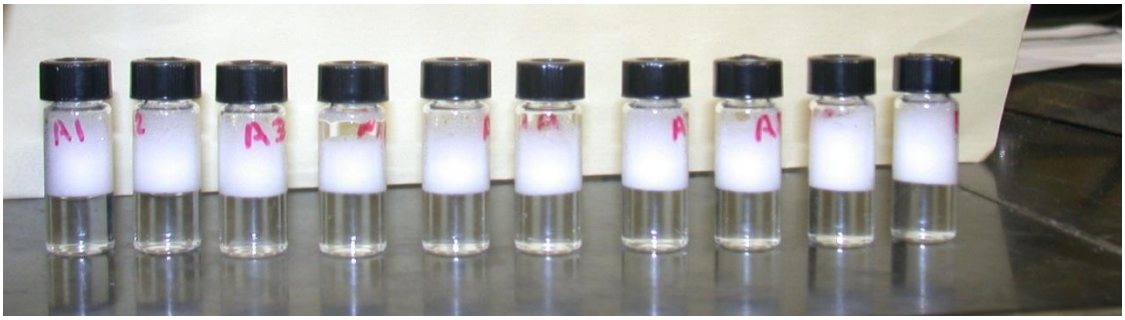

Figure B.3 Tergitol NP-9 (0.1 wt%) with different salinity of NaCl (4,000-40,000 ppm)

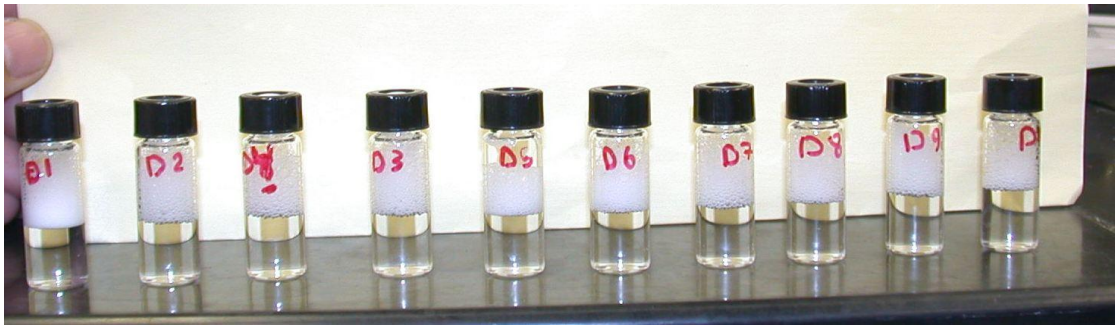

Figure B.4 Tergitol NP-9 (0.4wt%) with different salinity of NaCl (4,000-40,000 ppm)

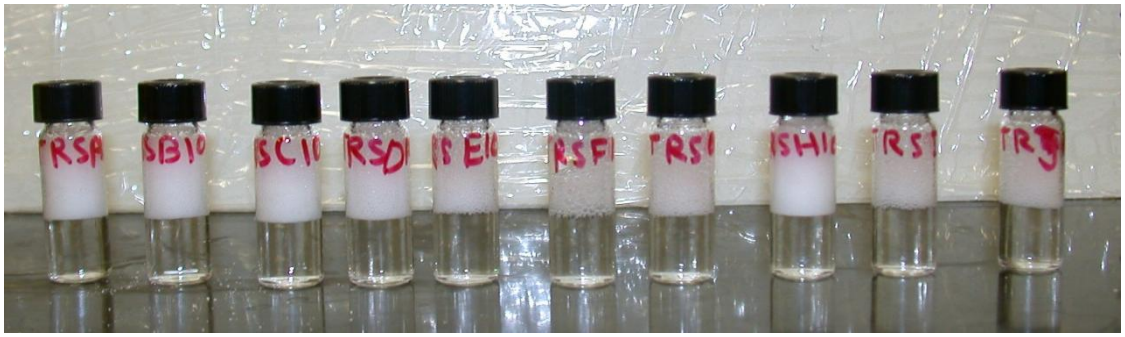

Figure B. 5 Triton X-100 (0.1-1 wt%) with 40,000 ppm soft brine

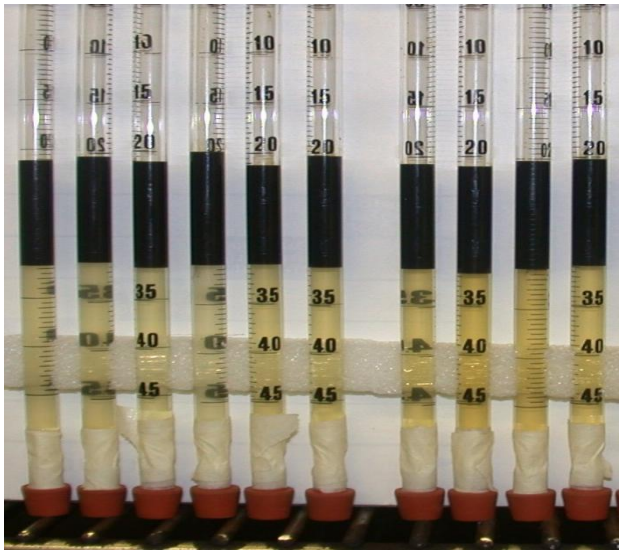

Figure B.6 Tergitol NP-9 (1 wt%) with (4,000-40,000) ppm NaCl at 50 ^{o}C

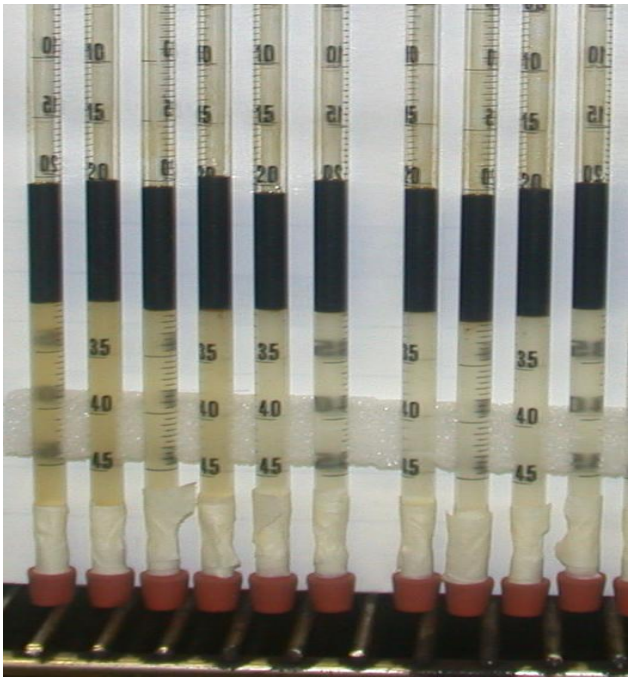

Figure B.7 Tergitol NP-9 (1 wt%) with (4,000-40,000) ppm NaCl at 77 ^{o}C

Appendix C **Surfactants**

Table C. 1 Capstone FS-50 Fluorosurfactant Properties

Product name	Capstone FS-50
Appearance	Clear amber-colored liquid
Chemical structure	Amphoteric fluorinated surfactant
Active ingredient, wt%	27
Solvent	Ethanol/water
Density at 20°C (68°F)	1.03
Viscosity at 20°C (68°F), cP	9.7
Thermal stability	Stable up to 175°C (347°F)
pH	5–6
Flash point (closed cup)	25°C (77°F)
Solubility at 25°C (77°F)	Soluble in water, ethanol

Table C. 2 Capstone FS-51 Fluorosurfactant Properties

Product name	Capstone FS-51
Appearance	Clear amber-colored liquid
Chemical structure	Perfluoroalkyl amine oxide
Active ingredient, wt%	40
Solvent	Ethanol/water
Density at 20°C (68°F)	1.07
Thermal stability	Stable up to 175°C (347°F)
pH	6–8
Flash point (closed cup)	25°C (77°F)
Solubility at 25°C (77°F)	Soluble in water, ethanol and ethylene glycol

Table C. 3 Capstone FS-61 Fluorosurfactant Properties

Product name	Capstone FS-61 Fluorosurfactant
Surfactant Type	anionic
Manufacturer	DuPont
Form	viscous liquid
pH	7 - 9
Boiling point	100 °C (212 °F)
Density	9.17 lb/gal
Specific gravity	1.1
Water solubility	soluble
Concentration	13 - 15 %

Table C. 4 Tergitol NP-9 Properties

Product name	TERGITOL™ NP-9: Nonylphenol
Surfactant Type	Nonionic
Manufacturer	Dow
Cloud Point, °C	54
HLB	12.9
Pour Point	-1
Appearance Pale	yellow liquid
pH, 1% aq solution	6
Viscosity at 25°C (77°F),cP	243
Density at 20°C (68°F), g/mL	1.055
Flash Pt, Closed Cup, ASTM D93	247°C 477°F
Actives, wt%	100
CMC	60
Surface Tension	32
Foam Height	105/90

Table C. 5 Triton X-100 Properties

Product name	Triton X-100
Surfactant Type	Nonionic
Manufacturer	Sigma-Aldrish
Appearance	Liquid, clear to slightly hazy, colorless to
Specific gravity	1.065 at 25 °C (approx. 1.07 gm/ml)
Viscosity at 25 °C, cps	240
Cloud Point (1% aq solution)	63-69 °C
pH, 5% aq solution	6.0 to 8.0
HLB	13.5
CMC	0.22 to 0.24 mM

VITAE

Name	:Ali Saleh Omar Ba geri
Nationality	:Yemeni
Date of Birth	:8/30/1983
Email	:asob.1983@gmail.com
Mobile	:0096701063690, 00966535101972
Address	: Bour Village, Seyion City , Hadhramout Governorate, Republic of Yemen
Academic Background	:M.S in Petroleum Engineering, May 2013 King Fahd University of Petroleum and Minerals Dhahran, Saudi Arabia. B.S in Petroleum Engineering, July 2007. Hadhramout University for Science and Technology, Hadhramout, Yemen.